AN EXPERIMENTAL OF THERMODYNAMIC PERFORMANCE OF A CASCADE REFRIGERATION SYSTEM FOR REFRIGERANT COUPLES

2023
Ph. D. THESIS
ENERGY SYSTEMS ENGINEERING

Adel Mohmed A KRAIM

Thesis Advisor
Assist. Prof. Dr. Şafak ATAŞ

AN EXPERIMENTAL OF THERMODYNAMIC PERFORMANCE OF A CASCADE REFRIGERATION SYSTEM FOR REFRIGERANT COUPLES

Adel Mohmed A KRAIM

Thesis Advisor
Assist. Prof. Dr. Şafak ATAŞ

T.C.
Karabuk University
Institute of Graduate Programs
Department of Energy Systems Engineering

Prepared as
Ph. D. Thesis

KARABUK
February 2023

I certify that in my opinion the thesis submitted by Adel Mohmed A KRAİM titled "AN EXPERIMENTAL OF THERMODYNAMIC PERFORMANCE OF A CASCADE REFRIGERATION SYSTEM FOR REFRIGERANT COUPLES" is fully adequate in scope and in quality as a thesis for the degree of PhD.

Assist. Prof. Dr. Şafak ATAŞ .....
Thesis Advisor, Department of Energy Systems Engineering

This thesis is accepted by the examining committee with a unanimous vote in the Department of Energy Systems Engineering as a PhD thesis. 01/02/2023

Examining Committee Members (Institutions)	Signature
Chairman : Prof. Dr. Mehmet ÖZKAYMAK (KBU)	.....
Member : Assist. Prof. Dr. Şafak ATAŞ (KBU)	.....
Member : Prof. Dr. Kurtuluş BORAN (GU)	.....
Member : Assoc. Prof. Dr. Volkan KIRMACI (BU)	.....
Member : Assoc. Prof. Dr. Alper ERGÜN (KBU)	.....

The degree of PhD by the thesis submitted is approved by the Administrative Board of the Institute of Graduate Programs, Karabuk University.

Prof. Dr. Müslüm KUZU .....
Director of the Institute of Graduate Programs

"I declare that all academic ethical principles have been taken into account in submitting and presenting this thesis to obtain a doctorate degree, I also declare that according to the regulations of the two laws in force and the academic principles, everything related to this dissertation."

Adel Mohmed A KRAIM

ÖZET

Doktora Tezi

SOĞUTUCU AKIŞKAN ÇİFTLERİ İÇİN KADEMELI BİR SOĞUTMA SİSTEMİNİN TERMODİNAMİK PERFORMANSININ DENEYSEL OLARAK İNCELENMESİ

Adel Mohmed A KRAIM

Karabük Üniversite
Lisansüstü Programlar Enstitüsü
Enerji Sistemleri Mühendisliği Bölümü

Tez Danışmanı:
Dr. Öğr. Üyesi Şafak ATAŞ.
Şubat 2023, 110 sayfa

Bu tez sayesinde, düşük basınç çevriminde (LPC) R32 soğutucu akışkanı kullanılmasının, yeni oluşturulan karışım gazına (%90R32+%10R600a) göre küresel ısınma potansiyeline (GWP) daha büyük zarar verme potansiyeli olduğu kanıtlanmıştır. R407C soğutucu akışkanı kullanılan yüksek basınç çevrimi (HPC) bir ısı eşanjörü (HEX) ile iki soğutma devresini birbirine bağlayan mini bir kademeli soğutma sistemi (MCRS) kullanılmıştır. Ayrıca bu araştırma ile GWP'nin mümkün olan en düşük değerde tutmak için bir karışım kullanılarak istenilen en iyi sıcaklık (T) (-32°C) değeri elde edilmiştir. Ayrıca yeni karışım ile (-32.18°C) ve R32 ile (-32.46°C) değerlerine deneyler sonuçunda ulaşılmıştır. Her iki çevrim için aşırı kızdırma (Sh) değeri, evaporatör (Evap) ve kondenser (Cond) basıncı (P), kompresörlerin (Comp), HEX'nin, Cond ve Evap ün her birinin giriş ve çıkışının T değeri ölçülmüştür. Bu

sayede, MCRS de enerji tüketimi değeri, soğutma odası T düşüşü ile karşılaştırılmış ve iyi bir sonuç elde edilmiştir. Güç girişi ve performans katsayısı (COP) faktörü hesaplandı. HEX'nin (T_3) LPC'sinin T çıkışı, soğutma odasındaki T_e değeri T ile eşleştirilir. Sonuç olarak, MCRS'de aynı deneysel koşullar altında yeni karışımın ve R32 akışkanı kullanılan çevrimleri COP_{MCRS} 'nin sırasıyla 1.63 ve 1.78 olması nedeniyle yeni karışımın R32'nin sonuçlarına çok yakın olduğu kanıtlanmıştır. Yeni karışımın kullanılması sayesinde GWP değeri R32'den 63 daha düşüktür. Kullanılan sistem modelini simüle etmek için Refprop yazılımı kullanılmıştır. R600a ve R32 gazlarının her ikisininde yanıcı olmasından dolayı yanıcı olmayan alternatifler aranması önerilmektedir.

Anahtar Kelimeler: Mini Kaskad Soğutma Çevrimi, Küresel Isınma Potansiyeli, R32, R600a.

Bilim Kodu **:** 92808

ABSTRACT

Ph. D. Thesis

AN EXPERIMENTAL OF THERMODYNAMIC PERFORMANCE OF A CASCADE REFRIGERATION SYSTEM FOR REFRIGERANT COUPLES

Adel Mohmed A KRAIM

Karabük University
Institute of Graduate Programs
The Department of Energy Systems Engineering

Thesis Advisor:
Assist. Prof. Dr. Şafak ATAŞ
Febuary 2023, 110 pages

Through this thesis, it was proved that in the low-pressure cycle (LPC) when using R32 the greatest potential for damage to global warming potential (GWP) of the new mixture (90%R32+10%R600a). A mini cascade refrigeration system (MCRS) was used based on two refrigeration circuits connected by a heat exchanger (HEX) using the high-pressure cycle (HPC) with R407C. Furthermore, through this research, the best temperature (T) was (-32°C) by obtained by using a mixture at the lowest possible value of GWP events. Moreover, results were taken from the experiment with the new mixture at (-32.18°C) and with R32 at (-32.46°C). Superheat (Sh) and the pressure (P) of the evaporator (Evap) and the condenser (Cond) for both and, the T of the inlet and outlet of each of the compressors (Comp), the HEX, the Cond, and the Evap have been taken. Therefore, the energy consumption has been compared with the cooling chamber T drop and has a good result using MCRS. The power input and coefficient

of performance (COP) factor were calculated. The outlet T of the LPC of the HEX (T_3) is matched by the T in the refrigerating chamber (T_e). Consequently, it was proved that the new mixture under the same experimental conditions in MCRS is very close to the results of R32 as R32 and COP_{MCRS} is 1.63 and 1.78 for the new mixture. Therefore, the new mixture has a lower GWP of 63 than R32. Software Refprop was used to simulate the system model used. Therefore, from this, recommend looking for non-flammable alternatives to gases or mixtures because both R600a and R32 are flammable.

Keywords **:** Mini Cascade Refrigeration System, Kürese Isınma Potansiyeli, R32, R600a.

Science Code: 91408

ACKNOWLEDGMENT

Your interest and support guided me throughout my undergraduate and graduate education my very dear teachers; Thesis Supervisor: Assist. Prof. Dr. Şafak ATAŞ and Prof. Dr. Mehmet ÖZKAYMAK, with their financial and moral support, are always there for me. I offer my big thanks and gratitude to my dear wife and my family, to provide assistance and support to complete this thesis successfully.

Also, I will not be able to finish counting their names; or their support with their knowledge, experience, and friendships. To my esteemed professors, friends, Karabuk University Family and I would like to thank my dear family members.

CONTENTS

Page

Page

Page

LIST OF FIGURES

Page

Page

LIST OF TABLES

Page

SYMBOLS AND ABBREVIATIONS

SYMBOLS

W_C : Work by the Compressor

T : Temperature

P : Pressure

°C : Degrees Celsius

°K : Degrees kelvin

kW : Kilowatts

kWh : Kilowatt hour

X : Exergy

Q_C : Condenser capacity (W)

Q_E : Evaporator capacity (W)

W : Power

h : Specific enthalpy Joule per Kg (kJ/kg)

S : Specific entropy Joule per Kelvin (J/K)

$\dot{m}$: Mass flow rate (kg/s)

$\dot{V}$: Volumetric flow

kj : Kilojoule

kg : Kilogram

m^3/h : Cubic meters/ hour

bar : Bar pressure measurement

kPa : Kilopascal

Mpa : Megapascal

η_{vol} : Volumetric efficiency

η_{carnot} : Carnot efficiency

η_{is} : Isentropic efficiency

CO_2 : Carbon dioxide

NH_3 : Ammonia

H_2O : Water

O_2 : Oxygen

O_3 : Ozone

C : Carbon

H : Hydrogen

F : Fluorine

Br : Bromine

Cl : Chlorine

SO_2 : Sulfur dioxide

h_p : Horsepower

cc : Cubic centimeters

m : Meter

m^2 : Square meter

cm : Centimeter

mm : Millimeter

AC : Alternating current

Sh : Superheat

Sc : Subcooling

A : Ampere

V : Volt

L : Liter

” : Inch

ABBREVIATIONS

GWP : Global Warming Potential

CRS : Cascade Refrigeration System

LPC : Low-Pressure Cycle

HPC : High-Pressure Cycle

MCRS : Mini Cascade Refrigeration Systems

EES : Engineering Equation Software

COP : Cooling Performance Coefficient

EEV : Electronic Expansion Valve

CM : Cooling Machine

TEV : Thermostatic Expansion Valve

CFC : Chlorofluorocarbon

HCFC : Hydrochlorofluorocarbon

HFC : Hydrofluorocarbon

HEX : Heat Exchanger

Evap : Evaporator

Cond : Condenser

Comp : Compresser

PART 1

INTRODUCTION

Refrigeration and cooling systems are an important part of our lives. Cooling technologies, which are frequently needed for the high quality of life and food preservation, emerged in the mid 19th century while living spaces were being built. It plays a very important role in both domestic and commercial and industrial use. Refrigeration and cooling systems have played an important role in our lives since then. Cooling systems; It is widely used in areas, food preservation, production areas of various sizes, storage, commercial workplaces, and chemical and pharmaceutical industries. Therefore, it is very important to develop CM, increase their efficiency, be suitable for human health and be environmentally friendly. Today, many cooling applications are used. However, heat pump cooling systems are The coolest type of cooling nowadays. Appliances such as refrigerators and air conditioners that we often use in our daily life are the most common examples of heat pump systems.

Because a region or country has a hot climate, there is a need for cooling or lowering its T. CM; It is widely used in food storage, production, and storage of various sizes, commercial workplaces, and chemical and pharmaceutical industries. Therefore, the COP of CM should be increased, they should be made suitable for the atmosphere and people to be healthy, and the GWP and ODP values of the refrigerants used should be low values. Refrigeration devices are called CM. Main CM is known as vapor compression, absorption, and multistage CM.

In some areas such as the pharmaceutical-chemical industry, health, and laboratory applications, cooling at very low T may be required. Single-stage heat pumps (vapor compression refrigeration cycles) have difficulty in meeting adequate efficiency in LPC, as well as their costs and energy consumption, remain high. As it is clearly seen in the literature, CRS is more efficient system for low T cooling than single-stage heat

pumps. The energy consumed and the Comp outlet T in CRS (two-stage) cooling systems used in very low T cooling areas are lower than in single-stage systems.

Absorption cooling applications can also cool at very low T when used gradually. However, this type of CM used today is not suitable for use in all areas, as they are large-scale and more complex CM.

Today, the most widely used cooling system in cooling applications is vapor compression CM. These systems depend on Comp, Cond, EEV, and Evap respectively. Heat drawn from a higher T environment is thrown into a low T environment. In order for this process to take place, external work is given while the refrigerant is circulating in the CM. During this process, the refrigerant undergoes a number of processes and changes phase. Some CM require very low T. CRS come to the fore in order to perform cooling at desired low T.

Experimental setup is designed and produced. In the experimental setup, computer-connected T and P measuring devices and EEVs were used to measure and record the experimental data. In this thesis, the CRS in which R32-R600a refrigerant and its mixtures are used in the low-pressure cycle (LPC) and R407C refrigerant in the high-pressure cycle (HPC) will be examined experimentally. Heat exchanger (HEX) be a link between the two sessions. The data obtained as a result of MCRS will be given in the sixth chapter of this research.

PART 2

HISTORY OF COOLING AND LITERATURE

2.1. COOLING APPLICATIONS FROM PAST TO PRESENT

In this chapter; The first cooling methods, the first alternative cooling studies, the first chemical cooling applications and the first mechanical cooling (CM) applications in history have been trying to be summarized. It is aimed to explain the importance of refrigeration in human history and to introduce the firsts in vapor compression refrigeration cycles based on the thesis topic. Various cooling applications have been needed since the beginning of human history. The cooling needs, which it has seen basically to preserve foods for a long time without spoiling and to lower T room [1]. Although the exact dates cannot be reached in the first cooling applications, we see various examples in ancient civilizations. As an example, the İnsuyu cave located in Burdur, Turkey, from the geography of Mesopotamia, can be shown in 333 BC. In archaeological studies, the city's BC, the cave was used for cold storage of food in Sagalassos, the ancient city of Pisidia. The cave, which is 900 m above sea level, has large and small sections, is 597 m long, and has a T of 13°C in all seasons of the year [2]. Many examples such as Karabük Bulak-Mencilis Cave, and Gaziantep Kaleoğlu Cave show us that natural methods have been used from ancient times to cool food in Anatolia, the cradle of civilizations. The common features of the caves used for food storage are that they are at the same T in all seasons of the year, due to the effect of being in a karstic structure [3].

In Ottoman history, we see that the snow and ice trade was carried out, where in the last periods of winter, snow was collected, compacted with molds, buried in deep wells, and stored. During storage, thermal insulation would have been provided by utilizing the low heat transmission coefficient of straw and soil. In case of need, the ice floes extracted from the wells during the summer were used for cooling purposes,

especially for food [4]. When it comes to the 16th century, the first examples of chemical cooling methods are seen. It has been found that when chemicals such as sodium nitrate is mixed in water, the water t drops. The first known creator of the steam p refrigeration cycle was Oliver Evans (1755-1819). O. Evans found that when the vacuum is made from a container filled with water, the boiling point decreases and the water cools slightly. He described in his drawings that a reciprocating vacuum pump or a compression cylinder must generate heat in a Cond to produce this effect [5]. The first known example of mechanical cooling was applied in 1756 by William Cullen, a professor at the College of Physicians and Physicians at the University of Scotland Glasgow. He reduced the P and T of Diethyl ether in a non-air-permeable tank using a manual vacuum pump. As a result of this experiment, it was succeeded in producing a very small amount of ice. It has produced commercial-grade samples for meat products and the brewing industry. The first use of refrigerators in residences took place in America in 1911. The basic cooling methods, which are based on the principle of discharging the heat from the space (or mass), are used much more effectively today [6].

The refrigerant couples used in CRS are on the rise in recent research. The sterilization and blood storage industries, for example, need low T of less than -30°C, and in many cases, these industries need small spaces that can meet MCRS. The LPC and the HPC are connected to a HEX to form CRS. The HEX represents the Cond for the LPC and the Evap to the HPC, while the main Evap is to the LPC and the main Cond to the HPC. By CRS performance CPO and flow rate ṁ were calculated using R744/R717 according to A. Messineo [7]. It is recommended to use EES to calculate the simulations of CM. The main attraction of R744 natural refrigerant blends is that it has lower GWP, ODP, and flammability than safety cooler. It considers the possibility of using CO2 blends in applications below -56°C [8]. According to reference [9], CRS must be improved to reduce cost and increase COP, and this comes by calculating the analysis of the condition of the refrigerant and the stages of its transformation from liquid to gas and vice versa.

Y. Zhang et al. (2022) In this thesis worked with containing R1270 with carbon dioxide. A CRS working with two reciprocating Comp was produced. The results show

R1270 as a good alternative in the HPC to replace NH3 and R290 [10]. Moreover, Refrigerants can be classified into A3 highly flammable, A2 medium flammable, and A1 low flammable at 101 kPa and 21°C. The mixtures have a similar flammability and toxicity rating as R407C class A1, R32 class A2, and R600a class A3 [11]. Sun et al. (2019) article, R41, and R23 refrigerants were used in the LPC, while refrigerants R32 and R290 were used in the HPC [12]. Likewise, Roy and Mandal Compare the Exergy analysis of CRS R404A in HPC and R41 in LPC [13]. Mofrad et al. (2020) thermodynamic simulation and analysis for CRC are examined. The optimization results concluded that heat recovery CRS increases the COP by 7.6% and the exergy efficiency by 12.5 [14]. Also, according to Y. Ust and A. S. Karakurt, the R23/R717 refrigerants proved to be better [15].

Moreover, MCRS should be user-friendly refrigerants for the environment. Correspondingly, a system secures all working conditions in following as below:

- Increased demand in the refrigeration industry.
- Low energy consumption compared to a single Comp unit.
- CRS can be manufactured in different sizes.

Bhamidipati et al. (2020) In this study, aimed aims to investigate the use of R32 as a possible substitute for R134a. R134a has a higher GWP than R32 [16].

It is also compulsory to mature both freezing rotations to rise the competence of the MCRS. Recently, the science of two-phase refrigeration has received significantly devotion. A mixture composed of R32/R600a where the pressure deviation was 13% and 0.0089 respectively [17]. Bingming et al. (2009) carried out the work in this article Analyze the COP of CRS by using NH3/CO2. The effects of the T difference in the cascade HEX of the LPC on the COP were investigated. Use cascade cooling for better COP for T below -40°C [18]. Furthermore, The HPC and LPC cycles form the MCRS and are connected by a HEX. R32 can be used in LPC because its vapor point is from 0 to -70°C and R407C can be used in HPC because its vapor point is from 0 to -60°C. Both cycles are subject to entropy analysis of the expansion process. Using R23/R404A proved to be less effective than R23/R404A in terms of COP.

Furthermore, according to [19], the heat gained from the Comp is subtracted by the Cond of each of the two cycles.

2.2. LITERATURE RESEARCH

Khalilzadeh et al. (2019) designed a system based on that the Cond squandering heat get from the CRS is used in an Organic Rankine cycle with the reinforcement of solar collectors, and the generated electrical energy is reused in the CRS. The CRS used has a cooling capacity of 100 kW at -55°C and has an electricity consumption of 3253.44 kWh/day. In addition, the overall energy efficiency of the designed CRS was calculated as 84.53%, and the total exergy efficiency was calculated as 37.05%. In this way, the electrical energy that the CRS cycle will receive from the network has decreased by 82.57%. As extend the COP of the CRS increased from 4.23 to 5.74 [20].

Singh et al. (2021). COP, exergy efficiency, and system cost ratios were compared to determine the best alternative refrigerant pair. It was concluded that COP and exergy competence achieved was 1.917% and 39.14%, respectively. Analysis of R717/R290 is the best in terms of thermodynamics and economy [21]. R134a is the first gas that does not affect ODP. The COP and flow rate of the mixture with a weight ratio of (70/5/25) consisting of (R32/R600a/R290) less global warming potential than R134a at 33°C condensation and -5°C evaporation. Using a refrigerator, an alternative to R134a was searched for in a practical experiment conducted by [8]. Choosing R32 is the recommended choice as it is the least environmentally destructive. It is also rated R32 as having a low GWP [22].

Llopis et al. (2016) experimentally investigated and analyzed the effects of the internal HEX used in the LPC of a CRS with a two-stage HEX. COP was equivalent 3.7 by experiments. In addition, it has been observed that it reduces the amount of heat in HPC in the HEX 4.4% to 5.2% [23]. Massachetto et al. (2019) By a CRS, six types of refrigerants were tested. By using pure gases, the percentage was raised to 32% from 18% for the COP [24]. When the oil mixes with the coolant, the P increases by 22%. Test R32 for ignition effect at a mixing rate $\dot{m}$ at 200 g/min tested by Liang et al., as announced by [25]. Wang et al. (2020) the overexploitation control method in order to

achieve precise T setting values in a CRS. The over-cooling control get the desired T with a deviation of 0.8%, and it was determined that the system COP by 10.6%. Extreme seeking control provides instant controls by quickly detecting system parameters with dynamic algorithm software [26].

López-Belchí et al. (2017) R32 was suggested as an alternative to R410A refrigerant. Using a small channel condensate and refrigerant exchanger, a theoretical and practical research was carried out. Therefore, prove that the energy efficiency of the system is increased by using R32 and the environmental impact is reduced [27]. In a practical experiment using the CO2/R32 mixture (20/80 %) by mass, the energy consumption was 12%, which has a lower global warming potential compared to R410A gas, which produces it with an energy consumption of 16%, according to the reference [28]. Massuchetto et al. (2019) used in a CRS. Thermodynamic performance comparisons of R744/R1270, R744/R717, and R744/RE170 fluid pairs were made. R744/RE170 liquid couple reached the highest COP value with a value of 2.34. The experiments were carried out in a cycle, it had a capacity of 100 kilowatts [29].

Sun et al. (2016) An alternative to R23 refrigerant gas has been proposed with a gas better than it with environmental specifications using R41. The study was comprehensive to LPC and HPC with vital cooling agents for both from evaporation to condensation of the refrigerant medium. The COP was better and the input power was lower when using the R41 compared to the same experience of the R23. Record (g) energy consumed, (X) energy loss, (COP), and Comp input power. The CRS that was used suggested theoretically that the R41 is better than the R23. The result was 42.98% when using the R23/R404A, while the result was 44.38% with R41/R404A for maximum energy. The highest COP is achieved when the degree of condensation is as low as possible [30].

However, Environmental problems have become a major factor in determining the quality of carbon mixtures and the possibility of using them or not. The oils used to lubricate the Comp in the refrigeration cycle are of great importance because of the possibility of interaction with the refrigerant gas, so the refrigerant oil used with R410A was changed with new oil that is compatible with the alternative gas R32, and

it is less energy consuming and less capable of causing global warming, so R32 is a good alternative to gas R410A (2014) [31]. Wang et al. (2020) carried out A low T equal to -80°C was reached by using an additional LPC of HEX in a laboratory experiment. It has been proven that the decrease in T is faster than the decrease in COP and cooling capacity [32].

Tan et al. (2015) in this study; Suggest a lower T cooling cycle by using an ejector cooling with CRS. -30°C is the T reaches as the lowest possible T in this experiment [33]. The best experimental rate and the lowest energy consumption with the lowest gas charge by weight were when using R600a/R290 mixture (54.8/45.2%) by mass as an alternative to R134A gas. Mohanraj et al. (2009) [34] Prove that the mixture used reaches a lower T in the Evap, 1% is the mixing ratio of the oil with the refrigerant when using POE oil. Sun et al. (2016). Using a successive refrigeration cycle with a practical experiment R23/R404A compared to the refrigerant pair R41/R404A by a thermodynamic analysis method. As a result of the experiment, it was noted that a mixture could be used instead of pure R41 gas due to its high flammability [35]. Kilicarslan et al. (2010) In this study, the irreversibility analysis was done with a computer code that optimizes energy using 12 different refrigerant pairs, among which was R404A and R290. This research adopts that it replaces R507/R23 with the proposed couple R404A/R23 the COP of a system decreases as the T of the Cond increases [36]. conducted with R600a and a mixture of R600 with R290 at a ratio of (40/60%) by mass to replace HFC-134A as stated in [37].

Dalkılıç (2012) made COP comparisons of various refrigerants in a CRS with his experimental analysis. In the study; A comparison of R12, R22, and R502 refrigerants and alternatives such as R134a, R152A, R404A, R407C, R290, R600a, R717, and mixed refrigerants consisting of R134a, R152A, R600a, R290 is presented. In mixed fluids, it was stated that the azeotropic R152A/R134a (86/14%) and R600a/R134a (18/82%) both by weight mixtures reached higher COP values than the non-azeotropic R290 / R600 (55/45%) mixtures. It was confirmed that R600a was used in refrigerant mixtures that were used during the experiment, and the mixture charge quantities were less than other gases. In the comparisons made; Reaches the highest COP value when using R717 refrigerants in the HPC and R152a refrigerants in the LPC. As a result of

the analysis, it was stated that R152a and R717 fluids reached higher COP values and these fluids required less charge amount [38].

Sun et al. (2019) In this article, the Comp operating conditions, as well as COP of CO2/R32 mixtures. In this study, they observed that the CO2/R32 mixtures significantly reduced the cooling treatments [39]. According to Rui et al. (2016) confirmed the value for which the Evap is designed to be wet can be converted to the drying value of the Evap if large quantities are used as the load for the Evap inside the cold rooms. Atalay (2019) developed a refrigeration simulation for real cooling cycles, it is stated that the results are quite compatible with each other and can be used easily and effectively in the application areas. With the developed simulation models, CRS analyses of R290/R290, R600/R600, and R290/R600 fluid couples were performed. In the comparison of refrigerants, it was determined that the R290 fluid gave a higher COP value. The data obtained as a result of the simulation were compared with the internationally valid REFPROP 9.0 program and it was observed that the results obtained from both programs were compatible with each other. However, it was observed that higher COP values were obtained in the simulation using R600 refrigerant in both cycles [41].

Kochenburger et al. (2015) The CRS using mixed refrigerant in this study offers a possible for the HPC from 55 to 70 K. Oxygen is used in the HPC and a mixture of nitrogen and neon is used in the LPC [42]. Furthermore, the components of the mixture have an effect on the system used according to the proportion of each component in the mixture, and the effect is clear about condensation, evaporation, and performance coefficient. The results of the experiment mentioned the relationship between COP and P [43]. Cimşit (2018) theoretically made thermodynamic analyzes of NH3/H2O fluid couple in a CRS [44]. Pico et al. (2020) conducted a study was conducted to reduce increased GWP, the system is running R410A replaced by R32. By selecting two different temperatures the POE oil was tested [45].

In the same way, Shaik and Babu (2017) R22 was suggested to be replaced with a mixture of 10 refrigerants in different proportions consisting of two main gases, R290 with R1270. 50 is the condensing T and -30 to 10 is the evaporation T using the least

amount of refrigerant possible [46]. Rupesh et al. (2015) in their experimental study; Thermodynamic analyzes of a CRS using R134a/R23 fluid couples were carried out. COP_{MAX} for R134a/R23 by 0.8 [47]. He et al. (2016) this research proposes ingredients for the mixture R32/R290. Using an R22 air conditioner, a mixture was tested to be replaced by the mixture composed of R32 68% with R290 32%. R410A has a higher heat transfer coefficient than the mixture. The study presented an improved design of the refrigeration unit through the results obtained for the mixture [48]. The result of the research is that the cooling factors for the added cooling cycle are very important factors for obtaining good results for the system, such as Sc and Sh of a study conducted by [49]. Yin et al. (2016) developed a control-supervision mechanism to excess the energy of CRS. In the light of the data obtained, it has been stated that the developed control unit provides 5.8% less energy consumption than a standard CRS. In the HPC, a mathematical model using a PI controller has been developed to optimally meet the demands between cooling demands and Sh degrees [50].

Yao et al. (2017) In this study, the application of R32 refrigerant identical COP for R410A was investigated. DEAFAHU through R32 can sustain performance and operate safely at 90°C. There is a clear trend towards replacing R410A and R32 [51]. Therefore, use a mixture of R600a added to R290 as an alternative to R134a for a heat pump. R134A was considered a natural alternative to R290. To provide adequate flow they recommended the use of a larger compressor with the R600a. With the possibility of using a compressor with the same specifications and refrigerant oil for both R600a and R134A gases [52]. Campbell et al. (2007) designed and manufactured a system and conducted various experiments on this system examine the cop of the single rotation using R744 (CO_2) fluid. They compared the benefits and practical results of using natural fluids such as CO_2 (R744) in commercial cooling devices. As a result of their studies, they determined that the 25-kW CRS (R404A/R744) releases up to 1274 tons of CO_2 less in 10 years compared to conventional single-stage systems with the same capacity. They observed that using the R404A/R744 CRS saves energy and significantly reduces CO_2 emissions compared to conventional systems [53]. Ma et al. (2014) In this study, they investigated a CO_2/NH_3 CRS using a falling film Evap-Cond by way of a HEX. When using CO_2 and NH_3, it is possible to benefit from this study in the field of design [54].

Similarly, Oktaviani [55] has employed the mixture of R134a as well as R32 which was applied under an absorption cooling experiment at T ranging from (25°C to 75°C) on activated carbon powder. Ceylan (2002) studied CRS operating at low T. It also formulated methods to be used in determining the materials used in multistage refrigeration cycles [56]. Sanz-Kock et al. (2014) In this study, Used CRS with R134A and CO_2. All system cooling factors are taken into account to calculate COP. The highest degree of Cond is 50℃; the highest degree of Evap is -30℃, the lowest degree of Cond is 30℃, and the lowest degree of Evap is -40℃ [57]. Consequently, when applying the mixture R32 / R290, Pipe connections and Comp capacity must be checked when using the mixture as declared in [58]. In his study, Menlik (2005) designed and manufactured a two-stage cooling system and conducted efficiency-performance experiments. The COP of the system at this operation was calculated as 1.05. A brazed plate was chosen for the HEX, which is considered the most sensitive element in the CRS. the Evap T is -88°C which 2°C lower than the designed T value and -75°C ambient T in 5 hours [59]. Sholahudin & Giannetti (2016), it is investigated a CRS by means of a mix of C_3H_8 in HPC and a C_2H_6/CO_2 in LPC. The result was more positive than expected in terms of economics and thermodynamics [60].

Using a refrigeration cycle that uses CO2 and R404A proves that the Comp has the greatest value in system energy loss. The more energy loses, the lower the COP [61]. Bayrakçı et al. (2010) made energy analyzes of one-stage and double-stage (CRS) with R744 refrigerant at identical cooling loads and compared their costs. When they compared the annual energy consumption of single and two-stage systems, it was revealed that the energy cost of the one-stage refrigeration cycle is upper than the CRS. In their studies, they determined that the CRS had higher COP values [62]. Şahin (2020) analyzed different refrigerants using the EES (Engineering Equation Solver) program in his CRS study. Exergy and COP efficiencies were compared for each refrigerant when operated with different parameters. ODP values are the same, GWP values are different [63]. Bouaziz (2014). R32 with a mass fraction of approximately 0.22 amounts to 150 GWP [64]. Zubair (1998) determined in their studies that a two-stage vapor compression system would be more appropriate in order to eliminate the extreme P differences between low and high P of single-stage systems operating at low T. With this simulation based on thermodynamic analysis, they showed that the COP

value of the CRS would be higher than one-stage. In their study, they made thermodynamic analyzes of single-stage and CRS refrigeration cycles operating at identical loads [65]. In his study, Yilmaz (2018) CRS using R744/R717 refrigerant. It has been observed that the NH_3-CO_2 mixture has a higher cop in CRS in LPC [66]. When using R32 by increasing the mass fraction, the system T of condensation and evaporation increases [67]. Kılıçarslan (2004) aimed to increase the low COP efficiency due to the large difference in low and high pressure at high condensation and low evaporation T in a system using a single-stage R134a refrigerant [68]. Elitok (2017) experimentally investigated the CRS in his study. R134A in the HPC and R404A in LPC. It observed that while T_e were changed from -27°C to -17°C, Cond T varied from 47°C to 57°C [69]. Zhou et al. (2017) It is presented a study to analyze the transformation of the refrigerant medium from a gas to a liquid and vice versa for a single gas or a mixture. R134a Replace with refrigerant mixtures of R290, R600a and R32. It is recommend using REFPROP software [70].

Kaynaklı and Yamankaradeniz (2003) According to the COP factor of an absorption cooling system through the HEX. They used NH3 and NH3/H2O as refrigerants in the absorption cooling system [71]. Güney (2014) made the exergy of energy and energy analysis for R744/R134A in the CRS in his study. COP of the general CRS was 1.14. The environmental and thermophysical properties of the refrigerants used were examined, and measurements were taken from certain points on the system used [72]. The COP of the mixture was better in this search [73]. Kizilkan (2004) In his theoretical work, Kızılkan made thermodynamic and thermoeconomic analyzes of Evap, Cond, Sh, and Sc values in a cooling system. In the investigations, Evap, Cond, superheat and Sc T values are considered variable parameters of the system. In the last stage of the study, the thermoeconomic optimization method was applied to the entire cooling system [74]. In the Kaya (2014) study, the most commonly used R32, and HC, R290, and R600a, refrigerants. It has been observed that refrigerant mixtures have an important role in the determination of environmentally friendly. The mentioned refrigerant mixtures were analyzed according to their thermodynamic and economic properties [75]. Kilicarslan and Hosoz (2010) They used five types of refrigerant compounds with R23 refrigerant by computer code. The cooling load is 100

watts, evaporating and condensing degrees -40℃ degrees Celsius -27℃ degrees, respectively, with Sh at 7℃ [76].

Özkaymak (2008) By means of a refrigeration compression system, an extensive analysis of all components of the system was carried out economically and thermodynamically. COP improvement of the system by using three different types of coolant depending (R502, R12, and R22) on the second and first law of thermodynamics for all system elements. The T of the water entering and exiting the cooling vessel was determined at 15℃ and 20℃, and for the Cond, the water exit T was 25℃, and at the entrance of the Cond was 20℃ [77]. Kedersiz (2014) used Four pairs were proposed that rise to be among the best cooling fluids in terms of their suitability for the environment. The best proposals of this study were R407C-R507A as the best COP rate. The Evap operates between -40℃ and -30℃, and the Cond operates between 60℃ and 50℃, with a capacity of 10,000 watts in CRS. [78]. Moreover, the study included R507 was suggested as an alternative to R404a. Kalla et al., (2017) have performed reached the result of changing the refrigerant oil suitable for working with R407C when using it as an alternative to R22 in a theoretical study [79].

Özkaymak et al. (2010) studied thermoeconomic optimization using alternative refrigerants by a Comp system. The calculations, they calculated the ideal surface areas for the Evap and Cond in HEX according for given in a range of degrees. R22, R410A, and R407C refrigerants, calculations were made by taking the Cond 35 °C to +55 °C, and Evap -10°C to +10°C. By analyzing the law, they optimized the system in terms of thermoeconomic. In this study, thermoeconomic optimization of Cond and Evap have been carried out [80].

In the study of Akalan (2013), Use ammonia in CRS features and isotherms with CO2. Under the same conditions, ammonia was better than NH3/CO2 in the study result [81]. It was announced by [82] that the enthalpy and entropy charts with P can be calculated with great accuracy for both the inertia of the mixture and the quality of its COP. Additionally, with a practical and theoretical study, replace R22 with a mixture of two gases, R32 by 30% and R134a by 70%, using an air conditioner. Uysal (2018),

his experimental work, conducted experiments to determine the appropriate Sh value to be used in cold storage applications. As a result, he stated that the ideal Sh value for Comp life and energy efficiency is 8ºC. The warehouse T set value was determined as -10ºC and used R404a refrigerant. In these experiments, he measured COP, Comp surface T, energy consumption, and Comp on-off numbers. It was used an EEV and cold room control unit to control Sh values in the experimental setup, it was designed and manufactured [83]. In the study of Ismaeel (2012), The study confirmed that the ambient T affected the cooling system by 2.36% of the annual total cost using CRS [84]. In the same way, Chen and Yu (2008) Air conditioner R32 has been used extensively in recent times, so a suitable oil must be developed for it, as the usual oils mix with it, which reduces the viscosity of the oil [85].

Özkaya et al. (2009) Different refrigerants of domestic refrigerators, it found that R404A and R407C fluids are more efficient in high-pressure systems. According to the results obtained from the experiments, they determined that R134a refrigerant is more suitable for domestic use than R404A and R407C refrigerants. They conducted separate experiments and calculated the COP, using R134a, R404A, and R407C refrigerants, without making any changes in the system elements, in household type coolers that generally use R134a and R22 refrigerants [86]. Carbon dioxide, T, P, cooling COP, capacity, etc. The main Cond varies between 32.67 kW and 8.12 kW, and the required Comp power varies between 9.45 kW and 3.89 kW. Cooling effect coefficient for whole CRS is between 1.693 and 0.853, and efficiency for whole system is between 0.375 and 0.189. The results show that the upper stage evaporation T from -15°C to -45°C, the cooling capacity varies between 20.54 kW and 3.74 kW [87]. Besides, prove that the oil used with R410A can be used with R32 [88]. Qi et al. (2010) worked on the development T of Sh control in commercial air conditioning systems, a controller has been developed to increase the cooling efficiency by simultaneously changing the added heat degree. It was spotted ideal the added heat degree must be actively changed for maximum efficiency due to the speed change of the variable flow Comp [89]. Karaöz (2010) researched the applications of CO_2 systems in his study. CO_2 is one of the famous gases for this research, with both its thermodynamic properties and environmentally friendly rates [90].

Additionally, for lower T with a heat pump load, use a mixture of R32 at 20 percent with R1234yf at 80 percent. The heating rate increased by 13%, the COP increased by 16%, the cooling capacity increased by 16%, and the heating capacity increased by 20%. Xu et al. (2017) have mentioned that when the Evap T rises, this leads to an increase in the T of the Comp intake line, which was calculated to be equal to 110 degrees Celsius [91].

Usta et al. (2006) by CRS study, performed performance tests using the R404A/R508B refrigerant couple. As a result of their studies, they stated that the most critical part of CRS is the cascade HEX. They used R404A fluids in the HPC and R508B fluids in the LPC. They showed the results of their experiments at different ambient T in graphs [92].

Arcaklioğlu (2002) it was used by mixing in different proportions as double, triple, and quadruple. As a result, R290/R600a (56/44) with a 0.4% COP increase instead of R32/R134A (35.2/64.8) by weight [93]. Prove the low global warming potential of gas R32 and elaborate extensively on the advantages and disadvantages of this gas. Moreover, this gas has flammability, but it is better than most refrigerants consisting of hydrofluorocarbons, which have a high potential for global warming events. As they mentioned, one of the advantages of this gas is that it reduces both the operating energy of heating and cooling and by adhering to safety rules in the charging and unloading operations, dealing with the gas is safe even when it is used with other gases as a mixture [94]. Prove that mixtures of refrigerant gases can reduce the GWP, even if one of the mixture's components has GWP, depending on the proportion of those gases in the mix as declared by [95]. In developed countries, R404A was replaced by a mixture of R455A with R454C, as the COP value increased to 15 percent from what it was in the past. as informed in [96].

The refrigerant oil must be changed when replacing R22 refrigerant with mixtures containing R32 compound. The humidity is high for modern types of POE oils that are stable by chemical interaction with the coolant after developing these oils from older types of PAG as reported in [97]. The results of the research are summarized that in order to reach the best possible outcome for the refrigeration system, the search for

alternatives to the refrigerant medium must be continued, except if it is pure gas or a mixture consisting of several gases, in order to reduce the toxicity of the gas or mixture in addition to the environmental risks described in [98]. The system recorded the lowest energy consumption using two alternative gases for R404A. Both alternatives, R453A and R442A, had good results and were better than the old results with R404A at three fixed T for both the Cond and the Evap [99]. Hydrocarbon gases are shipped in a higher quantity inside the refrigeration system compared to R32 gas, which is 73 percent less than the internationally permissible limit for the potential for global warming, as it is widely used in Europe and America, and it is a good alternative to R410A. The laboratories, laboratories, and factories of developed countries, such as Japan, confirmed the replacement of the R22 refrigerant gas with a mixture or a pure gas from the R32 refrigerant by adding gas to the mixture or more to form the mixture [100].

Declared 750 as the maximum global warming potential value for any refrigerant according to the laws in force in the European Union, and it was also approved to work as an alternative to R410A gas for systems 3000 grams of refrigerant and recommended the use of R32 [101]. Confirmed use of an alternative mixture of R744 20% with R32 refrigerant 80% to replace R410A as declared by [102]. Adopt a maximum of 150 to the GWP of any gas or mixture that acts as a refrigerant by 2022 within the European Union as reported in [103].

For MCRS in our search there is not enough scientific and practical research to refer to refrigeration media unless it is composed of one gas or a mixture of several gases. Most researchers, companies, and laboratories in the fields of refrigeration and air conditioning are striving hard to find new refrigeration media that are better than the ones that exist now, except if they are pure gas or a mixture to reduce GWP, as is evident through the latest research papers recently published on this topic. Gas or mixture less likely to cause global warming was the target of our current research. A sealed reciprocating Comp was used to reach an Ejection line of P_2 for the refrigerant consisting of R600a by 10 percent and R32 by 90 percent. The Cond expels the heat gained from the system Q_H and subtracts it from the outside air at condensation T_c. In HPC, T_8 represents the entry T to HEX in the HPC, while LPC, which is the LPC,

takes a measurement of the outlet of the HEX T_3, and the difference between the two degrees ΔT has a significant impact on the system according to the laws of thermodynamics. The cooler T_8, the better the COP of the MCRS.

Table 2.1. Some results published in CRS of LPC and HPC

Refrigerant couples		**Information Studies**
LPC	HPC	
R23	R12, R22,	Cond T of HEX in CRS
R744	R404A	Cond T of HEX in CRS
R744	R290	Cond T of HEX in CRS
R744	R717	Cond T of HEX in CRS
R32	R407C	Cond T of HEX in CRS, cost, size
R32/R600a (90/10 by mass%)	R407C	Cond T of HEX in CRS, cost, size

Cooling pairs used during this research are show in the last two experiences.

PART 3

THEORETICAL BASICS OF COOLING AND COOLING SYSTEMS

3.1. INTRODUCTION TO THE DEFINITION OF COOLING

Refrigeration technology is constantly evolving and has become an integral part of life in today's environment. In refrigeration cycles, Moisture and heat are taken from the cooling space to the surroundings. Cooling is the transfer of warmth from one place to another and keeping the temperature in that place at a temperature below the ambient temperature.

3.2. COOLING METHODS

In this chapter; vapor compression cooling system, absorption cooling system, two-stage cooling system, and cascade cooling system will be briefly explained; Cascade cooling systems will be discussed in detail in the fourth chapter. Different cooling systems are used depending on the reasons. Commonly used cooling systems can be listed as follows: Vapor compression cooling system, absorption cooling system, two-stage cooling system, and CRS. The most common refrigeration cycle to use is the compression cycle, which the medium used for refrigeration alternately Evap and Cond and is Comp while in the vapor phase. Today, the material to be cooled, its amount, cooling place, desired T value, etc.

3.3. ABSORPTION COOLING CYCLE

The absorption circuit consists of the refrigerant separator, which performs the work of the Comp in the compression cycle, and the rest of the cycle parts are similar. An absorption chiller varies from other chillers and does not have a Comp. The cooling load is met by an Evap. Instead, it uses heat to generate cooling. Lithium Bromide is

more common. Conventional coolers are not used with absorption circuits in refrigeration. There is a pump to circulate the water in the cycle.

The water evaporates in the Evap as a result of its low P after leaving the expansion valve, and in the Cond the vapor is condensed into liquid after the heating process in the separating vessel to Sh the water from the salt.

3.4. STEAM COMPRESSED COOLING CYCLES

There are some differences in the materials that make up the cycle according to their purpose of use and shape, their basic principles are the same. It is used extensively in many areas such as food storage, industry, air conditioning, and laboratory environments. According to the II of thermodynamics, the transfer of heat from hot to cold space. Therefore, another name for vapor compression refrigeration cycles is "Heat Pump". Although vapor compression refrigeration cycles actually work with the same principle, they enable us to transfer heat from a low-temperature place to a high-temperature environment by taking advantage of the phase changes of the refrigerants. We can classify vapor compression refrigeration cycles under four main headings according to P-h, T-s diagrams, and designs. These; Single-stage vapor compression cycles, Double-stage vapor compression cycles [95].

3.4.1. Single-Stage Vapor Compression Cooling Cycles

It needs equipment when it wants to transfer heat from a cold place to a hotter place, according to what was stipulated in Law 2. The cycle shown in Figure 3.1 is the most basic form of the cycle pressure. A simple cycle pressure is displayed from Figure 3.1. Four components are the incorporating parts. Evap, Compr, Conde, expansion element are those components that must be present in all circuits.

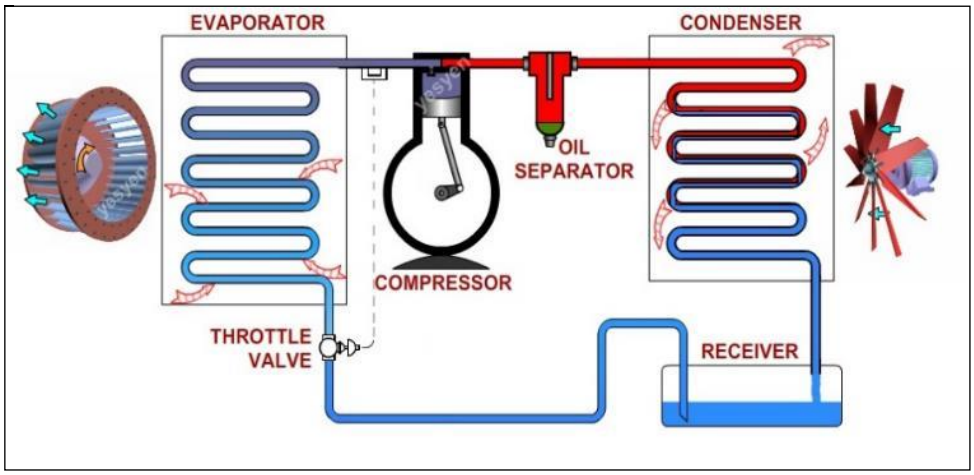

Figure 3.1. Simple single-stage diagram [121].

3.4.2. Two-Stage Cooling Systems

In compression, as the T gets too high when coming out of the Comp, the lubricating oil might burn and all parts of the Comp may wear out easily and become unusable in a short time. In compression, the T limit in the fumigation device changes between (-15°C) and (-25°C). Generally, it is desirable that the T that can be reached not greater than (100). For the desired lower T, CRS is preferred.

3.4.3. Cascade Cooling Cycle

CRSs are systems designed to obtain very low-slung evaporation T by combining two vapor compression refrigeration systems for cooling. CRS be a good choice when some specialized industrial applications, food storage, or special laboratory work require refrigeration at very low T. This may cause the Cond P to rise above the refrigerant critical point P, approach the solidification T of the refrigerant as a result of the Evap P being too low, or cause the Comp efficiency to drop too low and similar problems. In order to prevent this, CRS using two or more vapor compression cycles are made in applications where low T are required. Since heat is drawn from the environment during evaporation, the cooling process takes place [95]. The hot and high-pressure fluid coming from the Comp condenses by dissipating an external environment. It evaporates by taking heat at low P in the Evap, comes to the Cond after being conditioned with high P in the Comp. The liquid and high-pressure fluid

coming from the Cond is passed through a very small and narrow opening in the expansion element and evaporates with the effect of the P difference.

3.5. ELEMENTS, WHICH USE IN NORMAL HEAT PUMP CYCLES

(1) Sight glass: It is positioned between the expansion element and the Evap [98]. It is used to check whether there is moisture or liquid fluid in the fluid passing through the expansion element. (2) Dryer filter: It is positioned between the Cond and the expansion element. It is used to filter the water vapor and solid particles that may be in the refrigerant. (3) Oil separator: Since the amount of separated oil may be high in large-capacity systems, the oil is sent back to the Comp via a By-Pass line. In case the Comp oil is mixed with the refrigerant and transported, it ensures the separation of the oil from the fluid from the refrigerant. (4) Receiver: It is a liquid tank of the refrigerant reservoir. It is used to store the excess fluid that has become liquid in the Cond. (5) Accumulator (gas separator): It is a liquid separator from the vapor. It prevents the liquid fluid coming from the Evap from damaging the Comp.

3.6. IDEAL VAPOR COMPRESSION COOLING CYCLE

The important elements for forming the idea of compression circuits are an evaporation device, a P device, a condensing device, and an expansion device. It is not possible to have a real physical cycle without losses in P and T. In all components of a real refrigeration circuit, there is a decrease or increase in both T and P, and this includes pipes and other components.

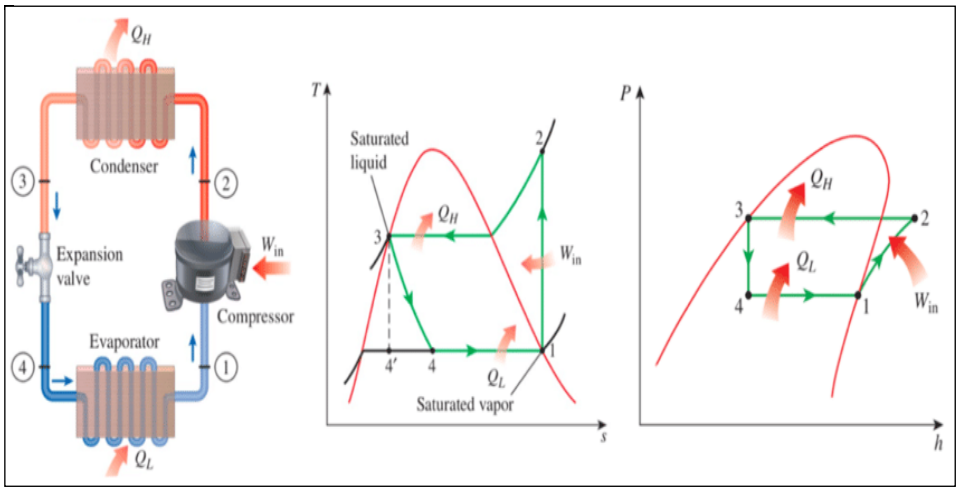

Figure 3.2. (P h) and (T S) diagrams [122].

At point (1), the lowest P in the system is equal to the evaporation P. At (2) the greatest P is equal to the condensation P. At point (3) it is a liquid with condensation P. At (4) it is saturated vapor at low Evap P, as shown in the figure 3.3.

3.7. WORKING PRINCIPLE AND THERMODYNAMIC INVESTIGATION

The refrigerant is at a T below the ambient T where it is located, and the refrigerant leaves the Evap as a satiate. The refrigerant in the high-pressure Cond condenses, and then throttles to a certain P as wet steam. The cycle is completed by condensing the refrigerant vapor in the Cond coming from the Comp.

3.8. PHASES OF THE CYCLE AS IN FIGURE 3.2

- 1 TO 2; The refrigerant gas is drawn at low P at (1) by the Comp, which raises its P to the condensing at (2).
- 2 TO 3; The hot gas at (2) turns into a liquid at (3) by the Cond.
- 3 TO 4; First throttling of the fluid (3) in the expansion element, then its expansion and P drop in (4).
- 4 TO 1; Heat is withdrawn by the refrigerant gas as a result of its p drop at (4) and its exit from the evap at (1).

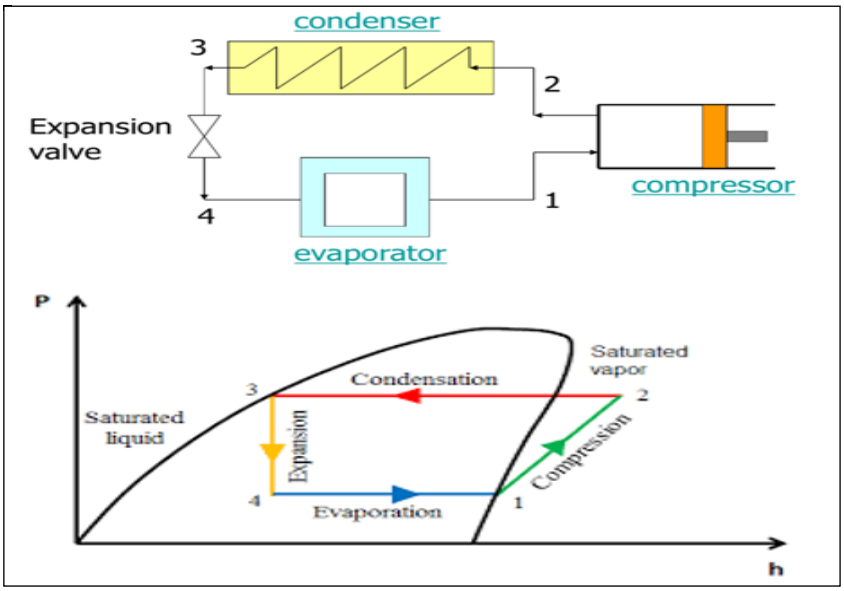

Figure 3.4. Ideal (P h) diagram [123].

P-h in Figure 3.3, it understand vapor compression refrigeration cycles is (pressure-enthalpy). The formulas are taken from the work titled “Thermodynamics with an Engineering Approach” by Yunus Ali Çengel and Michael Boles [95]. It can obtain the following formulations of calculations;

- Evap capacity by unit [kW];

$$Q_E = \dot{m}_R \ (h_1 - h_4) \tag{3.1}$$

$$Q_E = Q_C - W_{COM} \tag{3.2}$$

- Refrigerant mass flow rate ṁ by unit [kg/s];

$$\dot{m}_R = \frac{Q_E}{(h_1 - h_4)} = \frac{Q_C}{(h_2 - h_3)} = \frac{W_{COM}}{(h_1 - h_2)} \tag{3.3}$$

- Cond capacity: The heat released from the Cond by unit [Kw];

$$Q_C = \dot{m}_R \ (h_2 - h_3) \tag{3.4}$$

$$Q_C = Q_L + W_{COM} \tag{3.5}$$

Reversible adiabatic compression work, Comp work, system work by unit [Kw];

$$W_{1-2} = W_{COM} = \dot{m}_R \ (h_1 - h_2) \tag{3.6}$$

Basically, The heating or cooling performance in a cooling cycle is determined by the heating-cooling COP.

- Calculation COP without a unit of measure;

$$COP = \frac{Cooling\ load\ achieved}{Work\ consumed\ on\ the\ compressor} \tag{3.7}$$

Coefficient of Heating Effect of Comp work W_{COM} & Heat gained from an Evap Q_E & Heat lost by a Cond Q_C ;

$$COP_C = \frac{Q_E}{W_C} = \frac{h_1 - h_4}{h_2 - h_1} \tag{3.8}$$

Coefficient of Cooling Capacity;

$$COP_E = \frac{Q_C}{W_{COM}} = \frac{h_2 - h_3}{h_2 - h_1} \tag{3.9}$$

3.9. REAL VAPOR COMPRESSION REFRIGERATION CYCLE

The ideal cycle differs from the real cycle in P and heat losses. The two main sources of irreversibility are; friction coefficient and undesirable interchange with the external environment outside the Cond-Evap. These are mostly due to the irreversibility of the elements that make up the cycle.

The system should be designed has some heat vapor at the compressor. However, this condition cannot be fully fulfilled in practice because it is almost impossible to

precisely control the phase state of the fluid. Ideal cycle, the fluid leaving the gas enters the Comp as a saturated vapor. The purpose here is to prevent the fluid from going to the Comp [95].

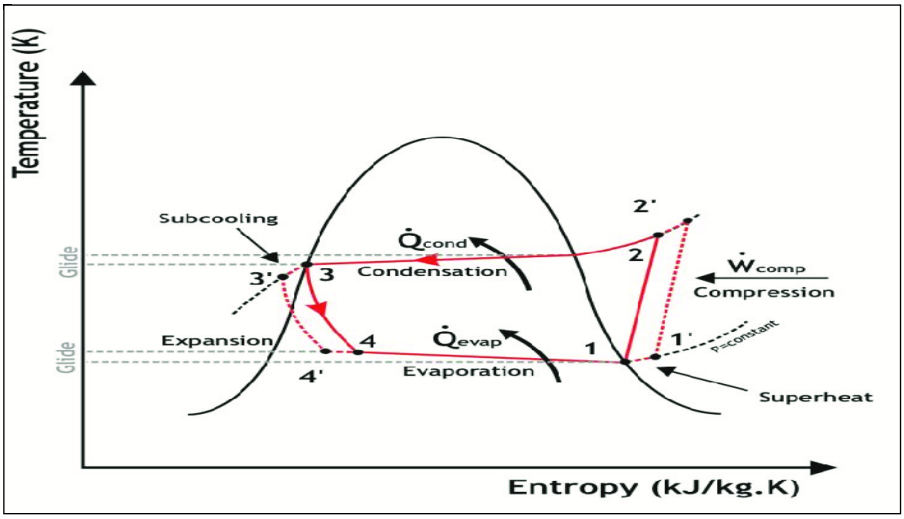

Figure 3.5. Real (T S) diagram [124].

During actual compression process, entropy of cooling medium may increase (1-2 process) or decrease (1-2' process), whichever is dominant. In the ideal cycle, it is isentropic. the compression process is internally reversible and adiabatic. In real compression, however, there is flow friction and heat transfer that affect entropy. It is sometimes more desirable for the compression to occur according to a 1-2' process rather than isentropic.

It is desired that the fluid be completely liquid before entering the expansion element. In the real cycle, there are P losses between the Comp outlet and the expansion element due to friction and T differences. Since the saturated liquid state is difficult to realize in practice, the exit state from the condenser is usually compressed liquid. In the ideal cycle, the outlet P fro condenser and the outlet P from Comp is the same in the saturated liquid state.

The most accurate results can be obtained with the values measured in the actual application of the cycle [95]. Therefore, calculated with ideal cycle formulas, tables, and graphs; Cycle values such as system efficiency, COP, Evap-Cond T, heat load,

and ideal Sh T differ in practice. Due to these factors occurring in practice in Figure 3.4.

3.10. CASCADE VAPOR COMPRESSION COOLING CYCLES

A simple CRS diagram is given in Figure 3.5. For this, in CRS, at least two flow, tube type, or plate type HEX must be used. Heat transfer between the two cycles is provided by a HEX. Because the thermodynamic properties and Comp of the fluids used in the low P environment and high P circuit are different. Fluids should never mix with each other. CRS used at low T are formed by the hybrid operation of two different refrigeration cycles.

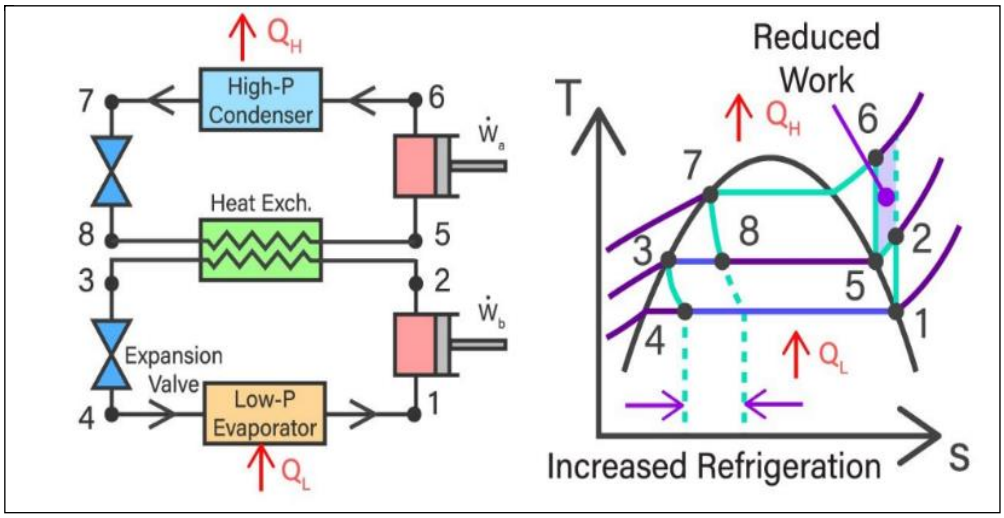

Figure 3.6. Cascade vapor compression refrigeration cycle diagram [125].

In CRS, cooling can be done at low T by working together with two cooling cycles at standard capacity and cost. On the other hand, larger Comp and more expensive materials must be used to cool at extremely low T of a one-stage cycle. In addition for its high cost, efficiency of cooling at very low T with single-stage systems will be lower and energy consumption will be higher. The most important factors in the use of CRS are cost and energy efficiency.

it enables two different systems to operate in an alternately and CRS manner [59]. In this way, the HEX works as an Evapr in the HPC, while it Cond in the LPC. One of the important and critical components of CRS is the HEX.

3.10.1. Working Principle of Cascade Vapor Compression Cycles

The HEX acts as an Evap in HPC and as a Cond in LPC. CRS is given in Figure 3.5. The connection of the LPC and HPC takes place with a HEX. Since the fluids do not mix with each other in the HEX, the gases in HPC and LPC do not have to be the same. Therefore, fluids with the best-desired properties can be used in each cycle. The process for LPC as; 1-2 with the Comp where the refrigerant gas is drawn from the Evap and compressed to the Cond The process 2-3 takes place in the Cond, where the hot gas coming from the Comp is condensed and converted into liquid in the HEX. The process is 3-4 expansion valve, which converts high P liquid into low P steam. And in the same way for the HPC.

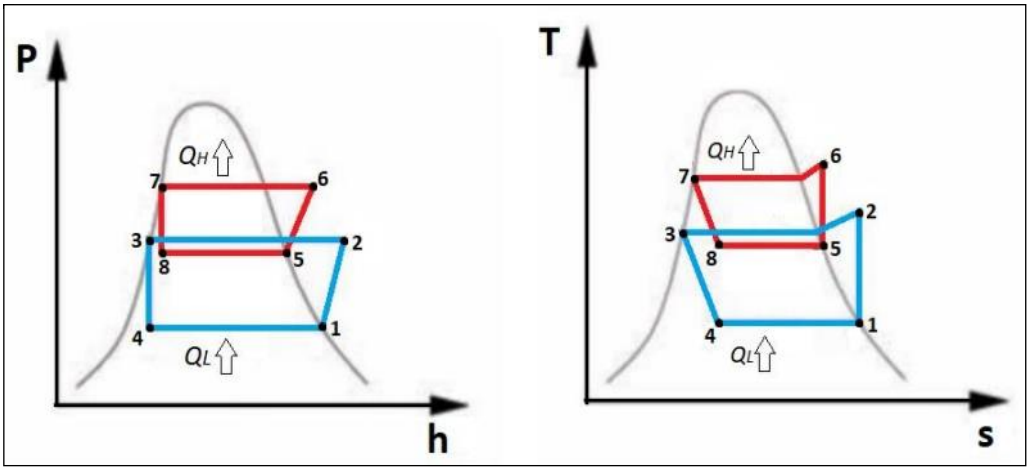

Figure 3.7. Cascade (P h) and (T S) diagrams.

3.10.2. Cascade Cycle Theoretical Calculations

- Ratio of CRS refrigerant flow rates:

$$\dot{m}_{LPC}\,(h_2 - h_3) \;= \dot{m}_{HPC}\,(h_5 - h_8) \tag{3.10}$$

$$\frac{\dot{m}_{HPC}}{\dot{m}_{LPC}} = \frac{h_2 - h_3}{h_5 - h_8} \quad (3.11)$$

- The efficiency coefficient of the CRS [95]. Wher $W_{COM.S}$ the total workload of the systeme for two Comp.

$$W_{COM.S} = W_{COM.LPC} + W_{COM.HPC} \quad (3.12)$$

$$COP = \frac{Q_L}{W_{COM.S}} = \frac{\dot{m}_{LPC}\,(h_1 - h_4)}{\dot{m}_{HPC}\,(h_6 - h_5) + \dot{m}_{LPC}\,(h_2 - h_1)} \quad (3.13)$$

$$COP = \frac{Q_L}{W_{COM.LPC} + W_{COM.HPC}} = \frac{Q_L}{W_{COM.S}} \quad (3.14)$$

3.11. SUPERHEAT

The process is called "Superheat" Sh, the evaporation is called "hot gas". Under normal atmospheric conditions, the water (H_2O) evaporates by boiling at 100°C, but if it can absorb some more heat before it evaporates, the steam temperature will be above 100°C; this steam is called Sh steam.

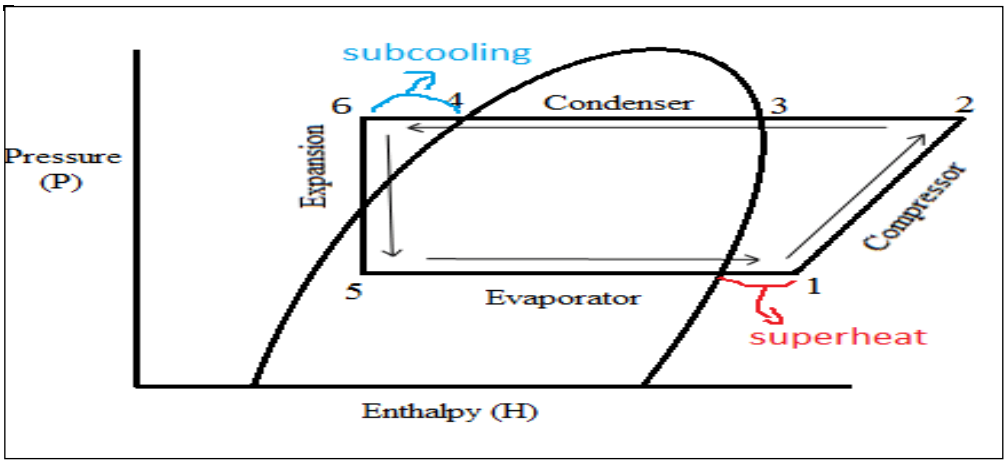

Figure 3.8. Demonstration of Superheat application on the (p h) diagram [126].

Sh values are very important for the system efficiency, as the Comp life, and determining the maximum capacity. Although the ideal Sh values differ from each other according to the cycle used, they vary between 3°C and 15°C [92]. It is not

desirable to always have high Sh values, as in Figure 3.7, the heat of the refrigerant increases due to Sh.

Thermostatic Expansion Valve (TEV), Automatic Expansion Valve (AEV), or Electronic Expansion Valve (EEV) is used to control the fluid passing through the Evap. The expansion element is of great importance here. Active Sh control cannot be provided in expansion elements such as capillary pipes that cannot be adjusted [101]. The degree of Sh is controlled by the flow of fluid passing through the Evap.

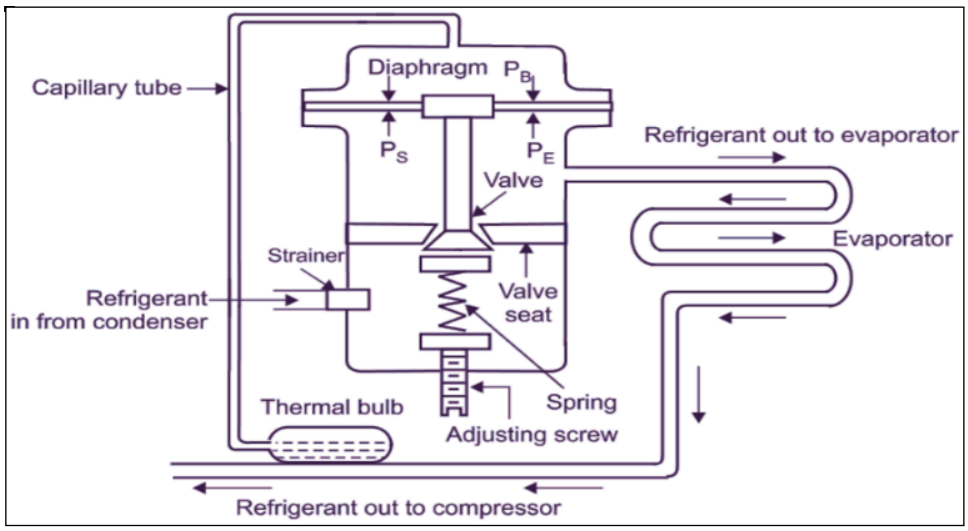

Figure 3.9. Working principle of the thermostatic EV [127].

As seen in Figure 3.8, it is a mechanical system and operates according to a predetermined constant Sh degree [104]. The thermostatic expansion valve regulates the fluid flow according to the Evap inlet-outlet T difference. In the automatic expansion valve, It is not a preferred expansion element because it cannot respond to T and load changes [107], the fluid flow is adjusted with the adjusting screw as in Figure 3.9.

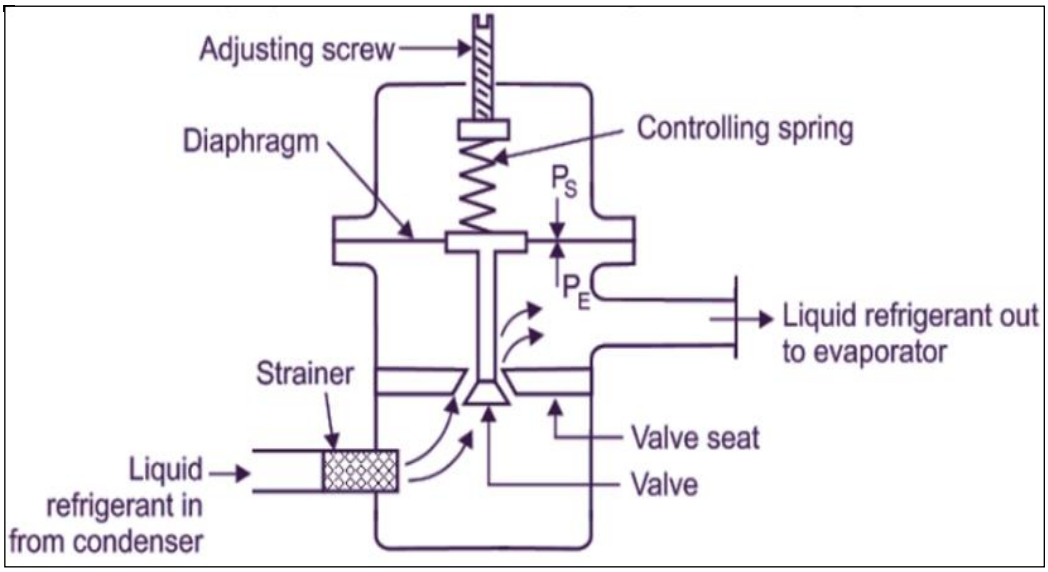

Figure 3.10. Automatic EV Working Principle [128].

Although there are different types of valves, the basic working principles are the same. An example electronic valve of Figure 3.10. It is considered to be the expansion elements that give the most correct reaction. The degree of Sh is instantly detected by the T difference corresponding to the measured T and the P value. A T sensor and a P sensor are located at the Evap outlet. Sh control is done by automatically adjusting the expansion valve opening. In electronic expansion valves, changes in Sh values can also be made [104], this way, faster and more accurate measurements are taken.

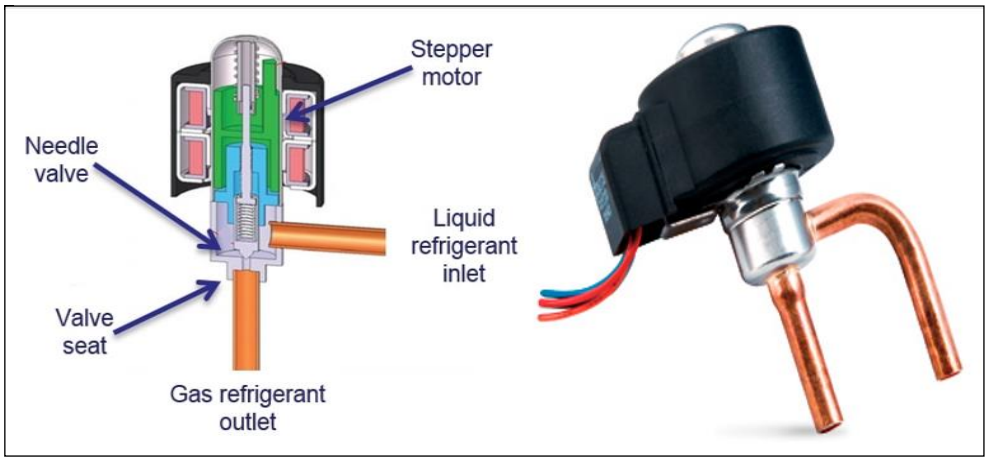

Figure 3.11. Electronic EV and section view [129].

3.12. REFRIGERANTS AND MIXTURES

Especially for vapor compression cycles, refrigerants, which are used as intermediate products in the transfer of heat from one environment to another in a refrigeration cycle, generally provide heat exchange by converting from liquid to vapor (refrigerant Evap circuit) and from vapor to liquid (refrigerant Cond circuit). Due to factors such as efficiency, thermodynamic properties, environmental factors, and human health, the search for alternative refrigerants has always continued [5]. Ether was used as the refrigerant in the first vapor compression cycle produced by J. Perkins in 1834, then in the following years, CO_2 and NH_3 gases started to be used. Today, even if there are fluids that provide these features, the search for alternative fluids continues fast to increase their performance values.

The basic properties sought for refrigerants are given in the following items; Especially for vapor compression cycles; Refrigerants, which are used as intermediate products in the transfer of heat from one environment to another in a refrigeration cycle, generally provide heat exchange by converting from liquid to vapor (refrigerant Evap circuit) and from vapor to liquid (refrigerant Cond circuit). The refrigerants used in this study were R32, and R600a in LPC and R407C in HPC. In order for refrigerants to fulfill their cooling function, they must have some physical and chemical properties. Various gases have been used in cooling systems until now. Some features of the cooler are more important depending on the operating condition and conditions, and in this case, other features can be ignored. The features required by the chiller vary depending on the application and operating conditions. The refrigerant cannot be reused in the cooling process and is discharged into the environment over time; It has caused the pollution of the natural environment, the increase of the greenhouse effect in the atmosphere, and the destruction of the ozone layer, which prevents harmful rays from the sun. These negative developments have initiated studies and research on new alternative refrigerants. The basic properties of refrigerants are as follows:

Its chemical structure should not deteriorate during the cycle. It should not be toxic. It should be environmentally friendly and harmless [92]. The fluid preferences in the refrigeration cycles used may differ from each other, where refrigerant selection is a

very important issue in a designed refrigeration cycle for gave the desired refrigerant properties. The main reasons for this can be as; Desired critical T values in the cycle (Condensation-evaporation) & Working P values & Usage areas (Home, Commercial or Industrial) & Cooling capacity & The size of the cycle & Environmental effects & Effects on human health & Safety and Cost. Refrigerants; When we consider the capacity, coefficient of cooling performance (COP), and performance factors, we see that gases such as R12 and R22 are quite efficient and have been used extensively in the industry for many years. However, such highly efficient and stable refrigerants cause serious environmental problems due to their chemical structure [112].

3.12.1. Environmental Effects of Refrigerants

The first used artificial refrigerants cannot be used for a long time in the process and are thrown into the environment; where causing environmental pollution, greenhouse effect, and depletion of the ozone layer. However, it also brought with them various environmental effects. After the Second World War, the use of artificial refrigerants became widespread. The ozone layer, also known as the Ozonosphere; is 30 km from the earth's surface. It is a gaseous layer that prevents ultraviolet rays from the Sun from reaching the earth and harming nature [38]. It is located above the atmosphere between the atmosphere and the stratosphere. The basis of the destruction of the ozone layer is the stability of Halon, CFC, and HCFC group gases, which makes them disadvantageous in their use. A free chlorine atom reacts with 100,000 ozone molecules and transforms it into an oxygen atom [112]. Figure 3.11 shows the reactions of ozone molecules and chlorine ions. O_3 (ozone) molecules that make up the ozone layer react with chlorine ions and turn into O_2 (oxygen) molecules. Since these gases are extremely difficult to decompose, they remain in the atmosphere for many years until they pass into the atmosphere.

It is these free chlorine ions that convert ozone molecules into oxygen molecules [81]. Because CFCs are extremely difficult to decompose. With the presence of intense ultraviolet solar radiation, the molecules are fragmented and as a result of this fragmentation, chlorine ions are released, at the root of the ozone depletion problem lies the inherent 'stability' property of the CFC. As a result of a study, the use of CFCs

in aerosol sprays was banned in the USA in 1978 [96], in 1974, M.J.Molina and F.S.Rowland conducted a study stating that the CFC has the ability to catalytically decompose ozone under high-frequency ultraviolet light and will erode the ozone layer by 7% in 60 years as in the Figure 3.12. below.

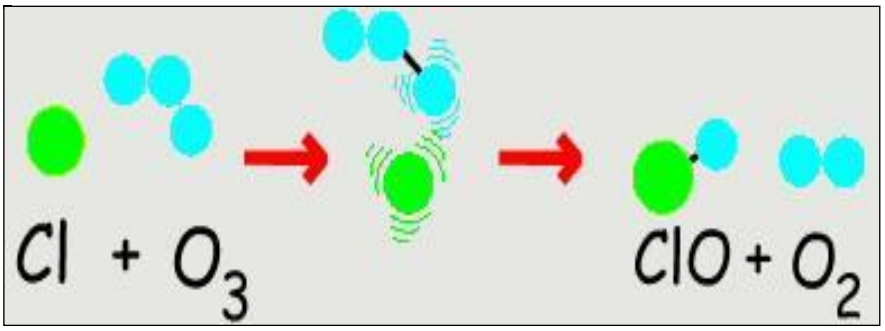

Figure 3.13. Reaction of chlorine molecules with ozone gas [130].

As a result of the increase in the greenhouse gas effect gases in the atmosphere, the T in the earth increases and leads to GWP [38]. Some of the reflected rays are trapped by gases with the greenhouse effect such as carbon dioxide, methane, and water vapor, causing the world to warm up. The world's warming occurs with the sun rays reflected from the Earth rather than the sun rays falling on it. On the other hand, the greenhouse effect is the T effect that occurs as a result of the sun's rays reflecting off the earth and not returning to space. The agreement was signed under the leadership of UNEP (United Nations Environment Program), for advisory purposes, the first attempt to maintain the ozone layer was the “Vienna Convention” signed in 1985. In 1987, among them; The “Montreal Protocol” was signed with the participation of 43 countries, including Turkey the USA, the USSR, European Union Countries, and Japan, according to this protocol, it was decided to completely abolish the use of gas that causes ozone destruction by 2000. In 1997, the "Kyoto Protocol" against greenhouse gas emissions was signed in Kyoto, Japan, with the participation of 161 countries [112]. However, the USA, which produces the highest greenhouse gas emissions, rejected the "Kyoto Agreement" accepted by all developed and developing countries because it contradicted its economic interests, unfortunately, this event remains current even in 2020.

3.12.2. Ozone Destruction Potential (ODP)

Although Chlorofluorocarbon (CFC) is a substance with high ODP values, Hydro chlorofluorocarbon (HCFC) have ozone depletion potential, but since this rate is very low, they are allowed to be used until 2030, provided that they are under control. The ozone depletion potential of a substance, which expresses the risk of damaging the ozone layer, is expressed with reference to the R11 molecule, which is considered ODP1 [99]. All refrigerants containing Chlorine (Cl) and Bromine (Br), which cause ozone layer destruction, cause ozone destruction at varying rates.

3.12.3. Global Warming Potential (GWP)

The GWP is calculated with reference to carbon dioxide (CO2), which is 1 GWP [99], wherein addition to ozone destruction, another harmful effect is the greenhouse effect. This value, which is defined as the Global Heating Effect, is also an important factor in the selection of the cooler. It is an indicator of the impact of greenhouse gas and planetary warming.

3.13. CLASSIFICATION OF REFRIGERANTS

Classification of refrigerants according to their chemical properties and their basic properties are presented in the following.

- Pure Refrıgerants: It is under two main headings organic and inorganic.

1) Inorganıc Refrıgerants: Refrigerants such as water vapor (H2O), carbon dioxide (CO_2), sulfur dioxide (SO_2), and ammonia (NH_3) are in this group of inorganic gases.

2) Organıc Refrıgerants:

a) Halon gases are the gases that cause the most ozone destruction. An example of this group is Halon1301 (R13b1) gas. Bromofluorocarbons (Halon) gases consisting of bromine, fluorine, and carbon atoms.

b) Chlorofluorocarbons (CFC): These are gases consisting of chlorine, fluorine, and carbon atoms, they are also known as Freon. CFCs, which have been used since 1930, started to be produced as an alternative to toxic refrigerants. They are quite safe as they are non-toxic and non-flammable. However, due to the chlorine atom in their structure, ozone destruction is the most common gas after holons. Examples of this group are the gases R11, and R12, the application flexibility, performance, and cheapness, and they have been widely used in a short time. Since their chemical structures are quite stable, they do not enter into chemical reactions much.

c) Hydrofluorocarbons (HCFC): Refrigerant gases consisting of hydrogen, fluorine, chlorine, and carbon atoms. It does not have as much chemical inertness as CFCs. R22 and R123 gases can be given as an example of this group. However, although their ozone destruction is low, they have a very high greenhouse effect. Therefore, since most HCFCs decompose before reaching the ozone layer, their ozone layer destruction is lower.

d) Hydrofluorocarbons (HFC): They have a lower greenhouse gas effect than HCFCs. Examples of this group are R134a, R23, R143, and R152a gases. These are gases consisting of hydrogen, fluorine, and carbon atoms. Since they do not contain chlorine atoms in their structure, they do not cause any damage to the ozone layer.

- B) MIXED REFRIGERANTS

With these mixtures, it is aimed to reduce the negative properties of the refrigerants and bring the desired effect to the fore. They are refrigerants that are formed as a result of mixing pure refrigerants with different combinations and ratios. There are many types of refrigerants with mixed gases. Some of them are experimental and some of them are successful in the commercial field. Many types of refrigerants have existed since the use of the first vapor compression cycle. Basically, we can classify them under two main headings.

1) **Zeotropic mixtures:** Gases of this type do not have a fixed boiling and condensing temperature. R401A (53% R22, 13% R152a, 34% R124) gas can be

given as an example of this type of mixture. Other than the systems developed based on these features, usage areas are not very common. The saturated liquid and saturated vapor phases of the gases forming these mixtures differ from each other in thermodynamic equilibrium. Such mixtures show temperature shifts during phase change.

2) **Azeotropic mixtures:** Gases such as R404A and R407C can be given as examples of this type of gas [112]. Such mixtures behave like a single fluid during phase change. Its components are in thermodynamic equilibrium in the saturated liquid and saturated vapor phases. For this reason, the most environmentally friendly and most widely used refrigerants are included in this class. In addition, these mixtures have the beneficial properties of their pure components and have their own thermodynamic equilibrium conditions.

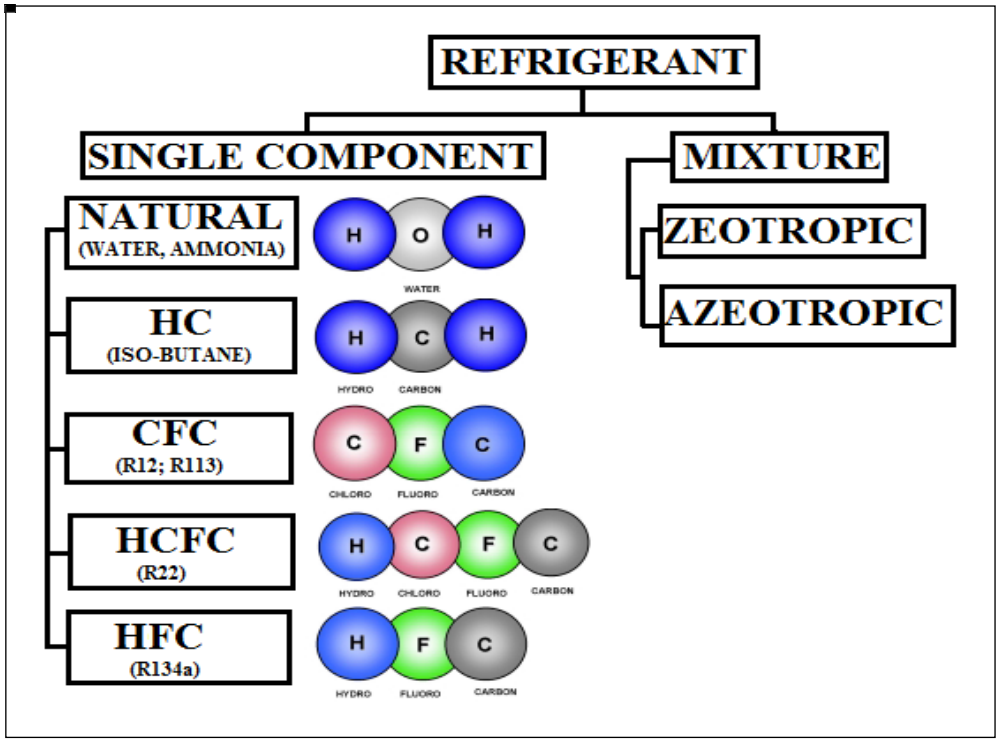

Figure 3.14. Hierarchical classification of refrigerants [131].

Some refrigerants, that have achieved commercial success, and have had and continue to be in widespread use are given below:

- **R717:** Also known as Ammonia (NH3). It is a colorless and foul-smelling gas. It has been used in various fields since ancient Egypt. It has been used as a refrigerant since 1878. It does not burn easily, but it burns when certain conditions are met and can cause violent explosions by mixing with air. A small amount of adjustment and control is difficult. Not suitable for small cooling loads. Therefore, it is widely used in absorption cooling machines due to its easy separation from water when heated. It dissolves easily in water and when it melts, its freezing point is lowered.
- **R744:** (CO2) Since it is abundant in nature, its cost is very low. It has been used as a refrigerant since 1870. Refrigeration cycles using CO2 have always been open to improvement, as they do not have ozone destruction, have a very low greenhouse effect, are not toxic-explosive-combustible, and are cost-effective. However, due to the low coefficient of cooling effect and high operating pressures, it has left its place to halocarbon refrigerants over time.
- **R11:** It is in the CFC group, it is non-flammable and odorless [116]. Production has been stopped due to ozone destruction. (CCl3F) It is a low-pressure chiller and is generally used in large capacity industrial water cooling units.
- **R12:** It is in the CFC group. It has a low operating cost and high efficiency. It has started to be used as an alternative to ammonia and carbon dioxide, but its use and production have been stopped due to its high destruction of the ozone layer [110]. It is heavier than air, colorless, and odorless. Since it can be easily mixed with oil, there is no obligation to use an oil separator in the system. However, (CFCl2) was the most widely used refrigerant in the industry.
- **R125:** HFC group is a refrigerant. (CF3CHF2). There is no ozone layer destruction. However, the greenhouse gas effect is quite high [116]. It is not flammable and non-toxic. It has been accepted as an alternative for R502 and R22 gases.
- **R134a:** It is an HFC group refrigerant. It is suitable for domestic and commercial use. It is one of the most widely used refrigerants today. (CF2CH2F) It is the closest refrigerant to R12.
- **R404A:** It is widely used in the home, commercial and industrial areas. There is no ozone destruction [116].

3.14. REFRIGERANTS WERE USED IN THE EXPERIMENT SYSTEM

R600a: It is suitable for air conditioning industries and is called C_4H_{10}. It is also used in most refrigeration systems, due to its purity, which reaches 99.5%. It has a small global warming potential of zero to deplete the ozone layer.

Figure 3.15. R600a was used in MCRS [132].

R32: HFC group is a refrigerant. It has been produced with the studies carried out that can be used alone and without loss of efficiency compared to its successors [110]. It does not have ozone destruction and the greenhouse effect is quite low, R32 has only about 1/3 the GWP of R410A. R32 is a gas whose chemical name is called “difluoromethane”. Currently, R410A is the most widely used refrigerant in developed countries.

Figure 3.16. R32 was used in MCRS [133].

R407C: There is no ozone destruction, Different concentrations are also sold according to the manufacturers. It consists of R32, R125, and R134a, which is considered an alternative to R502. R407C is mainly used in commercial and residential air conditioning systems and has very similar properties to R22. R407C It was used as an alternative to R22 in new refrigerant equipment.

Figure 3.17. R407C refrigerant was used in MCRS [134].

Table 3.1. Physical and thermodynamic properties of substances used as refrigerants in the search [104, 107, 111].

Refrigerant	**R407C**	**R32**	**R600a**	**R32/R600a (90/10%)**
ODP	0	0	0	0
GWP	1774	675	3	583
Molecular weight (kg/mol)	86	52	58,13	52,6
Boiling point (1 bar °C)	-44	-52	-11,7	-47.9
Critical Heat (°C)	86	78	135	84.33
Critical P (bar)	46	54	3,65	52.06
Alternative to Gas	R22	R410A		
Chemical Composition	R32 23%, R125 25%, R134a 52%	CH2F2	C4H10	R32/R600a (90/10%)
Safety level	A1	A2	A3	

PART 4

MATERIAL AND METHOD

4.1. CASCADE COOLING CYCLE

With the population increase, the cooling requirements increase dramatically and on a large scale, especially with regard to systems that operate at very low T, as in the field of medicine and laboratories, especially if they have an operating cost that is not of high value. T below -30°C require large Comp if one refrigeration cycle is used, so the use of Comp consisting of two cycles has spread to reach the required degree at the lowest costs. In addition to that, the use of CRS assemblies has become in all types of industries, as it reaches the degrees required to work in different sizes to suit the required work at normal condensing T. With this, the demand for these products increased in the field of medicine and food marketing. Where the CRS consists of two cycles a HPC and a LPC. In the selection of refrigerant gas, along with refrigerant properties. In CRS, Performance is greatly affected by the type of compound used in the cooling cycle separately. The HEX is an Evap for (R407C) in first stage HPC and the Cond of the second stage LPC (R32, R600a). Two-stage refrigeration cycles using R32, R600a, and R407C as refrigerants are shown.

The energy consumed in the two-stage CRS (R407C/ R32+R600a) is given in Figure 4.1 above. QE as equation below.

$$\mathrm{QE} = \frac{Q_{Evap\ 2}}{Q_{Comp\ 1} + Q_{Comp\ 2} + Q_{Evap\ Fanı} + Q_{Cond\ Fan2}} \tag{4.1}$$

4.2. CASCADE WORKING PRINCIPLE

In CRS, 2 independent cooling cycles are combined, although the HEX, titled the Evap-Cond, where it is condensed for LPC, throws the heat to the fluid in HPC. The

Cond of HPC is cooled to the ambient air, similar to conventional vapor compression units. Thus, the Evap-Cond works as an Evap for HPC and a Cond for LPC at a some P, and T. In each cycle of CRS, a diverse compound is used which is most suitable for the wanted. In request to balance for 2 circuits, the heat dissipated by the lower stage has to be absorbed by the higher stage. The cooling low P is attained in the Evap of LPC.

The coefficient of CRS at COP, is defined as the ratio of the cooling result generated in the Evap to the total work input of 2 Comp. If the kinetic and potential energies are neglected and the HEX is well insulated, the heat given by the LPC fluid in the HEX will be equal to the heat engrossed by HPC fluid. The assembly of the 2 loops in CRS is made by means of HEX that acts as HPC Evap and LPC Cond.

4.3. DESCRIPTION OF (P H) AND (T S) DIAGRAMS

The highest simulation values were determined for low condensation 15°C and high condensation 45°C while for low evaporation -50°C and high evaporation 5°C. The P-h for CRS in Figure 4.1. which LPC of R32. Here, R407C is used in HPC. CRS using R407C / R32 refrigerant couple is given.

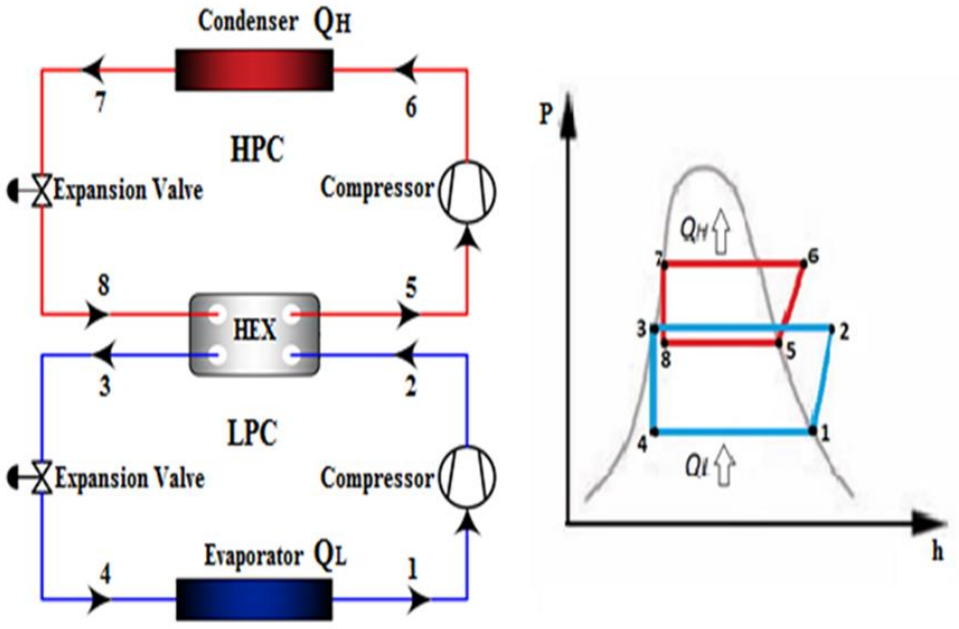

Figure 4.1. P-h diagram.

Under low P from point 4 to point 1 evaporation process, 3 to 4 expansion process, 3 to 2 densification process and 4 to 1 compression process. While R407C is used in the 1st stage, R32 is used in the 2nd stage. For the 1st stage; (5-6) compression in the Comp, (6-7) condensation, (7-8) EEV, and (8-5) evaporation. CRS be made up of two cycles.

4.4. THERMODYNAMIC CALCULATIONS

The calculations made are shown step by step below. Since the CRS works with two different fluids, first the thermodynamic properties of the refrigerant R407C were calculated. Comp, Cond, and Evap capacities are calculated on the (Refprop) program. While conducting the thermodynamic analysis of the R407C/R32 MCRS, as following:

Cond T is taken as 45°C, the Evap ability is accepted in place of 1000 W, and the Evap T was taken as -50°C. While performing these analyses, P losses between system elements, heat transfer from the Comp, EEV, and pipelines to the surrounding environment, and changes in internal energy during the flow of the refrigerant have been neglected, and it has been assumed that the MCRS elements operate according to the steady regime.

4.5. EXPERIMENT SETUP AND MATERIAL

In this section, the cycle elements that make up the experimental setup and their properties are shown. The cycle which is given in Figure 4.1, and the views of the manufactured experimental are given in Figures 4.1, and Figure 4.2. It is aimed to make the experimental setup more controlled by using auxiliary conversion elements and electronic expansion valves, which were previously described in Section 3.1.1. In this study, a MCRS using R32/R407C, and 90%R32+10%600a/R407C refrigerant pairs were studied. The leakage test of the experimental of MCRS, low P lines, and insulation of the room where the cooling will take place, and the refrigerant were transferred to the MCRS. Figure 4.1, shows MCRS and its components, Figure 4.3. displays the experimental and the place to be cooled.

Figure 4.2. Top view of the MCRS.

The experimental setup and cycle elements are shown in Figure 4.2 are given in Tables 4.1 and 4.2.

Table 4.1. Empirical control and intervention equipment.

I	**LPC refrigerant service connection**
II	LPC EEV
III	HPC EEV
IV	HPC refrigerant service connection
V	LPC cold room Sh control unit
VI	HPC cold room Sh control unit

Table 4.2. Cycle elements used in the experimental setup.

	Low Pressure Cycle (LPC)		**High Pressure Cycle (HPC)**
1	R32 Comp	13,14	R407C Comp and accumulator
2	EGV P sensor	15	Cond
3	EGV T sensor	16	Liquid tank
4	Plate HEX (Cond)	17	Dryer filter
5	Liquid tank	18	Sight glass
6	Dryer filter	19	High P manometer
7	Sight glass	20	EEV of HPC
8	High P manometer	21	Plate HEX (Evap)
9	EEV of LPC	22	EGV T sensor
10	Cooling cabinet	23	EGV P sensor
11	Accumulator (liquid trap)	24	Low P manometer
12	Low P manometer		

Figure 4.3. View of the cold room.

4.5.1. HPC Elements

Since the Comp used in the HPC is a self-accumulator, an extra accumulator is not used in the HPC. The image and label technical features of the HPC compressor are shown in Figure 4.4, and Table 4.3, has also been given.

Figure 4.4. HPC R407C Comp.

Table 4.3. HPC Comp specifications.

Marca - Model	**Panasonic Matsushita - 4PS164**
Comp Type	Rotary Comp (Constant peed)
Comp Power	1.5 h_p
Electrical Supply	50 Hz and 220 V
Cooler liquid	R407C
Suction Line	0.25”
Compression Line	3/8”

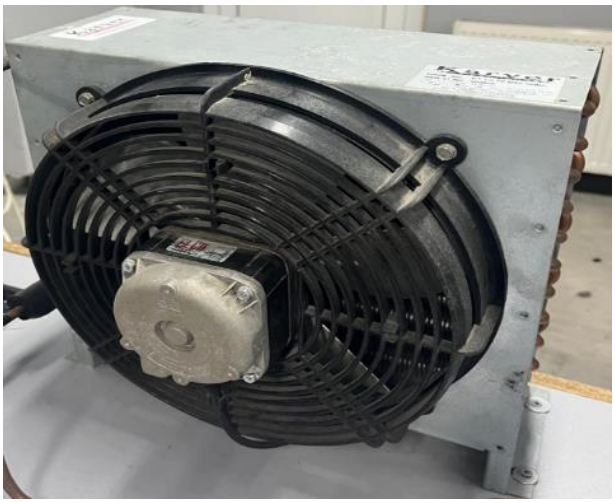

Figure 4.5. HPC Cond.

The appearance and label technical features of the air-cooled Cond used in the MCRS are in Figure 4.5, and Table 4.4.

Table 4.4. HPC Cond specifications.

Brand - Model	**Karyer - KT 1/2 HP DAV**
Cond Type	Electric Fan Hood Condenser
Surface area	1,9 m²
Material	Aluminum blades with Copper tubes
Fan Motor	65 W and 220 V
Fan Flow	500 m³/h

The appearance of the liquid tank used and the technical specifications of the label are given in Figure 4.6 and Table 4.5.

Figure 4.6. Liquid tank.

Table 4.5. Liquid tank features.

Brand - Model	**Erdem Cooling – ESSLR 01 Vertical**
Reservoir Capacity	1.2 L
Connection Diameter	0.5”
Maximum Working P	32 bar

Figure 4.7. Dryer filter.

The appearance of the drier filter used in the cycle is shown in Figure 4.7, and the label technical features are shown in Table 4.6.

Table 4.6. Drayer filter features.

Brand - Model	Erdem Cooling – ESSD
Filtration	20 micron
Connection Diameter	0.5”
Maximum Working P	45 bar

The view of the sight glass positioned before the entrance of the expansion element is given in Figure 4.8, and the features of the label in Table 4.7.

Figure 4.8. Sight glass.

Table 4.7. Sight glass features.

Brand - Model	SANHUA / SYJ-A00060
Connection Diameter	3/8”
Maximum Working P	45 bar

The appearance and label properties of analog manometers used for control purposes in the P gauge are given in Figure 4.9, and Table 4.8.

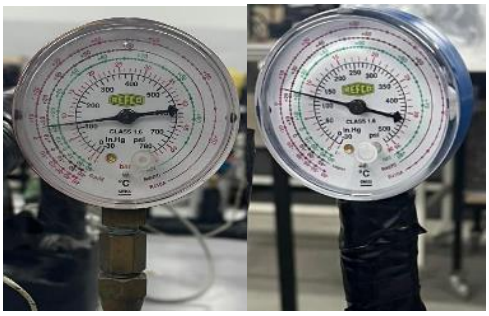

Figure 4.9. Low and high P manometers.

Table 4.8. Low and high P manometer features.

	Low P Manometer	**High P Manometer**
Brand	Refco	Refco
Operating P	-1/36 bar	-1/54 bar

EEV are used in both cycles and their specifications are given in Section 4.4.1. MCRS plate HEX acts as the Evapo of HPC. (Section 4.1.2)

4.5.2. MCRS HEAT EXCHANGER PLATE (HEX)

Although it is not possible to make a precise capacity calculation for the HEX used in MCRS, the most appropriate capacity selection can be determined experimentally. This is because the enthalpy of the refrigerant in both systems is not constant. Since heat transfer is desired between 2 different gases used in MCRS, the Ekin Industrial / Mit MB-01 brand plate HEX was used.

Figure 4.10. HEX Before and After thermal insulation.

Since high P differences will occur in HEX used in MCRS, a HEX with high P resistance was used instead of standard plate HEX as in Figure 4.10. The features of the HEX used in MCRS are given in Table 4.9. The refrigerant media flows between many channels sequentially between the parallel plates inside HEX to accumulate the largest area for HEX between the two circuits. Liquids and gases pass after entering through the openings in the corners of HEX and exit from another opening corresponding to it. HEX is in constant contact with the cold medium on the one hand and in constant contact with the hot medium on the other hand [102].

Table 4.9. Technical characteristics of the plate HEX of MCRS.

Brand - Model	**Ekin Industrial / Myth MB-01**
Number of Plates	28
Surface area	(n-2)*0,012 m² = 0,312 m² (n: number of plates)
Material (plate)	AISI 316L
Solder	Copper
Max. Operating P	45 bar
Stream Type	cross flow
Channel Pattern	H
Dimensions	192*76*73 mm

Since the amount of fluid passing through the HEX will be relatively less than in water MCRS, a high turbulent and cross-pass (H pattern) HEX has been chosen. In this way, it is aimed that the fluid can transfer more heat in the HEX without bypassing it. (H) type plates can increase P loss due to the high turbulence they create. However, it is aimed to increase the amount of heat transfer with turbulence in low flow systems. Since the P loss of low flow system is less than high flow system, turbulence formation is more preferred [118].

4.6. LOW PRESSURE CYCLE ELEMENTS

The images and technical specifications of the LPC elements given in Table 4.1 are given in the figures and tables below. The appearance and label specifications of the LPC Comp is in Figure 4.11, and Table 4.10.

Figure 4.11. Low T (R404A) circuit Comp.

Table 4.10. LPC Comp specifications.

Brand - Model	**Embraco Aspera -NEK 2134 GK**
Comp Type	Hermatik
Comp Power	0.5 h_p
Electrical Supply	220 V, 50 Hz
Cooler liquid	R32, R600a
Suction Line	0.25 ”
Compression Line	0.25 ”

HEX plate performs the Cond function of the LPC. Technical information on the HEX is given in Section 4.1.2.

Used in the HPC; The liquid tank, dryer filter, sight glass, electronic EEV, and manometers were also used in the LPC in accordance with the R404A fluid. Information about the auxiliary elements used in the cycle was previously discussed in section 4.1.1, has also been given.

Table 4.11. MCRS cooling cabinet technical specifications.

Cabinet Type	**Industrial type stainless steel cooling cabinet**
Cabinet interior volume	320 lt
Cabinet Dimensions	70*74*70 cm
Evap Type	Fan blown drip pan
Evap Surface Area	1.25 m^2
Evap Material	Copper tubes with aluminum strips attached inside a stainless steel frame
Fan Motor	20 Watt -220 Volt AC
Fan Flow	100 m^3/h

Figure 4.12. LPC fluid trap (accumulator).

The appearance of the accumulator positioned between the LPC refrigerator and its Comp is given in Figure 4.12, and the information of ıt are given in Table 4.12.

Table 4.12. LPC fluid trap (accumulator) technical specifications.

Brand - Model	**Gokceler Cooling / LTAG 6-28**
Tank Capacity	1.2 lt
Connection Diameter	28 mm
Maximum Working P	38 bar

4.7. THEORETICAL CALCULATIONS OF THE EXPERIMENT CYCLE AND APPLICATION OF EXPEIMENTS

Pairs consisting of R32/R407C and 90%R32+10%R600a/R407C refrigerants or mixtures, respectively, were used in the MCRS. In this investigation; In CRS, R407C refrigerant is used in the HPC, and 90%R32+10%R600a refrigerants are used in LPC. As a result for the studies, the amount of gas to be mixed and experimental studies were started, respectively.

For the analysis, the "Collpack 1.49" version, which has the MCRS cycle analysis feature, was used. The input parameters used in the program are given in Table 4.13. Before the experimental setup was designed, theoretical analyzes of the MCRS were made. The EES program was used for these analyses. Refprop is an excel-based analysis program.

Table 4.13. Values are entered into the Refprop program for calculations.

Parameters	**Values**
$\boldsymbol{Q_{R404a,Evap.}}$	1,0 kW
$\boldsymbol{W_{R404a,Komp.}}$	0,426 kW
LPC R32 evaporation T	-50 °C
LPC R32 condensing T	15 °C
LPC Comp isentropic efficiency	0,8
LPC Sh T	4 °C
LPC Sc T	4 °C
HPC R407c evaporation T	5 °C
HPC R407c condensing T	45 °C
HPC Comp isentropic efficiency	0,8
HPC Sh T	4 °C
HPC Sc T	4 °C

The equations used by the program in the thermodynamic analysis of the MCRS are given below;

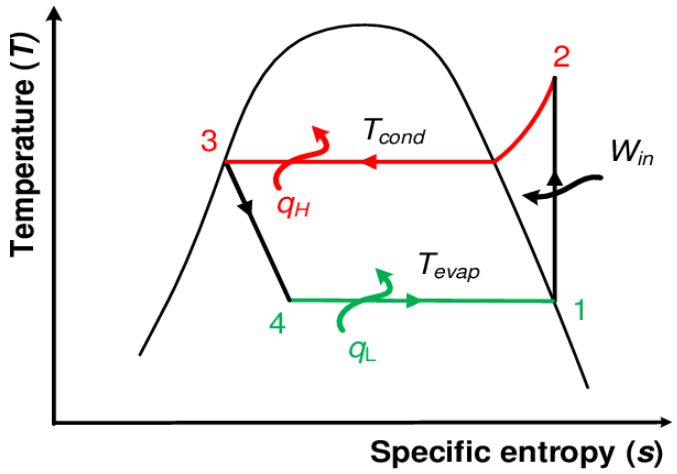

Figure 4.13. T-s diagram [124].

In the exergy and entropy calculations, the ambient (ambient) T (T_0) was accepted as 25°C (298 K), (T_F) the place to be cooled, (T_{cond}) Cond surface and (T_{Evap}) Evap surface T. Using the mass and energy conservation for a CRS, in next equations:

$$\dot{m}_1 = \dot{m}_2 = \dot{m}_3 = \dot{m}_4 = \dot{m}_A \quad (4.1)$$

$$\dot{m}_5 = \dot{m}_6 = \dot{m}_7 = \dot{m}_8 = \dot{m}_B \quad (4.2)$$

- Comp capacities;

$$W_{COMP,R32} = \dot{m}_{R32} \times (h_2 - h_1) \quad (4.3)$$

$$W_{COMP,R407c} = \dot{m}_{R407c} \times (h_6 - h_5) \quad (4.4)$$

$$h_3 = h_4 \quad (4.5)$$

$$h_7 = h_8 \quad (4.6)$$

- Cond capacity calculation;

$$Q_{COND,R32} = \dot{m}_{R32} \times (h_2 - h_3) \quad (4.7)$$

$$Q_{COND,R407c} = \dot{m}_{R407c} \times (h_6 - h_7) \quad (4.8)$$

- Evap capacity calculation;

$$Q_{EVAP,R32} = \dot{m}_{R32} \times (h_1 - h_4) \quad (4.9)$$

$$Q_{EVAP,R407c} = \dot{m}_{R407c} \times (h_5 - h_8) \quad (4.10)$$

- Cooling coefficient of efficiency;

$$COP_{R32} = \frac{Q_{EVAP,R32}}{W_{COMP,R32}} \quad (4.11)$$

$$COP_{R407c} = \frac{Q_{EVAP,R407c}}{W_{COMP,R407c}} \quad (4.12)$$

- Plate HEX calculation;

$$\dot{m}_3 = \dot{m}_4 \quad (4.13)$$

$$\dot{m}_5 = \dot{m}_6 \quad (4.14)$$

$$\dot{m}_3 \times (h_3 - h_2) = \dot{m}_5 \times (h_5 - h_8) \quad (4.15)$$

$$m_L \times Q_L = m_H \times Q_H \quad (4.16)$$

COP is the efficiency of CRS, and Q_E is the amount of enthalpy taken up by the Evap from the refrigerant compartment in LPC, W_{CA} and W_{CB} the energy consumed by the Comp HPC and LPC, respectively.

$$COP = \frac{Q_E}{W_{CA} + W_{CB}} \quad (4.17)$$

System Second Law Efficiency:

$$W_{izentropik} = Q_E \ ((T_0 / T_B) - 1) \quad (4.18)$$

$$W_{INPUT} = W_{KA} + W_{KB} \quad (4.19)$$

$$\eta_{II} = W_{izentropik} / W_{INPUT} \quad (4.20)$$

4.8. MANUFACTURING OF THE MCRS

On the left side of the platform, the voltage converters from 220 to 24 are located, which are necessary to operate the EEV control device, switches on and off the two cycles of high and low P, along with switches for operating the control devices, as seen in Figure 4.22. The only refrigeration compartment room is located under the installation table, and its parts are still located on the table . A wheeled workbench was used during manufacturing in order to carry the designed MCRS easily.

Figure 4.14. The experimental setup.

In the MCRS with copper piping, loop element fixings were made before welding. Then, all welding processes in the MCRS setup were completed using oxy-acetylene

welding and silver-copper solders. For leak test, manometers and service manifold P values on the assembly were checked and foam test was applied to all welding points. Leak tests were performed before gas filling to the MCRS with welded connections (Figure 4.23). After the P tests, the cycles were pulled to +1 bar P with a vacuum pump, and the MCRS was cleaned as much as possible by making a vacuum at this P for another 30 minutes. For the leak test, both cycles were first increased to 15 bar P and kept under P for a minimum of 1 day. After successfully passing these tests, the cycles were kept in a vacuum of -1 bar for at least 1 day, gradually refrigerant charges were made and an ideal gas charge was tried to be achieved.

Figure 4.15. Vacuum test and gas charge to the MCRS.

4.9. MEASUREMENT AND RECORDING OF MCRS DATA

The measurements taken were transferred to excel format and arranged and their graphics were created. T measurements were taken from multiple points with the Thermocouple-Data logger. While EEV equipment acts as a control mechanism, it also makes MCRS measurements. An electronic meter was used for electrical measurements. Various equipment was used to measure the MCRS data.

4.9.1. EEV and Control Unit

EEV is controlled by Emerson's EC2 unit. Emerson's EC2 control unit is used in conjunction and the EX2 valve is powered by a 24V AC. These valves can provide very precise T control. In the MCRS; Pulse width modulated EEV with replaceable orifices for two EX2 cold rooms are applied. Once Emerson's EC2 controller is set up and running, it is only necessary to plug in the Ethernet cable and type the default IP address into the web browser. It will automatically display the watch page. There is also the function of storing the data on a PC for later graphical visualization. MCRS in both cycles of the MCRS as in Figure 4.24.

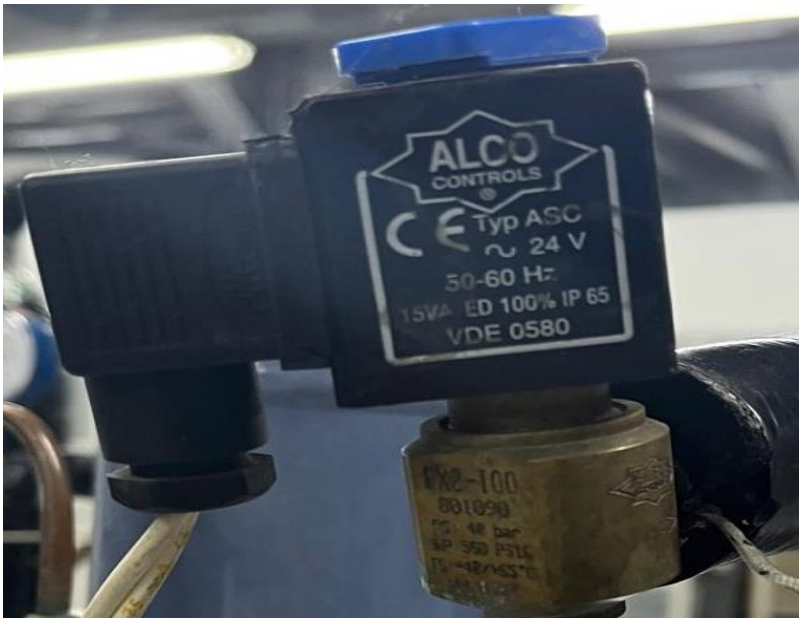

Figure 4.16. EEV.

Table 4.14. EEV features.

Brand - Model	Alco Controls / EX2-I00
electricity supply	120 V, 50-60 Hz
Pipe inlet-outlet diameters	3/8 ” - ½ ”
Electrical Supply	220 V, 50-60 Hz
Highest P	40 bar

The cooling medium incoming the EEV at high T and P then from it comes out low T and P values.

In EEV, one end consisting of copper pipe is mounted on the line at the Evap outlet, and the T is requested to be sensed, and thus the amount of refrigerant that will enter the Evap is adjusted by inside the EEV in the MCRS. EEV adjust the flow rate to the Evap according to the T of the fluid at the outlet of the Evap. Comp; The low P absorbs this evaporated refrigerant with slightly Sh vapor at low T then compresses it into a minor volume, causing it to become steam. It is clear to look at MCRS; It can see that its main elements are Evap, Comp, Cond, and EEV. Evap; It collects all the unwanted heat from the environment and transfers it to the cooler, this results in evaporation and boiling of the refrigerant.

EEV is therefore often found in senior MCRS, and a MCRS that require precise control. Also, the same valve can be used for different refrigerants after reprogramming. EEV is controlled by fever or compression devices. The use of EEV is increasing day by day and today the technology is developing gradually and has developed to meet the demands of the desired products. However, the cost of EEV is much advanced than a simple EEV valve. A T sensor is connected to the Evap outlet pipe to measure T. After the sensor measuring the P of the refrigerant is connected to the same line. Sh is the difference between the equivalent T of the measured P relative to the cooler and the measured T of the cooler. EEV control is performed by bringing the Sh value to the desired value. In command to rise the proficiency of the request or the chilling system, avoid unnecessary refrigerant charges, protect the life of the Comp, and make optimum use of the Evap, the desired Sh value is selected according to the characteristics of the MCRS. Sh is a value calculated using 2 sensors attached to the Evap outlet.

The device with the brand code Emerson EC2-352 given in Figure 4.25, also has to defrost, Comp control, and fan control features. A cold room control device was used in each cycle for the control of Sh values and the EEV in the MCRS.

Figure 4.17. Ports of Emerson EC2 controller.

The connection points are shown above as numbered in Figure 4.16, are given in Table 4.15. below;

Table 4.15. Emerson EC2 Controller Ports [108].

1	**Suction Line P Sensor**	**6**	**EX2 EEV**
2	Evap Outlet T Sensor	7	Comp Contact
3	Room T Sensor	8	Evap Fan Contact
4	Blowing T Sensor	9	Defrost Heater Contact
5	Defrost T Sensor	10	Computer Connection (RJ45)

This device can be used directly by plugging it into the computer and inputting TCP/IP. The device with the brand code Emerson EC2-352 shown in Figure 5.14 is available in the communication protocol to ensure that all EC2 devices authenticate with TCP/IP Ethernet and ensure the integrity of the data when sending or receiving data to the other party.

For the measured T and P values, the control circuit EEV directs the ON/OFF control. The EEV is an electronically controlled solenoid valve. ON/OFF control is used when working as the EEV. When the Comp is on, the EEV opens within 6 seconds, and when the Comp is off, it works as a solenoid valve. This type of valve works in all kinds of different conditions, such as filling or emptying the cooling compartment. The opening and closing time of the valve can be controlled, which determines its capacity. EEV components:

- Suction line P sensor.
- EEV.

- Comp start-stop contact connection.
- Cold room ambient T sensor.
- Evap fan.
- Evap blowing T sensor.
- Defrost heater contact connection.
- Evap defrost T sensor.
- Computer RJ45 network connection [120].

4.10. OBTAINING THE DATA OF THE EXPERIMENTS

In this study; while obtaining the MCRS data, various measuring devices and computer software were used. K, J type thermocouple and Ordel brand UDL200-05/20 Data Logger were used for T measurements from certain points of the MCRS.

DALI08 software was used, which enables configuration via computer and saving the values taken from the device on the computer. The measured T values are devices that enable Ordel brand SBA 200 USB converter signals to be converted to USB interface and transferred to the computer environment.

This EEV works in conjunction with a suitable electronic connection. Its valve is used with standard ALCO brand ASC coils. It needs sensors, valve control unit to operate. There is also two pulse-width modulated (PWM) EEV in the MCRS.

Again, the data was transferred to the computer with the “SBA200” RS485-USB converter device belonging to the Ordel company, and records were taken in instant periods in Figure 4.26. For T measurements, “Ordel UDL200 Data Logger” device operating in RS485 (Modbus) standard was used. For the T measurements of the MCRS, in addition to the cold room control device, an external T sensor was used at 10 different points.

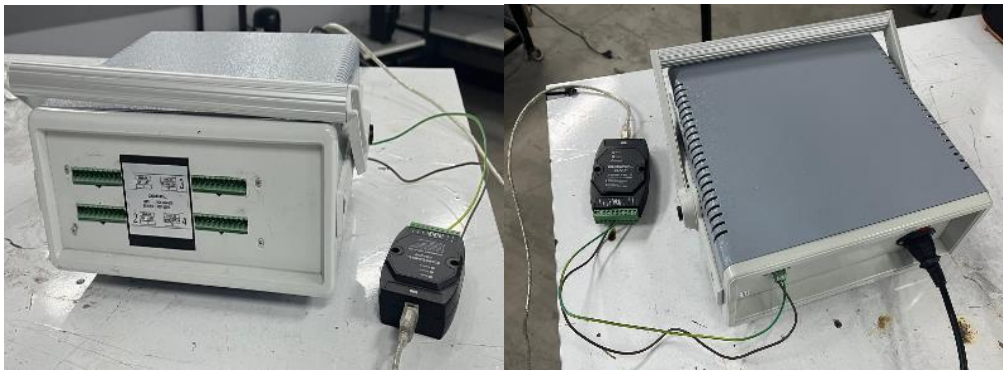

Figure 4.18. Ordel brand UDL200-05/20 data logger [119].

The prominent features of the Data Logger device used are;

- Thermocouple, mA, mV, Volt input options.
- 750 ms Sampling Period.
- Internal Cold End Compensation.
- MODBUS RTU Communication Protocol.
- DaLi 485 Monitoring and Recording Program.
- Unlimited Recording Capacity.
- Reporting in Excel, Acces, Text, HTML, PDF Format.
- Definition and Creation of On-Demand Graphics [43].

4.11. RETRIEVAL OF MEASUREMENT RECORDS

In this MCRS, the measurements obtained from 3 different pieces of equipment were recorded with a computer. In this way, all devices can be controlled with a computer. With the Emerson EC2 interface, both these devices were controlled and the data obtained from the devices were recorded. The first is Emerson EC-352 cold room control devices that control EEV, Sh, and T. Both devices are connected to a router-modem with an RJ45 (Ethernet) cable. Ordel SBA200 RS485-USB converter records the T values and memorizes them in an excel table.

During the MCRS, the photo of the counter data was taken every 10 minutes and these data were recorded in the excel file (Figure 4.27). The energy consumption per unit of time was calculated by finding the difference between the two measurement values.

The energy consumption values of the MCRS were measured with a digital electricity meter (Makel M310.2218).

Since the experimental system was operational, electrical energy consumption was recorded every 30 minutes. The meter connection power was measured in kilowatts (kW), and the electrical energy consumed by the test of MCRS was measured in kilowatt-hours (kWh). Makel M310.2218, a single-phase, electronic electricity meter was used to measure electrical energy consumption.

As shown in Figure 4.27. below, the current drawn by the test of MCRS every 30 minutes was measured and recorded in the Excel file. The clamp meter allows current to be measured without disconnecting the circuit. M266C clamp meter does amount of the current drawn by the MCRS.

In order to measure the consumed electrical energy and the currents drawn by the MCRS, Makel M310.2218, a single-phase electronic electricity meter, and a Clamp meter have been installed as shown in Figure 5.15. In order to take the MCRS measurements, the Ordel brand UDL200- 05/20 data logger device was installed on the MCRS in Figure 5.13, and thermocouple connections were made to the determined points on the MCRS.

Figure 4.19. Makel M310.2218, single phase, electronic electricity meter, Current measurement application with a clamp meter.

4.12. APPLICATION OF THE EXPERIMENT

Use an electronic electric meter and a thermometer for several connection points with the thermostable. The cooling room was also controlled by the computer to take measurements of the process T.

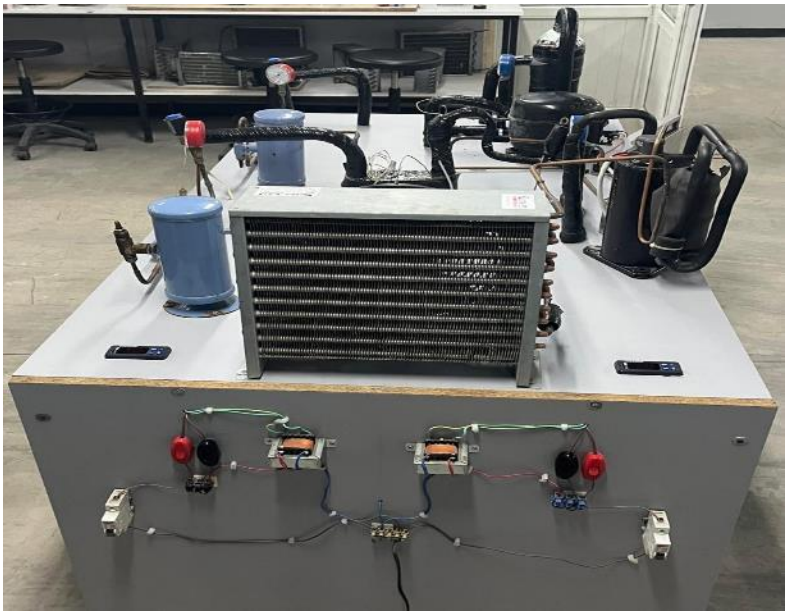

Figure 4.20. MCRS during taking measurements.

Only the Sh T set values differ between the MCRS. Except for the Sh set values, all set values, operating mode, and test method in the MCRS setup was kept constant. Figure 4.28, there are 10 different MCRS performed and the measurements were recorded continuously. In each experiment, the Sh set point values of the two cycles were kept equal, and a total of 10 different experiments were carried out from 3°C to 12°C. Each experiment was carried out at the same time of the day in periods of 120 minutes. Experimental measurements were not taken in cases where the ambient air conditioning conditions were different. Only the Sh T setting values were kept different between the experiments.

It is very important to measure the T of the air surrounding the laboratory and balance it with the temperature of both the cold room and the heat load equal to 15 half-liter plastic bottles. The water T inside the cooling chamber is recorded with a thermostable sensor as shown in Figure.4.29.

For all studies after refrigerant charging, data be located at the matching period interval, the next day. Afterward the end of the experiments, the LPC refrigerant and its mixtures were evacuated by providing the necessary conditions for the next experiment, and preparations were made for the next experiment. Each time in the experiments, another study was performed in which the opening of the EEV was manually changed for two hours after a fixed eight-hour operation, a total of ten hours of operation was performed for each experiment. In studies; Experiments were carried out by operating the refrigerant charge on the first day, and the system, which became stable the next day, in the same order, and such a method was followed for each experiment. In all experiments, the operating mode, clock, and test method of the system were kept the same.

At the end of the experiment, the recorded data were converted to excel format. Electrical energy and current every 30 minutes. Measurement was taken and recorded in an excel file. Excel files were examined for each experiment, and their conversions were made as 1-5-10 minutes and 1 hour, respectively. The received data was recorded in seconds for ten hours using the computer program Dali 08 and Emerson TCP/IP Ethernet.

Figure 4.21. Heat load study for the space to be cooled.

For all the experimental studies, 7.5 litters of water in 0.5-liter plastic bottles to create a heat load by the system as shown in Figure 4.21. The water was renewed each time

for the three experiments performed. In the study, in pairs where R407C/R32, and R407C/R32+R600a refrigerant, and mixtures were used, LPC of the test MCRS was placed under vacuum for the next test after the experiments. After the leak test application, the refrigerant or mixture charge applications were made, and then it was ready to collect the experimental data.

The supply of measurement and computer equipment was provided from a different source. The energy consumption of the loop elements in the experimental setup was provided from a single point, and the energy consumption was measured with a digital electricity meter. At least 1 day was left between the two experiments in order to ensure the equilibrium of the temperature and pressure values. MCRS can take a long time to reach equilibrium and reach maximum T depending on their size. The low heat load, it reached an equilibrium between 80 and 110 minutes. For this reason, all experiments were performed for 120 minutes (2 hours). Experiments were carried out at the same time of the day and only one experiment was taken on the same day. Before the experiments, attention was paid to ensure.

The aim of this study; The aim is to compare the cooling performance values under the same operating conditions, consisting of the same ODP values and different GWPs, alternative fluid mixtures used in two-stage cooling systems. In the MCRS; The system was investigated experimentally by using R32, R600a, and R407C refrigerants with the same ODP values and different GWP values, using fluid and fluid pairs under the same operating conditions.

Thermocouple connections were made between the Data logger device and the determined points so that T measurements could be taken when the test system was operational. Before the refrigerant is charged to the experiment system, the low-P lines and the insulation of the room where the cooling will take place are performed respectively. As a result of the work done, the MCRS was brought to a state where the refrigerant can be charged. The test system was taken to vacuum for a leak test and it was concluded that there was no leakage.

Figure 4.22. Vacuum application to the test system.

Gas charging was applied to the MCRS by using a refrigerant mixture Elitech brand LMC 300 precision digital balance. In MCRS, on the case that the refrigerant R407C in HPC remains constant, on LPC side, using a mixture of R32 refrigerant and R32, R600a refrigerant mixture, it is operated for ten hours.

Figure 4.23. Elitech brand LMC 300 precision digital balance.

The refrigerant mixture was charged with gas, with a total of 1000 gr 10%R600a 10 gr, 90%R32 900 gr. Gas charging was applied to the MCRS using R32 refrigerant, Elitech brand LMC 300 precision digital balance. In the MCRS, a total of 1000 gr of refrigerant for the LPC. including 10% R600a 100 gr. The tube was brought to the horizontal position and loaded in liquid form. Then, by making the test system operational and keeping the tube in an upright position, 90% R32 900 gr. gas charged.

Figure 4.24. R600a refrigerant charging application.

The MCRS was ready and the test results were taken the next day. After the test results were obtained, the R32, and R600a gas mixture on the LPC side was evacuated by providing the necessary conditions, the test system was put into a vacuum again and it was cleaned from unwanted gases and made ready for the next experiment, where only R32 refrigerant would be used.

In the cascade test system; in the next experiment, a gas charging application was made using R32 refrigerant digital scale. The MCRS was put into operation, with a total of 1000 gr of refrigerant R32, and gas was charged by keeping the tube in an upright position. After the test results were obtained the next day, the refrigerant R32 on the LPC side was evacuated by providing the necessary conditions, the test system was taken to vacuum again, and it was cleaned from unwanted gases and made ready for the next experiment, where the R32, and R600a refrigerant mixture would be used.

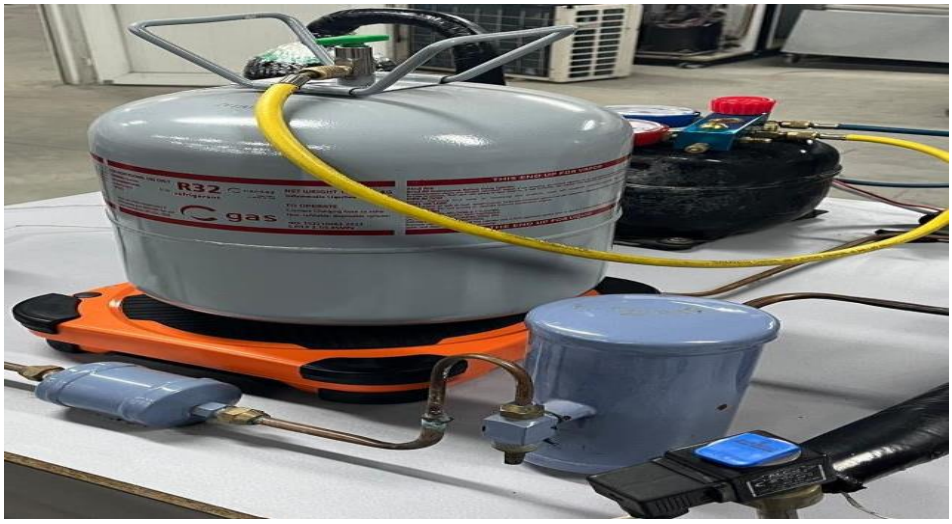

Figure 4.25. R32 refrigerant charge application.

Likewise, in the MCRS test in the first try; Gas charge application was made by using R32 + R600a refrigerant mixture digital scale. Refrigerant total 1000 gr as 100% R32 gas charged.

The MCRS was in the second experiment ready and the experiments were taken the next day. The tube was brought to the lying position and loaded in liquid form. Then, keep the tube in an upright position. gas charged. LPC refrigerant total 1000 gr. 10% R600a 100 gr and 90% R32 900 gr.

PART 5

MCRS MEASUREMENTS AND EVALUATION

Only the energy consumption values were manually read from the electronic meter and recorded at 10-minute intervals. The recordings were taken at intervals of 60 seconds, the arithmetic average of each 5-minute recording was taken, and the MCRS graphics and recording charts were created as 5-minute values. Records taken from computer-connected measuring devices were transferred to Excel format.

In the comparison of the MCRS, the graphs of the data between 60 and 120 minutes when the MCRS stabilized were used. Measurement points and connection diagrams of the MCRS setup are given. These are; COP values of MCRS, Condenser outlet T, Energy consumption values, cooling cabinet room T, Evaporation P, Comp outlet T.

5.1. THEORETICAL MODEL OF MCRS

After taking the theoretical results from software Refprop. Energy consumption measurements were taken for the MCRS, consisting of two different cycle in the refrigerant used and connected by the HEX, so that the first in LPC was with the R32 refrigerant in the first experiment, and then in the second experiment, the new mixture was used. While the HPC had R407C as the coolant for both experiments in the MCRS.

5.2. DESCRIPTION OF MCRS

Using a HEX suitable for the MCRS, the components of the assembly of form 5.1 with the P and enthalpy diagram of MCRS and including EEV, Cond, Evap, and Comp can be described as follows:

- The HEX is the main link between the two cycles of MCRS. As the Cond is connected to the LPC and the Evap to the HPC. It should be noted that the main Evap is in the LPC while the main Cond is in the HPC. It also has a Comp and an EEV for both LPC and HPC.
- To convert the refrigerant gas into a liquid, the appropriate Comp must be chosen carefully and in proportion to the refrigeration cycle. Any type of gas or mixture of materials used in the refrigeration cycle determines the size and type of Comp suitable for the cycle.
- 1.2 liters of coolant reservoir was used enough to store volume for each cycle which operates with approximately one liter. It is also possible to choose the parts of the MCRS after choosing the appropriate Comp, such as the Evap and the Cond, and determine the thickness of both and the pipes used in the connections between the parts of the MCRS.

However, the heat lost by the main Cond in the HPC is equal to the heat gained by the main Evap in the LPC. The Evap takes the quantity through which the required cooling can be obtained through the refrigerant liquid. In the liquid tank for each cycle separately, as stated in [19]. Figure 5.1, shows MCRS as HPC and LPC with p-h diagrams of it.

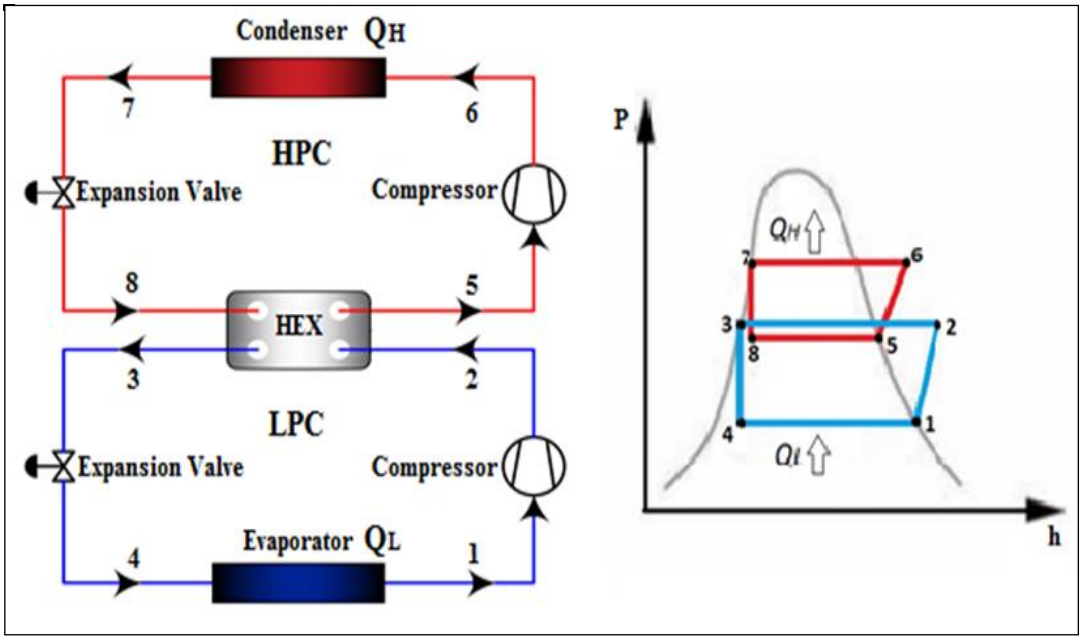

Figure 5.1. MCRS matches the (p h) diagram.

The new mixture proposed and used during this research consists of R32 with a mixing percentage equal to 90%, and plus R600a with a percentage of 10%. Two experiments were carried out, the first with pure R32 gas with a capacity of about one liter, and the second experiment using the new mixture in LPC. During the two experiments, R407C was used in an HPC with a capacity of approximately 1 liter. The MCRS performance rate COP_{MCRS} increases as the T of the main Evap T_e and the T of the main Cond decrease T_c.

5.3. THERMODYNAMICS IN ORGANIZATION DESIGN FOR MCRS

Assuming the following values in the simulation design for MCRS:

- In the connections and lines of connections between the components of the MCRS, P and heat losses are neglected.
- In the connections between each of the Evap, the Cond, the Comp, and the EEV, the stability in the condition of the refrigerant is considered in MCRS.
- Sh for HPC and LPC are 4˚C.

Table 5.1. In the simulation of Refprop maximum values below are imposed for MCRS.

Parameters	Value	Measuring Unit
Maximum convection (Q_e)	3	kW
Openair T (T_a)	35	˚C
Cond T (T_c)	45	˚C
Evap T (T_e)	-35	˚C
Sh of LPC	4	˚C
Sh of HPC	4	˚C
ΔT = T_3 - T_8	15	˚C
Comp efficiency η_{LPC} and η_{HPC}	80%	

Calculations were made for all P and T by REFPROP on each of the LPC, and HPC in this MCRS, and the expected values were obtained for the volumetric flow (ṁ) and system performance COP_{MCRS}. One of the rules of thermodynamics is that dividing the

Q_e cooling effect by the work done by the MCRS equals the performance rate COP_{MCRS}. The following equations were used in making the calculations of this thesis.

For each cooling cycle separately as documented in [7, 8].

Effect of Refrigeration LPC = $Q_e^{LPC} = h_1 - h_4$ (5.1)

Enthalpy at input Comp LPC h_1, enthalpy at EEV LPC h_4.

Comp work is equal = $W_c^{LPC} = (h_2 - h_1)$ (5.2)

Enthalpy of the output Comp h_2

$$COP_{LPC} = \frac{(h_1 - h_4)}{(h_2 - h_1)} \quad (5.3)$$

A mass flow rate ṁ of LPC

$$\dot{m}_{LPC} = \frac{Q_{LPC}}{(h_1 - h_4)} \quad (5.4)$$

Work in LPC as equation below:

$$W_{LPC} = \frac{\dot{m}(h_2 - h_1)}{\eta c,LTC} = \dot{m}_{LPC}\,(h_2 - h_1) = \frac{Q_L\,(h_2 - h_3)}{(h_1 - h_4)} \quad (5.5)$$

flow rate ṁ in HPC:

$$\dot{m}_{HPC} = \frac{Q\,W_{LPC}}{h_s - h_g} \quad (5.6)$$

W_T total work and the W_{HPC} work in HPC as equations below:

$$W_T = W_{LPC} + W_{HPC} \quad (5.7)$$

$$W_{HPC} = \dot{m}_{HPC} (h_6 - h_7) \quad (5.8)$$

Determine the mixing ratio of both gases R32 and R600a theoretically by software Refprop and practically by means of the accurate and sensitive device of a type precision digital balance. Before working with the proportion of the mixture in the MCRS. The results from EES of Refprop are shown in Table 5.2.

Table 5.2. Refprop results.

Mixture R32/R600a by mass % Respectively	**T_e (˚C)**	**Liquid phase P (MPa)**	**Vapor phase P (MPa)**	**Liquid phase Density (kg/m^3)**	**Vapor phase Density (kg/m^3)**	**Liquid phase Enthalpy (kj/kg)**	**Vapor phase Enthalpy (kj/kg)**	**Liquid phase Entropy (kj/kg-K)**	**Vapor phase Entropy (kj/kg-K)**
(90/10)	-35	0.23220	0.23067	1053.0	6.6151	136.18	488.15	0.76425	2.2302
(80/20)	-35	0.23284	0.19981	961.39	5.7392	137.08	477.54	0.75626	2.2077
(70/30)	-35	0.23146	0.13256	886.43	3.7633	135.07	472.07	0.74856	2.2393
(60/40)	-35	0.23185	0.098376	824.82	2.7940	133.17	468.13	0.74124	2.2538
(50/50)	-35	0.23571	0.077800	773.99	2.2212	131.37	466.87	0.73425	2.2628

In the first horizontal box in Table 5.2, the program Refprop results were recorded for the mixture used during this research, which represents 10 percent of pure gas R600a added to pure gas R32 at a rate of 90 percent. It is worth noting that if the percentage of R600a gas is less than 10 percent of the amount of charge in the system, the MCRS will have a discharged state. Data on the new mixture and the gas R32 are collected in the Table 5.3, below:

Table 5.3. The new mixture and R32, properties.

Refrigerant	**T (˚C)**	**P (MPa)**	**Liquid phase Density (kg/m^3)**	**Vapor phase Density (kg/m^3)**	**Liquid phase Enthalpy (kj/kg)**	**Vapor phase Enthalpy (kj/kg)**	**Liquid phase Entropy (kj/kg-K)**	**Vapor phase Entropy (kj/kg-K)**
R32	T_3=7.4	1.02339	1029.1	27.903	213.07	516.40	1.0465	2.1277
R32	T_e= -32.46	0.24676	1158.2	6.9266	145.43	505.28	078948	2.2845
R32/R600a (90/10%)	T_3=9.0	1.0875	921.07	30.398	216.61	502.90	1.0588	2.0732
R32/R600a (90/10%)	T_e= -32.18	0.25966	1072.4	7.4056	140.74	489.48	0.76887	2.2184

Table 5.4. Properties of R407C.

Refrigerant	T (˚C)	Liquid phase Pressure (MPa)	Vapor phase Pressure (MPa)	Liquid phase Density (kg/m^3)	Vapor phase Density (kg/m^3)	Liquid phase Enthalpy (kj/kg)	Vapor phase Enthalpy (kj/kg)	Liquid phase Entropy (kj/kg-K)	Vapor phase Entropy (kj/kg-K)
R407C & R32	T_7= 40.3	1.7619	1.5535	1066.2	68.746	260.89	424.56	1.2041	1.7312
R407C & R32	T_8= -5.13	0.47893	0.3835	1254.6	16.466	192.76	406.97	0.97352	1.7829
R407C & mixt	T_7= 41.19	1.8316	1.6195	1061.6	70.549	262.35	424.75	1.2086	1.7301
R407C & mixt	T_8= -4.21	0.49405	0.39655	1251.4	17.010	194.06	407.43	0.97829	1.7817

Table 5.5. The basic properties of the refrigerants.

Refrigerant	R407C	R32	R600a	R32/R600a (90/10%)
Safety level	A1	A2	A3	
Boiling point ˚C	-43.8	-52	-11	
T_{Cond} **˚C**	86.4	78.4	137.7	
P_{Cond} **bar**	46.3	53.8	36.4	
ODP	0	0	0	
GWP	1650	650	-20	587

The heat Q_{Hex} load of MCRS for HEX as shown in the following equation:

$$Q_{Hex} = \dot{m}_{HPC} \cdot (h_5 - h_8) = \dot{m}_{LPC} \cdot (h_2 - h_3) \tag{5.9}$$

The COP is given for MCRS by the equation:

$$COP_{MCRS} = \frac{\dot{Q}_{LPC}}{\dot{W}_{HPC} + \dot{W}_{LPC}} \tag{5.10}$$

$$COP_{MCRS} = \frac{\dot{m}_{LPC} \cdot (h_1 - h_4)}{\dot{m}_{HPC} \cdot (h_6 - h_5) + \dot{m}_{LPC} \cdot (h_2 - h_1)} \tag{5.11}$$

The performance factor of MCRS is as follows. By enthalpy COP equation:

$$COP_{MCRS} = \frac{(h_1 - h_4) \cdot (h_5 - h_8)}{(h_2 - h_1) \cdot (h_6 - h_7) + (h_1 - h_4) \cdot (h_6 - h_5)} \quad (5.12)$$

The platform prepared to install the MCRS's devices is equipped with wheels with brakes to facilitate the movement of the MCRS and ensure that it does not move during operation. Moreover, the refrigeration chamber is located on the lower level of the MCRS equipment installation platform, while the rest of the equipment is on the upper level, which is for both LPC and HPC, the Comp, the Cond, the liquid tank, and the Evap, respectively, in addition to the high and low P gauges for both LPC, HPC. With regard to the LPC, HPC operating switches, and the voltage transformers from 220 to 24 V, that operate the control units of the EEV, they were installed on the vertical side of the left side of the assembly platform.

The Figure 5.2, below shows the diagram indicating the main components of the MCRS used during this doctoral dissertation.

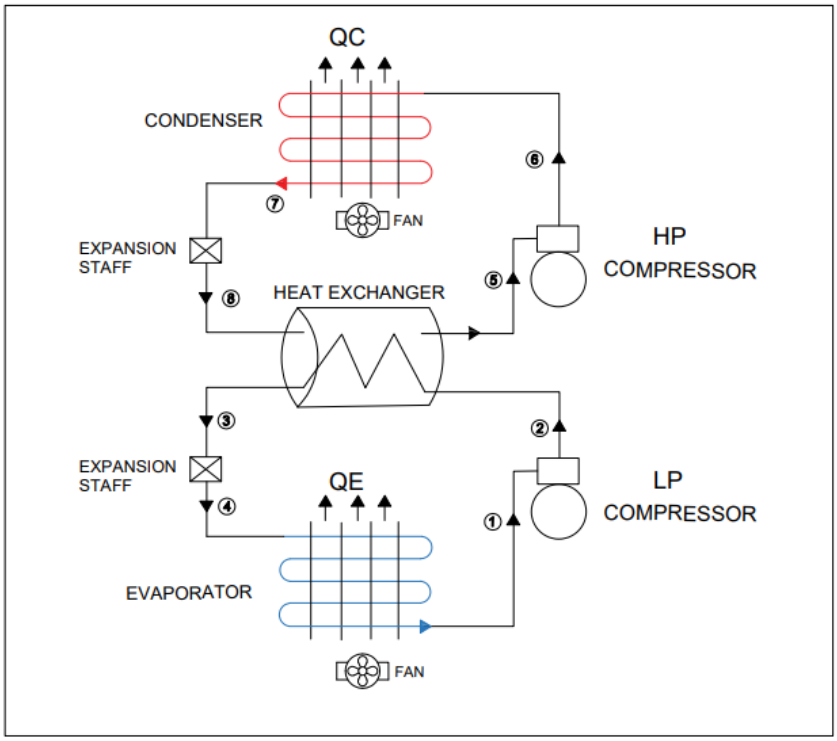

Figure 5.2. Schematic diagram of the MCRS in this research [125].

5.4. EXPERIMENTAL METHODOLOGY

The priorities for implementing the experimental research can be summarized as follows in the MCRS used:

- Use the very accurate Elitech brand LMC 300 precision digital balance to charge the MCRS with refrigerant gases, each according to the percentage required for each of R407C gas, R32 gas, and the new mixture with R600a gas.
- Use the vacuum pump when charging and discharging each experiment separately, the first with R32 only and the second with the new mixture. The high and low P gauges permanently installed in the pipelines were also used.
- The power drawn from the circuit was calculated using a movable jaw ammeter. The amount of current drawn by the coil per second was also measured by an electric measuring clock.
- Use oxygen and acetylene welding with silver skewers to weld between copper and copper tubes with welding aid when welding iron tubes with copper tubes for all connection points between the parts of the MCRS.
- By checking the application of the information taken from the latest scientific papers published recently in the field of CRSs the use of a HEX with a total capacity of 28 slices was extracted.

From recording the data taken from the Data Logger, 10 points were recorded for the MCRS connected by the thermocable of the device Data Logger. To connect the database device to the computer, an Ordel SBA200 RS485-USB adapter was used to record the information from the dataset into Excel spreadsheets on the computer. In addition to that, a program prepared by Ordel Company was dealt with as a computer application through which data is taken from the database and recorded accurately in tables on the computer. It should be noted that both cycles contain an EEV that is controlled by opening and closing from a computer. The Sh value was constant at 4˚C for both LPC and HPC.

5.6. BOTH CYCLE COMPONENTS OF MCRS

The difference between HPC and LPC parts are shown in Table 5.6.

Table 5.6. The HPC parts and the LPC parts.

The HPC Parts	**The LPC Parts**
Rotary Comp **1.5 Hp 220 V, 50 Hz, efficiency 0.8**	Reciprocating type hermetic-lock Comp 0.5 Hp 220 V, 50 Hz, efficiency 0.8
Comp gas **R407C**	Comp gas, mixture R32, R600a
Cond-Fan, amply 1.9 m², aluminum blades attached to a copper tube	Cabinet 320 Liter, Sizes 70*74*70 cm, Evap-fan
Liquid tank 1.2 Liter	Liquid tank 1.2 Liter
Dryer Filter	Dryer Filter
Sight Glass - High P Gauge	Sight Glass - High P Gauge
EEV	EEV
Plate HEX as Evap **of 28 Plates,0.312 m²**	Plate HEX as Cond of 28 Plates,0.312 m²
EGV T sensor	EGV T sensor
EGV P device	EGV P device
Accumulator (Liquid holder)	Accumulator (Liquid holder)
Hhigh&Low P manometer	Hhigh&Low P manometer
High-P manometer Operating P, 1/36 bar	High-P manometer Operating P, 1/36 bar

5.7. APPLICATION OF MCRS EXPERIMENTATION

We take the T and P of the ambient air, and we prepare the electricity meter to measure the current drawn by the MCRS, and we install the T sensors for 10 points by means of a thermocouple to the digital device, and we connect the digital device to the computer. We run the system in the LPC first, followed by the HPC. And we make sure that the computer is running and the sequence of data transfer to Excel tables to take all the information related to P and T to be saved and used later in creating the relationship curves between the transactions. We install the Sh at 4°C and record the EEV data. We record the T at the inlet and outlet of the HEX, main Evap, main Cond, and Comps.

Fifteen half-liter water bottles were used to form the convection for the MCRS. A thermocable is fixed with adhesive tape to one of the bottles inside the refrigerator compartment to record the convection T regularly. It is very important to ensure the thermal balance between the components of the MCRS and the ambient air before starting operation. Furthermore, to ensure thermal equilibrium, at least one day should be left between each experiment and the next experiment. The same devices were used for all experiments after the process of calibrating them and determining their accuracy before using them by recording data for each experiment. It should also be noted that each experiment was repeated at least five times to ensure the validity of the results by matching them with the previous experiment. The device reaches the state of equilibrium between the LPC, and HPC after two hours of starting the operation. It was left for four hours to record the data from the MCRS and save it in Excel tables, as an average of 8 hours of operation for each experiment.

PART 6

EXPERIMENTAL FINDINGS

6.1. ANALYSIS OF MCRS MADE ACCORDING TO THE REFRIGERANT PAIRS USED

Experiments were carried out under very close ambient-climatic conditions, at the same time of the day, and as one experiment per day. All system parameters were kept constant. In this thesis, a cascade vapor compression MCRS setup was fabricated and two experiments were carried out.

In MCRS experiments, it was seen that HPC reached T_e values faster and was more stable. Therefore, experimental data were compared between 60-120 minutes. MCRS can take a long time to stabilize. In the experiments, it was observed that the cycle became stable between 50 and 80 minutes due to the small MCRS setup and the low heat load.

Since these T differences are high and liquid fluid is likely to go to the Comp, it has been seen that an accumulator (liquid trap) should definitely be used in both cycles in MCRS. HPC compressor T averages varied between 29°C and 70°C according to the experiments. It has been observed that the output T of the HPC Comp are more affected by the Sh values. Between the 60-120 minutes when the test data were compared, the average of the outlet T of both Comp was calculated.

While there is a direct link between the Evap P of the LPC fluid and the cold room T, it has been determined that it reacts later than the HPC fluid. In addition, it has been observed that the Evap P of R407C and R32 give different responses to Sh values and ideal T_3.

It has been determined that while the HPC fluid is more affected by the outdoor T, the LPC fluid is mostly affected by the heat transfer rate in the HEX. Therefore, it has been observed that the LPC fluid gives a later and smaller response. It is worth saying that the cold room T is not directly related to the Cond outlet T, but is directly related to the amount of heat dissipated in the Cond.

Considering the energy consumption, room T, Comp outlet T, and COP values, it has been seen that the mixture experiment and the -30°C value provide more ideal data.

In this study, the data obtained by using the cooling medium pairs used in the CRS are given in graphic form using the Excel program. The test MCRS was operated for 8 hours and the measurements after the 2nd hour when it stabilized for each applied experiment were discussed. The Sh value of the MCRS using refrigerant R32/407C, and 90%R32+10%R600a/R407C pair was set as in both cycles.

After the MCRS reaches a stable state, P, and T data are recorded and stored from all points on which 2 high-P and 2 low-P gauges are installed, and thermocouple T sensors with 10 points. It should be noted that data is not taken when the Comps stop running. Work, i.e., data is recorded when Comps are running only. Intake and expulsion P were also recorded for each of the Comps. In addition, the amount of opening and closing of the two EEVs was recorded, with the Sh value being 4°C for both LPC and HPC. The mixture used is considered a new mixture and has not been used or published in scientific research and scientific publication papers. It consists of 90 percent pure R32 gas added to it and 10 percent of pure R600a gas. After recording and storing all the necessary information in Excel tables, curves were drawn showing the relationship by means of a graph between the various P, T, COP_{MCRS}, and the opening and closing of EEVs, by fixing the obtained information with horizontal and vertical axes, so that it is clear and clear all the information related to the MCRS and the results of this scientific research for Ph.D. It can be said that this research includes all the important scientific information for the operation of the MCRS and all the results related to knowing the details necessary to determine the COP_{MCRS} and the efficiency of the MCRS. The following points on which the MCRS depends can be monitored:

- 4°C is the value at which the Sh is fixed as if any change occurred during operation as a result of opening and closing the EEV controlled by the electronic control unit directly connected to the EEV, which operates at a low voltage of 24 volts, it is returned to the same value at 4°C by the special console attached to the computer.
- The value of P loss through the connections, elbows and connecting pipes of the constituent devices of the MCRS can be neglected to each other when the galaxies calculations during this scientific research.
- The P and T data are taken after the stability of the MCRS's work in both LPC, and HPC so that it is assumed that the condition is stable for all points recorded in the data of the MCRS recorded in Excel tables.
- The MCRS is considered thermally isolated from the surrounding medium so that it can be said that the heat does not transfer from it or to it.
- By software, Refprop is specified the volumetric flow rate and compares practical results with it.
- The most important link between LPC, and HPC is the HEX in MCRS, which works as a Cond for the LPC and at the same time works as an Evap for the HPC.
- The HPC Evap has a significant effect according to the laws of thermodynamics in both COP_L and COP_H separately.
- For each of the HEX, Evap, Cond, and Comps, the inlet and outlet T were recorded. It should be noted that the energy consumed by the MCRS increases with the increase in the P of condensation into the two gases R32, and R600a that make up the mixture.
- To determine the quality of the work of the MCRS, it was relied on to calculate the practical actual values of the COP_{MCRC}, which is equal to dividing the cooling effect T_e by the total work of the two Comp W_C in LPC, HPC, and this includes the calculation of all the inlet and outlet Comp T: T_1, T_2, T_5, T_6 in LPC and HPC.

6.2. EFFECT OF IDEAL T_3 ON T_e (LTC)

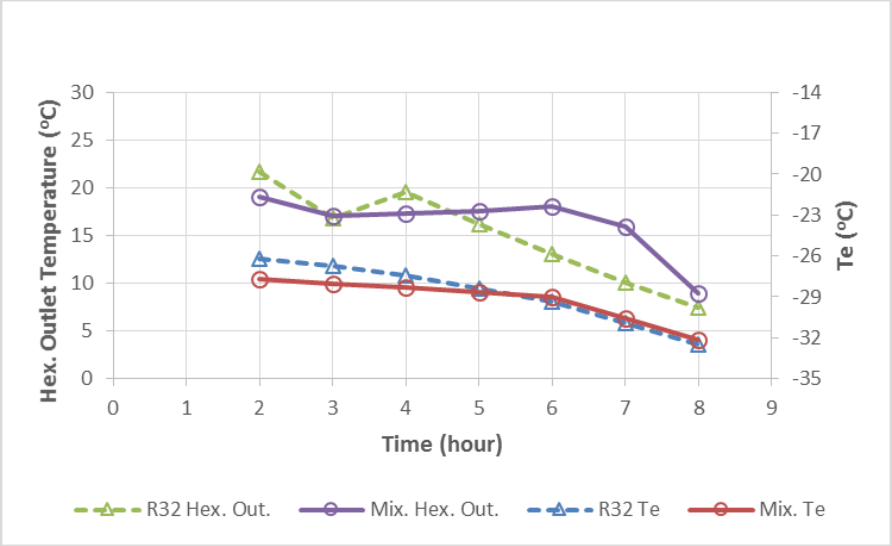

Figure 6.1. Effect of ideal T_3 on T_e LTC.

First experience with R407C/R32. This is followed by experiments using an R32+R600a refrigerant mixture in LPC, respectively. In two experiments in terms of room T, it was measured that there was not much T difference and it reached the desired low P values. As a result of two experiments using refrigerant and its mixtures, comparable curves were obtained as shown in Figure 6.1. As a result of the 8-hour measurements in the insulated room in the experimental MCRS, the results were similar in both experiments with R32, and the second with the new mixture 90%R32+10%R600a at the lowest degree obtained in the mixture. Also in Figure 6.1, the fluctuation of the T_3 curve of the HEX outlet T is due to the change in the opening of the EEV with the Sh value remaining constant at 4°C, as this effect appears on T_e in the same way. When the T_3 decreases, this leads to a decrease in the Evap T_e, the opposite is true when it rises. It should be noted that at the start of the operation of the two Comp work, T_3 is at a relatively high value, and at this stage, the COP of the two Comp is of a high value due to the two Comp not reaching high P values at the two Comp ejection line. In addition, an increase in T_3 leads to a decrease in the value of COP_L. It was also observed that both T_8 and COP_H both increased and decreased in HPC. What's more, it can be learned, after the MCRS reaches the lowest T in the Evap in LPC, when T_3 decreases from the recorded results, the system performance rate is lowest, while at the start of the accumulator operation, COP_{MCRS} with COP_L and COP_H

is at the highest value. The Cond T in both cycles LPC as well as HPC have a direct effect on each other, so the focus during this research was to reach the saturation T at the ideal T_3 in the MCRS to reach maximum COP_{MCRS}. For example, after 5:20 of starting the MCRS with R32 gas, the T of the main Evap drops to -27.8°C, and this time differs when using the new mixture to obtain it after three hours of starting operation, with a difference of 2.20 of the MCRS working hours, and this is what It appears that I preferred to work with the new mixture to reach the required degrees in the least amount of time, using pure R32 gas. Furthermore, each Evap T corresponds to an ideal T_3. For example, at -27.8 °C in the Evap, T_3 is equal to 18, which the mixture reaches after three hours of operation, while R32 gas reaches 22°C after 3:00 operation.

6.3. EFFECT ENERGY CONSUMPTION ON COP_{MCRS}

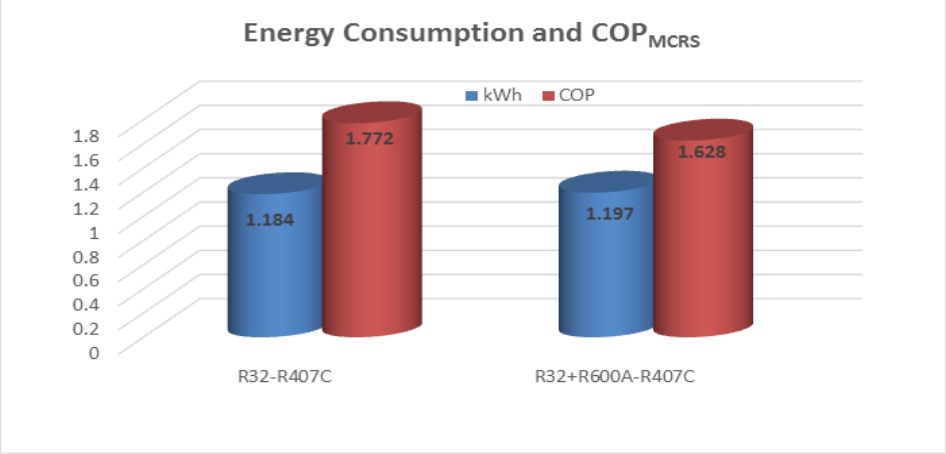

Figure 6.2. Effect energy consumption on COP_{MCRS}.

As a result of changing viscosity, energy consumption will increase together with frictions and will cause wear of the Comp in a short time. As a result of the fluid stage fluid entering the Comp, the T of the Comp oil decreases, and its viscosity is affected. In vapor Comp, the entering fluid must be in the superheated vapor phase. The phase state and T of the fluid incoming the Comp is an important factor in the energy consumption of the Comp.

Figure 6.2 explains the possibility of replacing R32 with the new mixture, as it is clear that both experiments have similar results for the mixture and pure gas R32. Figure 6.2, also indicates the closeness of performance rates in both trials. It can also be said that pure gas R32 has a higher COP_{MCRS} with a very small value than the new mixture, but here it is worth remembering that the mixture has a lower potential than R32 to cause global warming. The lowest total electrical energy consumption was measured in the experiment using the R32/R407C refrigerant couple. This was followed by R32+R600a/R407C refrigerant pairs, respectively.

6.4. EFFECT T_e ON ENERGY CONSUMPTION

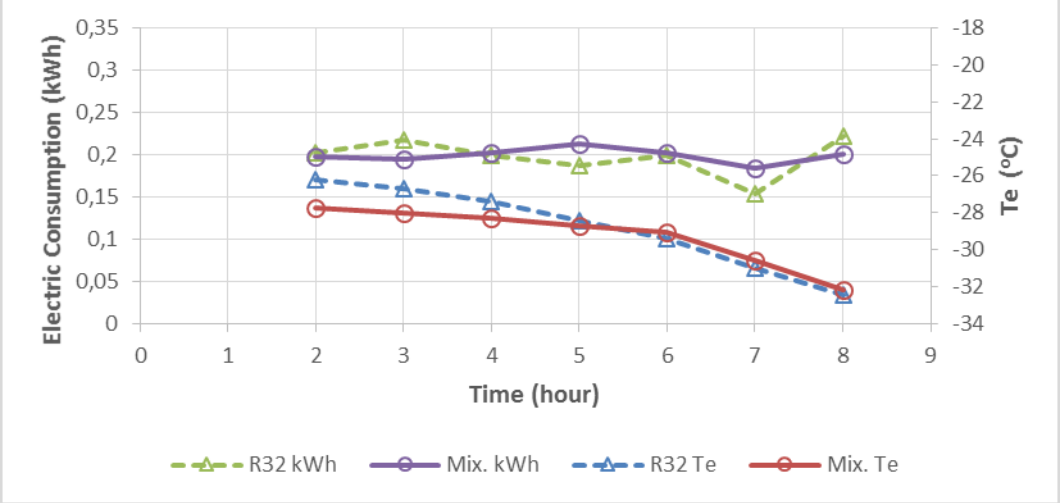

Figure 6.3. Effect T_e on energy consumption.

At -30.5°C, the lowest amount of energy consumed by the MCRS in both experiments is recorded and saved. It can be said that Figure 6.3, easily shows that the lower the Evap T_e, the lower the amount of energy consumed to reach that T. At -31.5°C is the lowest value of energy consumption for both experiments. Furthermore, it is noted from the curves that after the adsorbate reaches -29°C or less, the difference between the results of the mixture and the pure gas is almost equal. For each main Evap T_e, there is a value to the best performance rating COP_{MCRS} that is related to the T_3 of the LPC of HEX Through this research, we confirm that it is possible to improve the performance of the system COP_{MCRS} by choosing a suitable T for the outlet of the HEX T_3 in the LPC so that it can be changed by changing the capacity of the HEX.

At the lowest T_e in the Evap -32°C, the corresponding Cond T_c with the mixture will be 45°C and with R32 43°C. Figure 6.3 shows the similarity of the two curves in both experiments after the MGRS reached -30°C to -32°C, and the average performance value for both is similar in the two experiments, and this is due to both R32 and the mixture having similar cooling properties as a result of the close composition of both. The T of the outlet of the HEX T_3 rises slightly more than of the Evap T_e, and the reason for this is due to the high P of the exhaust line in the Comp, which leads to a rise in the T of the refrigerant. And since T_3 is one of the most important elements of the MCRS factors, it must be suitable and ideal due to its connection with the capacity of the HEX and the efficiency of the HPC.

It is worth noting that the new mixture has a lower energy consumption value than R32 when the Evap T_e is less than -30°C. In addition, the values in the Evap T_e curve are similar for the mixture and R32 at all points below -29°C. The relationship is also considered direct, meaning that it increases and decreases with each other for T_e, T_3, and COP_{HPC}. T_e, COP_{HPC}, and T_3 are the components of figure .6.3, where the relationship between them all appears in one illustrative curve. And this figure 6.3, adds that the new mixture has values greater than R32 in the T curve of the HEX outlet T_3 and this can be explained by the fact that the new mixture reaches the same T in the Evap in less time than the time it takes R32 gas to reach the same degree. It is noted that the lower the T of the Evap, the lower the degrees of entry and exit to the Comp in LPC T_1, T_2, and the Comp in HPC T_5, T_6.

T_3 can be considered as a major influencing factor in LPC as it is related to the efficiency of the performance of both cycles whose relationship to each other is shown in Figures 6.1, and 6.2. It was discovered through this research that the performance rate of the entire MCRS depends on T_3 in a positive relationship between them, they rise and fall together. Therefore, The relationship is inverse between the COP of each separate cooling circuit separately COP_L in the LPC and COP_H in the HPC at the start of the MCRS, where the COP is high in the HPC and low in the LPC in an inverse relationship, and The reason for this is that when the MCRS starts operating, the discharge P of the Comp T_2 is low. COP_{MCRS} improves with a decrease in the T_3 after

the system has stabilized. Comp outlet T_2 rises in the LPC. Here it is worth noting that COP_L also improves with the stability of the MCRS and COP_H decreases for the LPC.

6.5. EFFECT T_e ON COMPRESSOR INLET T_1 LPC

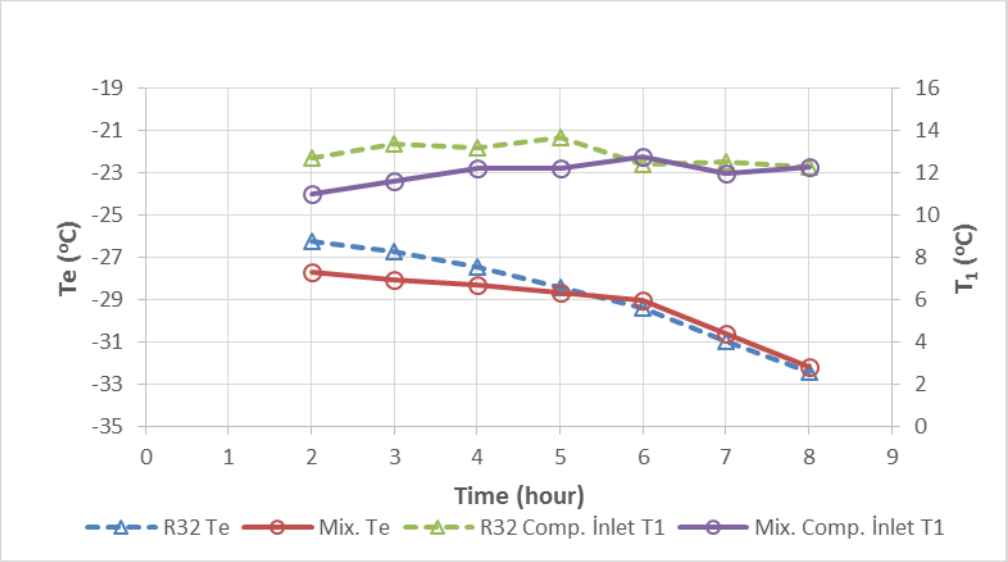

Figure 6.4. Effect T_e on Comp inlet T_1 LPC.

The consequence of this sudden reduction in the inlet T of the LPC HEX at the 7th hour is seen in Figure 6.4. In the MCRS, in which a mixture of refrigerant R32+R600a was used, a decrease in the outlet T of the Comp was observed as a result of a sudden decrease in the Comp inlet T in the 7th hour, as seen in the graph. As can be seen in Figure 6.2, it is seen that the Comp outlet T decreased over time in the two experiments. It was measured that the Comp outlet T reached its highest values in the experiment consisting of R32+R600a, R32 refrigerant, and mixtures, respectively.

As an outcome of such a situation, the heat transmission capacity of the Cond HEX will not change, and the MCRS will not be able to reach the desired cooling capacity, since it will not be able to fully discharge the heat, it needs to be removed. It is not desired that the refrigerant comes out of the Comp at a high T and enters the Cond.

T_1 an uneven curve but T_e a regular curve for two experiments. Growth at the beginning of T_1 curve, and after T_e decreases, the T_1 reductions. COP_{MCRS} reaches its

highest value when obtaining the lowest T in the main Evap, and it is noted that at this T the LPC Cond is cooler than any other T in the Evap. Furthermore, the main Evap is affected by the main Cond, although they are present in two different and separate cooling cycles LPC, and HPC, so the lower the T of the main Cond, the faster the required degree will be reached in the Evap. In other words, if the T of the air surrounding the main Cond is cooler, better for the COP of the MCRS and vice versa. For example, when the outside air-temperature T_a is equal to 20°C, the work of the condenser and the COP_{MCRS} value will be greater than if the T_a is 30°C.

In the LPC, T_1, the Comp inlet T in the intake line is affected by the Evap T_e, as shown in Figure 6.4. Figure, in both the LPC of the Comp outlet T_2 and in the HPC of the Comp outlet, when the higher they are, the lower the main Evap T_e. The lower the Evap T and the T_3 HEX outlet T, the lower the energy consumption. Furthermore, the energy lost and the energy used by the MCRS decreases with the decrease in the Evap T_e, and it can be said that at the outlet and inlet of both Comps, the decrease in the Enthalpy value h_1, h_2 in the LPC and h_5, h_6 in the HPC leads to a decrease in energy losses and energy consumed as in the Figure. 4.1.

6.6. INLET CONDENSER T_6 AND T_3 HPC

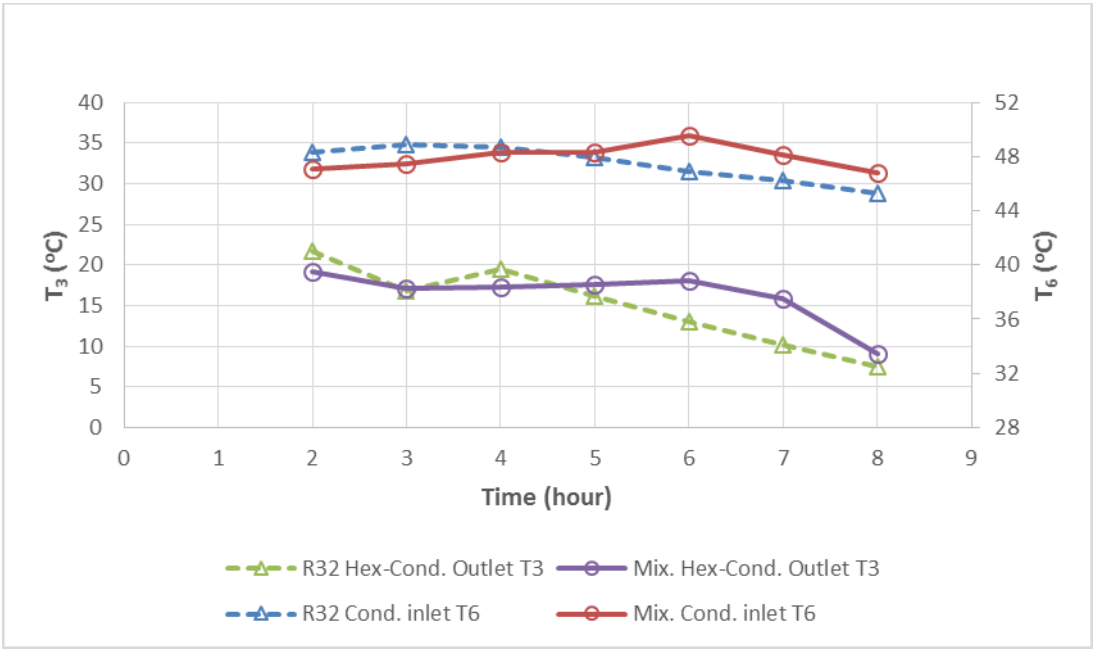

Figure 6.5. Inlet Cond T_6 and T_3 HPC.

As shown in Figure 6. 5, the inlet Cond T_6 of the HPC and outlet HEX T_3 in both R32/R407C, and 90%R32+10%R600a/R407C experiments, respectively, between the 2nd and 7th hours, is 4°C, 5.65°C, 4.51°C. The Cond, which is one of the elements of the MCRS, allows the refrigerant to pass from the superheated phase by throwing warmth into the environment.

It has been determined that the Cond outlet T are related to the heat transfer amount of the HEX as well as the Evap P values. It has been determined that the fluid flow rate decreases with increasing ΔT values in the R407C fluid, and the Cond outlet T decrease because the heat transfer rate in the HEX decreases. By reducing the EEV openings, the amount of heat transfer decreases with the fluid flow rate at increasing Sh degrees. Therefore, in R32 fluid, as the Sh degree increases, the Cond outlet T also increases as a result of the decrease in fluid flow and the inability to release heat. It has been observed that there is no direct correlation between R32 and R407C Cond outlet T. The Cond outlet T of the refrigerants are given.

The effect relationship of the entry T to the Cond T_6 on the exit T of the HEX T_3 between the use of the mixture that is equal to 1.5°C higher than the value when using R32 and this difference is considered very small. Moreover, it should be noted that the in the HPC, the inlet T of the Cond T_6 is lower than the outlet T of the Comp. Furthermore, in both experiments, -32°C is the best T for the MCRS in terms of stability, COP at the highest value, thermal load in thermal uniformity, and the energy consumed and lost from the MCRS, where it is the lowest value. In the LPC, the heat gained by the refrigerant (R32 or the new mixture) in the Evap as a result of its low P and the heat it absorbs in the form of heat content as a result of its high P in the Comp, in addition to that heat gained by R407C in the HPC from the HEX and transferred from the LPC and The heat that it acquires as a result of its high P in the Comp in the HPC, all of this affects the Cond inlet T in the HPC by increase or decrease. Therefore, the COP of the MCRS is inversely affected by T_6. Most of the results recorded in this thesis indicate that the difference between the refrigerant gas R32 and the new mixture is negligible, and here we emphasize the preference of the mixture from an environmental point of view, as it is less capable of causing global warming and does not deplete the ozone layer. It can be added that the energy lost and the energy

consumed decrease with the decrease of T_6 at the entrance of the main Cond in the MCRS. The MCRS's energy consumption and loss increase with an increase in the amount of heat T_6, as is evident when tracing the curve of the mixture in the figure above. Moreover, the lowest energy consumption with the mixture is when T_6 decreases from 49.8°C to 47°C during the last two hours, as shown in the figure.

6.7. EFFECT T_e ON CONDENSER OUTLET T_7 HPC

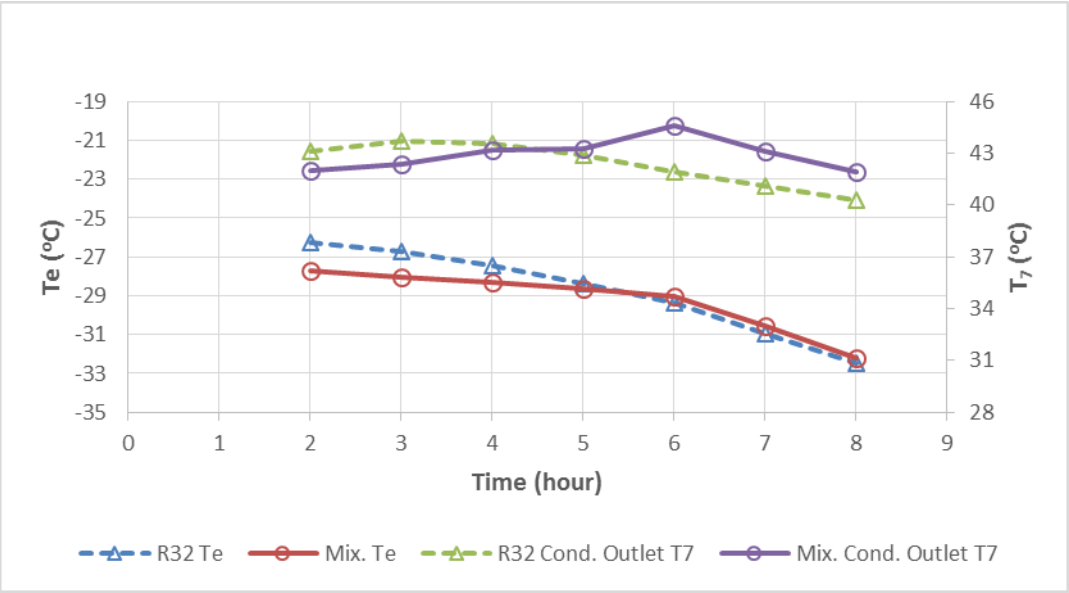

Figure 6.6. Effect T_e on Cond outlet T_7 HPC.

The above figure shows the result of the mixture formation of two different gases the curve represented by it is more volatile than the R32 curve of T_7. The curves indicate that the relationship is similar between T_e and its effect on T_7, especially in the last two runs. The outlet T of the Comp increases with the increase in cooling load in the refrigerating room, and in LPC the effect is more obvious when T_3 rises with T_e rise. In addition, for the mixture and R32 gas, there is no significant difference in the points in the curves shown in Figure 6.6. It is possible to compare the results between the mixture and R32 gas when they reached the lowest degrees in the Evap, so it will be as follows; First, the mixture obtained T_e was equal to -32.18°C. At the same time, the T of the mixture outlet from the HEX was equal to T_3 was equal to 16.3°C, secondly with regard to gas. R32 The results to the lowest degree obtained in the Evap T_e was equal to -32.46°C at the same time T_3 was equal to 14.95°C, which confirms the

similarity of the results in both experiments and the possibility of replacing the pure R32 gas with the new mixture. The above figure shows the great convergence in the results taken from the MCRS for the T_e of the refrigerating room so that it is clear in the case of using the mixture from -27.5°C to -32.18°C, but when using pure gas R32, the start is from -26.5°C to reaching the low degree at -32.46°C as the beginning and end of the two curves after the MCRS work has stabilized

6.8. SUCTION LINE PRESSURE P_1 LPC AND P_5 HPC

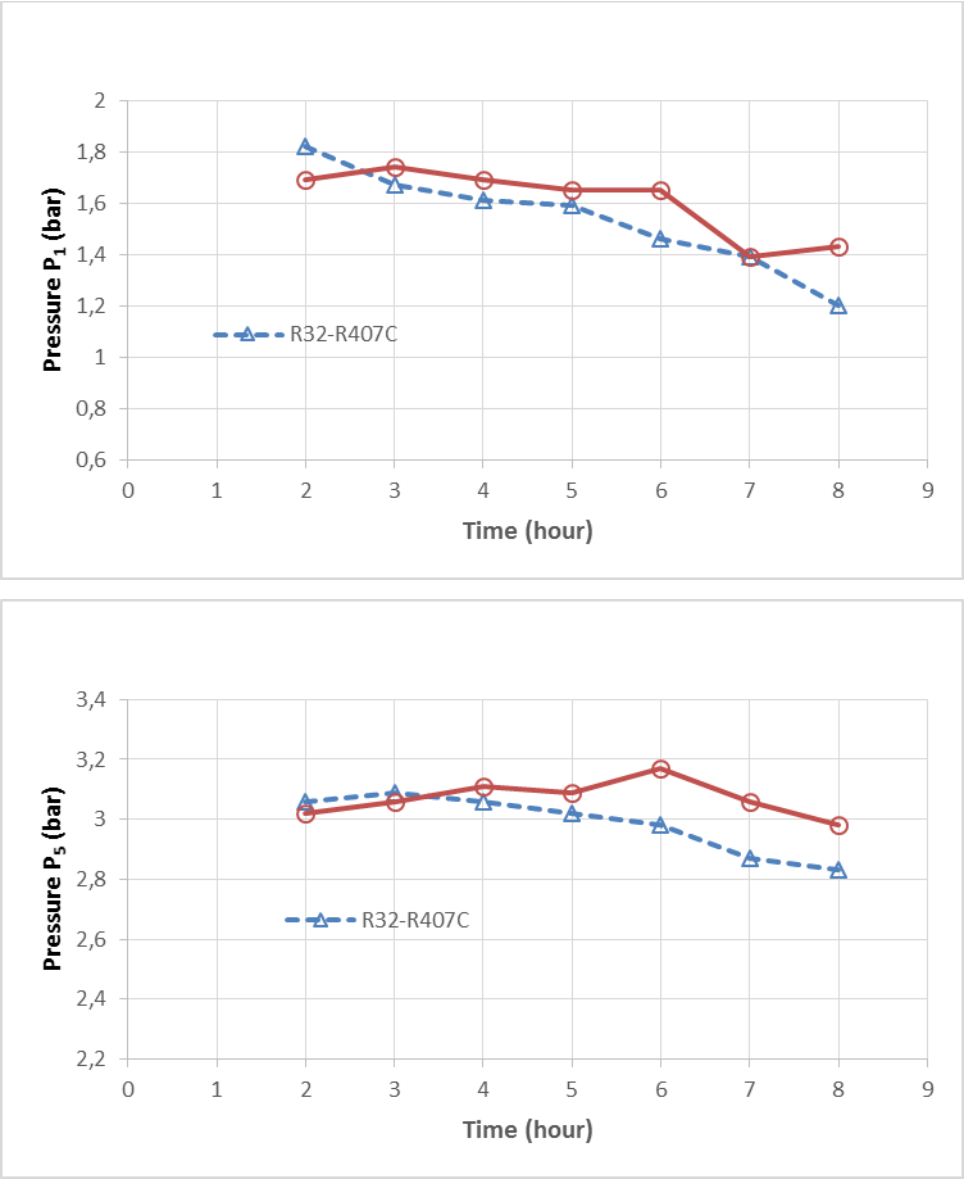

Figure 6.7. Suction line-Pressure P_1 LPC and P_5 HPC.

Likewise, high Comp T are also an important factor in reducing Comp life. This undesirable situation will force the Comp to work and may cause malfunctions in a short time. If the T of the fluid entering the Comp is too low, it may cause the liquid fluid to go to the Comp. Inlet-outlet T values are very important for the life operation of the Comp.

As presented in the Figure. 6.8. It should be noted that all measured P recorded in Excel tables as results for the MCRS was recorded without adding the value of atmospheric pressure equal to 1 bar, which have been written in the form in this study. Moreover, the difference between the P in the suction line P_5 in the two experiments can be neglected, which is equal to 0.19 bar for the mixture, which is higher than that with R32. In the same case, the T difference between the two experiments was equal to 2°C, for the mixture higher than that with pure gas R32 at the outlet of the HEX T_3 in the LPC, which resulted in a slight difference in the performance rate COP between the two experiments. In the same context, the difference between the two experiments with the suction line in the LPC P_1 was equal to 1.4 bar for the mixture, higher than it was with R32.

6.9. HEAT EXCHANGER INLET-OUTLET T_2 -T_3 LPC and T_8 -T_5 HPC

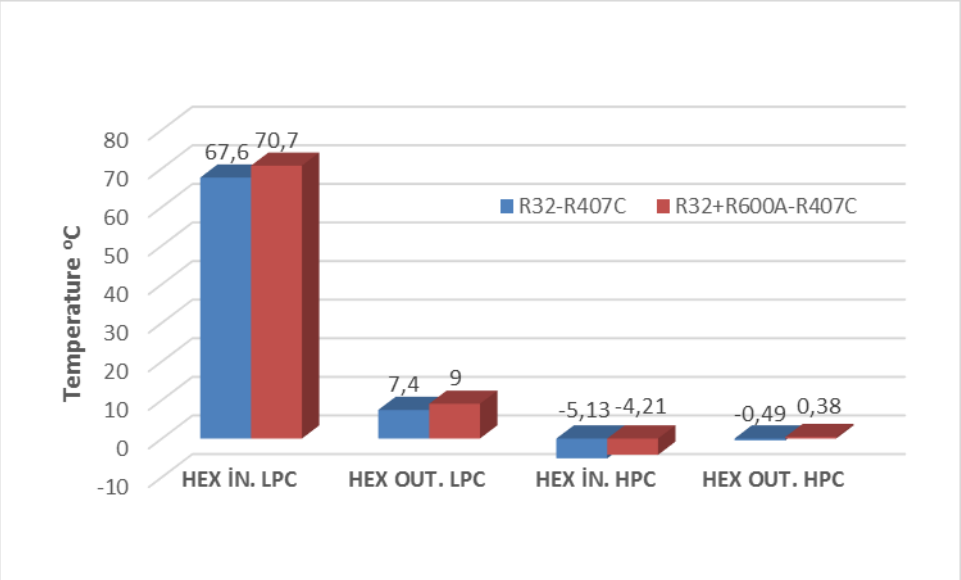

Figure 6.9. HEX Inlet-Outlet T_2 -T_3 LPC and T_8 -T_5 HPC.

As shown in Figure 6.4. the average difference variation the inlet and outlet T of the LPC HEX variation the 2nd and 7th hours in the R32/R407C, 90%R32+10%R600a/R407C experiments, respectively, was 55.42°C, 59.11°C, it was calculated as 56.44°C. The HEX functions as a Cond in LPC.

At the mixture HEX outlet T; There are many factors such as heat transfer rate, instantaneous thermodynamic properties of fluids, Comp T, and Evap T. However, it is clearly seen that the HEX outlet T are not directly related to the cold room T and are related to the amount of heat transfer in the HEX.

An element worth noting in the MCRS data is ($\Delta T = T_3 - T_8$) ΔT as it represents the relationship between both LPC, and HPC in line with thermodynamic laws. The relationship is in direct proportion so that it increases and decreases with each other for T_8 on T_3 T_5 on T_2. From the results of enthalpy tables 5.3 and 5.4, the Figure 6.10, has been drawn. The results of the effect of T on each sleeve of the inlet and outlet of the HEX in both LPC T_2 T_3 and HPC T_5 T_8 are shown in the above figure 6.8. Moreover, The results of the COP adopted the higher values to draw the above figure. Where the product of subtracting the inlet T of the HEX in the HPC T_8 minus the outlet T of the HEX in the LPC T_3 equal to ΔT is considered an important value in the results of the COP of the MCRS.

6.10. VALVE OPENING AND SUPERHEAT LPC

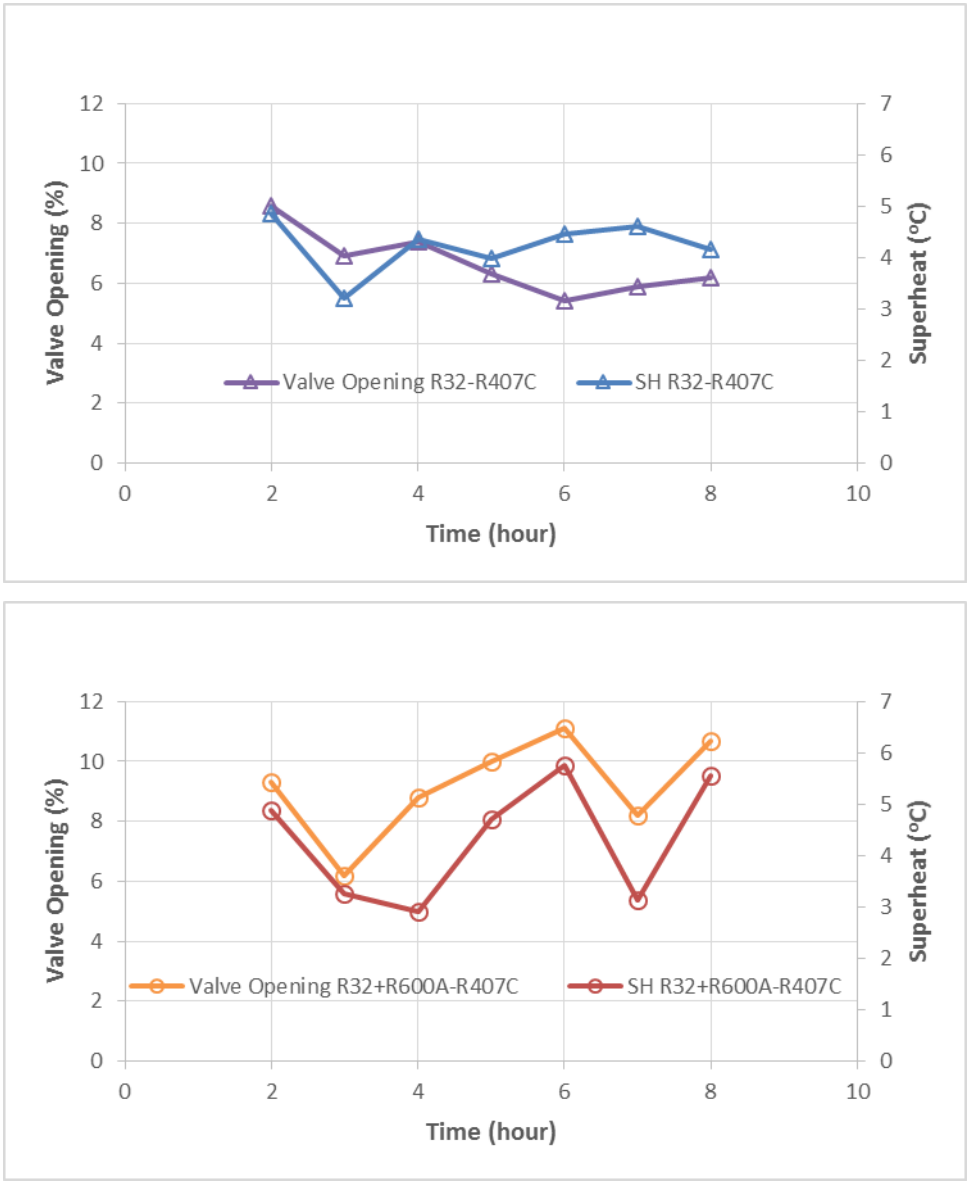

Figure 6.11. EEV opening and Sh in LPC.

Although R404A fluid P react later than mixture fluid, it is seen that the effect of T_3 values on Evap P is different. These fluctuations in the P curves are due to small changes in the EEV openings, the heat transfer rate in the HET, and the room T. Although there are fluctuations in the P curves, it is seen that the P reductions are in parallel with room T. As seen in Figure 6.9, there is direct parallelism between Evap P and T values.

Since there will be a decrease in the amount of fluid going to the Evap as a result of the decrease in the valve opening, the decrease in P was measured after the 6th hour as seen in Figure 6.9. In the experimentation where the 90%R32+10%R600a / R407C refrigerant couple was used, it was observed that the EEV opening decreased over time after the 6th hour.

As a result of the difference in the components of the mixture consisting of two pure gases, the above figure shows that the R32 curve is more regular than the mixture curve. In addition to that, the amount that enters the Evap when the valve is opened, it is not possible to know the ratio at which both gases that make up the mixture R600a and R32 enter, and this leads to an irregular increase and decrease in points. It can be concluded and interpreted the difference between the valve opening curves between the two experiments that when using a refrigerant with one gas, the curve is more regular than when using a refrigerant consisting of two or more gases. It can also be added to that which shows the Sh curves, which are fixed during the operating period of the MCRS at 4°C. When recording the practical results of the experiments, a difference in the Sh values is recorded as a result of the difference in the opening of the EEV, and then the same degree is returned to the same T at 4°C by the computer. It is noted in the results of this thesis that the excess T changes from the value fixed at it, which is 4°C, and this constant value is returned by opening or closing of the EEV, and it is worth mentioning in this important point that opening the EEV reduces the consumption the energy consumed and lost by the MCRS. It is proved by Figure 6.9, that in both experiments using the mixture or using one gas, the EEV opening curve was similar to both experiments. COP of MCRS when the EEV is opened, and at the same time, the value of energy consumed and lost from the MCRS decreases. Evap cooling increases as its T decreases with the EEV open.

At the same T, the COP is similar in the two experiments and with similar values for the input energy when the EEV is open. In addition, the slight difference between the R32 curve and the new mixture curve is due to the difference in the composition of the mixture from the pure gas. The results also show that each of the two experiments has a very close COP_{MCRS} when the Evap T is -32°C. Figures 6.9, 6.8, and 6.7 tell us that the energy consumption is relatively low when the suction head P of the Comp is low.

PART 7

CONCLUSION AND RECOMMENDATIONS

7.1. SUGGESTIONS

At the same time, by comparing this study with different refrigerants, it can be determined whether there is a difference between the ideal mixture's degrees. In addition to this MCRS, determining the ideal T_3 degrees of both cycles separately with the help of an automation MCRS can further increase cycle efficiency. According to the results obtained, T_3 values in MCRS; efficiency, energy consumption, and T values have been affected. Various improvements can be made in the HEX in order to reduce the stabilization time of the LPC in the MCRS and to reach the desired room T faster. In this context, it will be useful to conduct a comparative study on the MCRS of HEX and to determine the most efficient HEX type and method.

7.2. CONCLUSION

Using a small cascade refrigeration system, which we call (MCRS), this thesis proved using two separate experiments that the new mixture used for the first time, consisting of 90% of R32 gas added to it 10% of R600a gas, is better than using R32 gas alone in the low refrigeration cycle LPC, and it should be noted in both experiments, R407C gas was used in the high-pressure cycle HPC, and that is because of the lower potential of the new mixture to cause Global Warming Potential (GWP) than with R32 gas. The following points clearly explain the results obtained during this thesis:

- The new mixture and R32 gas have very close thermodynamic properties, and this scientific research prefers to use the new mixture instead of R32 gas because the mixture is less capable of GWP by 67 than when using R32.

- The performance rate COP_{MCRS} of the new mixture and R32 gas is close when the Evap T_e is -30°C, which both compounds reach at the same time from the start-up of the MCRS.
- In each of the first two experiments with gas R32 and the second with the new mixture, the values of energy consumption and energy losses were almost equal at different T measured in the Evap.
- The maximum value of the average performance is COP_{MCRS} there is an ideal t at the outlet of the HEX in the LPC T_3, and for each T of the main Evap T_e in the MCRS.
- This scientific research recommends that the search for non-flammable gases or mixtures be continued to work as a refrigerant in MCRS, since both gases used in this research, R600a, and R32, are flammable gases.
- The size of the MCRS used during this research is enough and suitable in size so that it can be installed on small cars that facilitate the transportation of medicines and vaccines, and it should be noted here that the rate of energy withdrawal of the MCRS is low and less than 1.2 kWh.

REFERENCES

1. Qi, Q., Deng, S., Xu, X., & Chan, M. Y., "Improving degree of superheat control in a direct expansion (DX) air conditioning (A/C) system", ***International Journal of Refrigeration,*** 33(1): 125-134 (2010).

2. Internet: Waelkens, M., "Sagalassos", **https://www.aktuelarkeoloji.com.tr /sagalassos483334**/(2020).

3. Sür, A., "Karst Landforms and examples from Turkey", ***DTCF Turkey Geography Research and Application Center Journal of Geography Studies,*** 3 (2): 1-28 (1994).

4. Turkmen, M. N., "Meeting the Needs of the Palace in the Ottoman Empire: "Snow and Ice Supply", **Gazi Academic View Journal,** 4(3): 8-19 (2011).

5. Shatchman, T., "Absolute Zero and the Conquest of Cold", ***1st Mariner Books Boston ,*** USA, 32-74 (2000).

6. Chisholm, H., "Cullen William", **Cambridge University Press,** UK, 616-617 (1911).

7. Messineo, A., "R744-R717 cascade refrigeration system: performance evaluation compared with a HFC two-stage system", ***Energy Procedia,*** 1(4): 56-65 (2012).

8. Di Nicola, G., Polonara, F., Stryjek, R., & Arteconi, A., "Performance of cascade cycles working with blends of CO2+ natural refrigerants", ***International Journal of Refrigeration,*** 34(6): 1436-1445 (2011).

9. Gholamian, E., Hanafizadeh, P., & Ahmadi, P., "Advanced exergy analysis of a carbon dioxide ammonia cascade refrigeration system", ***Applied Thermal Engineering,*** 13(7): 689-699 (2018).

10. Zhang, Y., He, Y., Wang, Y., Wu, X., Jia, M., & Gong, Y., "Experimental investigation of the performance of an R1270/CO2 cascade refrigerant system", ***International Journal of Refrigeration,*** 11(4): 175-180 (2020).

11. Froid, D. U., "Classification of refrigerants," ***Int. Inst. Refrig., no. Cl,*** 3(2): 1–6, (2001).

12. Sun, Z., Wang, Q., Xie, Z., Liu, S., Su, D., & Cui, Q., "Energy and exergy analysis of low GWP refrigerants in cascade refrigeration system", ***Energy,*** 17(10): 1170-1180 (2019).

13. Roy, R., & Mandal, B. K., "Exergy analysis of cascade refrigeration system working with refrigerant pairs R41-R404A and R41-R161", ***In IOP Conference Series: Materials Science and Engineering,*** 37(7):12-36 (2018).

14. Mofrad, K. G., Zandi, S., Salehi, G., & Manesh, M. H. K., "4E analyses and multi-objective optimization of cascade refrigeration cycles with heat recovery system", ***Thermal Science and Engineering Progress,*** 1(9): 100-613 (2020).

15. Ust, Y., & Karakurt, A. S., "Analysis of a Cascade Refrigeration System (CRS) by Using Different Refrigerant Couples Based on the Exergetic Performance Coefficient (EPC) Criterion", ***Arabian Journal for Science and Engineering,*** 39(11): 8147-8156 (2014).

16. Bhamidipati, A., Pendyala, S., & Prattipati, R., "Performance evaluation of multi pressure refrigeration system using R32", ***Materials Today: Proceedings,*** 2(8): 2405-2410 (2020).

17. Chen, J. X., Hu, P., & Chen, Z. S., "Study on the interaction coefficients in PR equation with vdW mixing rules for HFC and HC binary mixtures", ***International Journal of Thermophysics,*** 29(6): 1945-1953 (2008).

18. Bingming, W., Huagen, W., Jianfeng, L., & Ziwen, X., "Experimental investigation on the performance of NH3/CO2 cascade refrigeration system with twin-screw compressor", ***International Journal of Refrigeration,*** 32(6): 1358-1365 (2009).

19. Sun, Z., Liang, Y., Liu, S., Ji, W., Zang, R., Liang, R., & Guo, Z., "Comparative analysis of thermodynamic performance of a cascade refrigeration system for refrigerant couples R41/R404A and R23/R404A", ***Applied Energy,*** 18(4): 19-25 (2016).

20. Khalilzadeh, S., Nezhad, A. H., & Sarhaddi, F., "Reducing the power consumption of cascade refrigeration cycle by a new integrated system using solar energy", ***Energy Conversion and Management,*** 20(0): 112-830 (2019).

21. Singh, K. K., Kumar, R., & Gupta, A., "Comparative energy, exergy and economic analysis of a cascade refrigeration system incorporated with flash tank (HTC) and a flash intercooler with indirect subcooler (LTC) using natural refrigerant couples", ***Sustainable Energy Technologies and Assessments,*** 3(9): 100-716 (2020).

22. Kharat, A. E., Mate, D. M., & Kathwate, S. D., "Experimental study of alternative refrigerants to replace R134a in a domestic refrigerator", ***International Journal of Academic Research and Development,*** *3*(4): 28-35 (2018).

23. Llopis, R., Sanz-Kock, C., Cabello, R., Sánchez, D., Nebot-Andrés, L., & Catalán-Gil, J., "Effects caused by the internal heat exchanger at the low temperature cycle in a cascade refrigeration plant", ***Applied Thermal Engineering,*** 10(3): 1077-1086 (2016).

24. Massuchetto, L. H. P., do Nascimento, R. B. C., de Carvalho, S. M. R., de Araújo, H. V., & d'Angelo, J. V. H., "Thermodynamic performance evaluation of a cascade refrigeration system with mixed refrigerants: R744/R1270, R744/R717 and R744/RE170", ***International Journal of Refrigeration,*** 10(6): 201-212 (2019).

25. Liang, T. K., Ghadimi, A., Hong, L. C., Wei, P. S., & Meng, C. W., "The influence of mixing factors on the flammability of r32 refrigerant and compressor oil mixture", ***EURECA,*** 2(3): 1-8 (2016).

26. Wang, W., Zhou, Q., Tian, G., Hu, B., Li, Y., & Cao, F., "The intermediate temperature optimization for cascade refrigeration system and air source heat pump via extreme seeking control", ***International Journal of Refrigeration,*** 11(7): 150-162 (2020).

27. López-Belchí, A., & Illán-Gómez, F., "Evaluation of a condenser based on mini-channels technology working with R410A and R32. Experimental data and performance estimate", ***Applied Energy,*** 20(2): 112-124 (2017).

28. Hakkaki-Fard, A., Aidoun, Z., & Ouzzane, M., "Improving cold climate air-source heat pump performance with refrigerant mixtures", ***Applied Thermal Engineering,*** 7(8): 695-703 (2015).

29. Massuchetto, L. H. P., do Nascimento, R. B. C., de Carvalho, S. M. R., de Araújo, H. V., & d'Angelo, J. V. H., "Thermodynamic performance evaluation of a cascade refrigeration system with mixed refrigerants: R744/R1270, R744/R717 and R744/RE170", ***International Journal of Refrigeration,*** *10(6):* 201-212 (2019).

30. Sun, Z., Liang, Y., Liu, S., Ji, W., Zang, R., Liang, R., & Guo, Z., "Comparative analysis of thermodynamic performance of a cascade refrigeration system for refrigerant couples R41/R404A and R23/R404A", ***Applied Energy,*** 18(4): 19-25 (2016).

31. Tanaka, M., Matsuura, H., Taira, S., & Nakai, A., "Selection of a refrigeration oil for the R32 refrigerant and evaluation of the compressor reliability", ***International Compressor Engineering Conference,*** Purdue, 14-17 (2014).

32. Wang, H., Song, Y., & Cao, F., "Experimental investigation on the pull-down performance of a-80° C ultra-low temperature freezer", ***International Journal of Refrigeration,*** 11(9): 1-10 (2020).

33. Tan, Y., Wang, L., & Liang, K., "Thermodynamic performance of an auto-cascade ejector refrigeration cycle with mixed refrigerant R32+ R236fa", ***Applied Thermal Engineering,*** 8(4): 268-275 (2015).

34. Mohanraj, M., Jayaraj, S., Muraleedharan, C., & Chandrasekar, P., "Experimental investigation of R290/R600a mixture as an alternative to R134a in a domestic refrigerator", ***International Journal of Thermal Sciences,*** 48(5): 1036-1042 (2009).

35. Sun, Z., Liang, Y., Liu, S., Ji, W., Zang, R., Liang, R., & Guo, Z., "Comparative analysis of thermodynamic performance of a cascade refrigeration system for refrigerant couples R41/R404A and R23/R404A", ***Applied Energy,*** 18(4): 19-25 (2016).

36. Kilicarslan, A., & Hosoz, M., "Energy and irreversibility analysis of a cascade refrigeration system for various refrigerant couples", ***Energy Conversion and Management,*** 51(12): 2947-2954 (2010).

37. Energy, K. and Energy, T. F. "13 Space heating and cooling," ***U.S. DOE-EERE,*** USA, 335–336 (2005).

38. Dalkilic, A. S., "Theoretical analysis on the prediction of performance coefficient of two-stage cascade refrigeration system using various alternative refrigerants", ***1st Bilimi ve Tekniği Dergisi, J. of thermal science and technology,*** 32(1): 234-456 (2012).

39. Sun, Z., Cui, Q., Wang, Q., Ning, J., Guo, J., Dai, B., & Xu, Y., "Experimental study on CO2/R32 blends in a water-to-water heat pump system", ***Applied Thermal Engineering,*** 16(2): 114303 (2019).

40. Rui, S., Zhang, H., Zhang, B., & Wen, D., "Experimental investigation of the performance of a single-stage auto-cascade refrigerator", ***Heat and Mass Transfer***, 52(1): 11-20 (2016).

41. Atalay, H., "Determination of Optimum Operating Parameters of a Cascade Cooling System Using R290(Propane) and R600(N-Butane) Refrigerants", ***Dokuz Eylül University Faculty of Engineering Science and Engineering Journal,*** 21(63): 775-791 (2019).

42. Kochenburger, T. M., Grohmann, S., & Oellrich, L. R., "Evaluation of a two-stage mixed refrigerant cascade for HTS cooling below 60 K", ***Physics Procedia,*** 6(7): 227-232 (2015).

43. Wang, Q., Li, D. H., Wang, J. P., Sun, T. F., Han, X. H., & Chen, G. M., "Numerical investigations on the performance of a single-stage auto-cascade refrigerator operating with two vapor–liquid separators and environmentally benign binary refrigerants", ***Applied Energy,*** 11(2): 949-955 (2013).

44. Cimşit, C., "Thermodynamic analysis of vapour compression-absorption two stage refrigeration cycle", ***Karaelmas Fen ve Mühendislik Dergisi,*** 8(1): 218-226 (2018).

45. Pico, D. F. M., da Silva, L. R. R., Mendoza, O. S. H., & Bandarra Filho, E. P., "Experimental study on thermal and tribological performance of diamond nanolubricants applied to a refrigeration system using R32", ***International Journal of Heat and Mass Transfer,*** 15(2): 119-493 (2020).

46. Shaik, S. V., & Babu, T. A., "Thermodynamic performance analysis of ecofriendly refrigerant mixtures to replace R22 used in air conditioning applications", ***Energy Procedia,*** 10(9): 56-63 (2017).

47. Rupesh, P. L., Babu, J. M., Surryaprakash, D., & Misra, R. D., "Experimental and computational evaluation of temperature difference of a cascade condenser of R134a-R23 cascade refrigeration system", **In *2015 International Conference on Smart Technologies and Management for Computing, Communication, Controls, Energy and Materials,*** India, 659-663 (2015).

48. He, G., Liu, F., Cai, D., & Jiang, J., "Experimental investigation on flow boiling heat transfer performance of a new near azeotropic refrigerant mixture R290/R32 in horizontal tubes", ***International Journal of Heat and Mass Transfer,*** *10(2):* 561-573 (2016).

49. Kumar, B. and Scholar, Y. M. "A Review Analysis of Alternative of R-22 Using Vapour Compression Cooling System", ***International Journal of Engineering Technology and Applied Science,*** 2(9): 2395-3853 (2016).

50. Yin, X., Wang, X., Li, S., & Cai, W., "Energy-efficiency-oriented cascade control for vapor compression refrigeration cycle systems", ***Energy,*** 11(6): 1006-1019 (2016).

51. Yao, Y., Zhang, Z., & Hu, X., "Experimental contrast on the cooling performance of direct evaporative all fresh air handling units with R32 and R410A", ***Procedia Engineering,*** 20(5): 802-809 (2017).

52. Nawaz, K. Shen, B. Elatar, A. Baxter, V. & Abdelaziz, O. "Growing awareness of the potential environmental impacts of various refrigerants has led to the phase- down of hydrofluorocarbon (HFC) refrigerants and to initiatives replacing HFCs with hydrocarbons or other environmentally friendlier fluids. This study ", ***Appl. Therm. Eng.,*** 12(7): 870–883 (2017).

53. Campbell, A., Maidment, G. G., & Missenden, J. F., "A refrigeration system for supermarkets using natural refrigerant CO_2", ***International Journal of Low-Carbon Technologies,*** 2(1): 65-79 (2007).

54. Ma, M., Yu, J., & Wang, X., "Performance evaluation and optimal configuration analysis of a CO2/NH3 cascade refrigeration system with falling film evaporator–condenser", ***Energy Conversion and Management,*** 7(9): 224-231 (2014).

55. Oktaviani, J, "No Title No Title," ***Sereal Untuk,*** 51(1):51 (2018).

56. Ceylan, M., "Machine Design in Cascade Cooling Systems" ***Master Thesis, Gazi University Institute of Science and Technology,*** Ankara, 12-29, (2002).

57. Sanz-Kock, C., Llopis, R., Sánchez, D., Cabello, R., & Torrella, E., "Experimental evaluation of a R134a/CO2 cascade refrigeration plant", ***Applied Thermal Engineering,*** 73(1): 41-50 (2014).

58. Tian, Q., Cai, D., Ren, L., Tang, W., Xie, Y., He, G., & Liu, F., "An experimental investigation of refrigerant mixture R32/R290 as drop-in replacement for HFC410A in household air conditioners", ***International Journal of Refrigeration,*** 5(7): 216-228 (2015).

59. Menlik, T., "Design, Production and Performance Experiments of Alternative Fluid Two-Stage Cooling System", ***Ph.D. Thesis, Gazi University Institute of Science and Technology,*** Ankara, 45-67 (2005).

60. Sholahudin, S., & Giannetti, N., "Optimization of a cascade refrigeration system using refrigerant C3H8 in high temperature circuits (HTC) and a mixture of C2H6/CO2 in low temperature circuits (LTC)", ***Applied Thermal Engineering,*** 10(4): 96-103 (2016).

61. Yi, W. B., Choi, K. H., Yoon, J. I., Son, C. H., Ha, S. J., & Jeon, M. J., "Exergy characteristics of R404A indirect refrigeration system using CO2 as a secondary refrigerant", ***Heat and Mass Transfer,*** *55*(4): 1133-1142 (2019).

62. Bayrakcı, H. and Akdağ, A.E., "Comparison of Energy Consumptions of CO_2 Heat Pumps for the Same Cooling Load", ***Technological Research Paper,*** USA, 33-38 (2010).

63. Şahin, B., "Farklı Akışkanların Kullanıldığı İki Kademeli Soğutma Sisteminin Enerji ve Ekserji Analizi", ***Teknik Bilimler Dergisi,*** 10(2): 37-41 (2020).

64. Bouaziz, N., Lounissi, D., & Iffa, R. B., "Energy and exergy analysis of a double stage hybrid heat pump operating with water ammonia", **In *Proceedings of CONV-14: International Symposium on Convective Heat and Mass Transfer,*** **Begel House Inc.** Tunisia, 100-212 (2014).

65. Zubair, S. M., "Design and rating of a two-stage vapor-compression refrigeration system", ***Energy,*** 23(10): 867-878 (1998).

66. Yılmaz, İ.,"R-744/R-717 Kaskad Bir Soğutma Çevriminin Termodinamik Analizi", ***Yüksek Lisans Tezi, Süleyman Demirel Üniversitesi Fen Bilimleri Enstitüsü,*** Isparta, 60-62 (2018).

67. Zheng, N., Hwang, Y., & Zhao, L., "Thermodynamic performance assessment of R32 and R1234yf mixtures as alternatives of R410A", ***In 12th IEA Heat Pump Conference,*** China, 45-68 (2017).

68. Kilicarslan, A., "An experimental investigation of a different type vapor compression cascade refrigeration system", ***Applied Thermal Engineering,*** 24(18): 2611-2626 (2004).

69. Elitok, Ç., "Farklı buharlaştırıcı ve yoğuşturucu sıcaklıkları için kaskad soğutma sisteminin deneysel incelenmesi", ***Master's thesis, Hitit Üniversitesi Fen Bilimleri Enstitüsü***, Turkey, 34-57 (2017).

70. Y. Zhou, G. Chen, W. Cao, Z. Shen, and X. Yao, "Research on the sport majors college entrance examination system in guizhou based on data statistical analysis," ***Bol. Tec. Bull.,*** 55(11): 666–671 (2017).

71. Kaynakli, O., & Yamankaradeniz, R., "Effect of the Heat Exchangers used in Absorption Refrigeration Systems on Performance of the Cycle", ***University of Uludag, J. Faculty Eng. Archives,*** *8*(1): 111-120 (2003).

72. Güney, A., "*R744/R134A Kaskad Soğutma Sisteminin Enerji ve Ekserji Analizi", **Doctoral dissertation, Yüksel Lisans Tezi, Celal Bayar Üniversitesi, Fen Bilimleri Enstitüsü, Makine Mühendisliği Ana Bilim Dalı***, Manisa, Turkey, 32-88 (2014).

73. Xiao, B., Chang, H., He, L., Zhao, S., & Shu, S., "Annual performance analysis of an air source heat pump water heater using a new eco-friendly refrigerant mixture as an alternative to R134a", ***Renewable Energy,*** 14(7): 2013-2023 (2020).

74. Kizilkan, Ö., "Examination of superheating and subcooling effects in refrigeration systems with compressor in terms of thermoeconomics for different refrigerants", The ***Graduate School of Natural and Applied Sciences, Master Thesis***, Turkey, *117* (2004).

75. Kaya, H. "Soğutucu Akışkan Karışımlarının Kullanıldığı Soğutma Sistemlerinin Termoekonomik Analizi", ***Yüksek Lisans Tezi, Karabük Üniversitesi Fen Bilimleri Enstitüsü,*** Karabük, 98-105 (2014).

76. A. Kilicarslan and M. Hosoz, "The Influence of Mixing Factors on the Flammability of R32 Refrigerant and Compressor Oil Mixture," ***Energy Convers. Manag.,*** 51(12): 2947–2954 (2010).

77. Özkaymak, M., Kurt, H., & Recebli, Z., "Thermo-economic optimization of superheating and sub-cooling heat exchangers in vapor-compressed refrigeration system", ***International Journal of Energy Research,*** 32(7): 634-647 (2008).

78. Kedersiz, F., "*Kaskad soğutma sistemlerinin termodinamik incelenmesi", **Master's Thesis, Fen Bilimleri Enstitüsü,*** Turkey, (2014).

79. Kalla, S., "alternative refrigerants for HCFC 22—a review", ***Journal of Thermal Engineering,*** *4*(3): 1998-2017 (2018).

80. Özkaymak, M., and Özkaya, M.G. "Thermoeconomic Optimization Using Alternative Refrigerant in Vapor Compression Cooling System", ***Journal of New World Sciences Academy,*** 5(2): 381-398 (2010).

81. Akalan, O. B., "NH3 ve NH3/CO2 kaskad soğutma sistemlerinin karşılaştırılması", ***Master's Thesis, Namık Kemal Üniversitesi,*** Turkey, 56-77 (2013).

82. Wu, Y., Zhang, H., Zhang, Q., Qiu, J., & Rui, S., "The study of thermodynamic properties of zeotropic mixtures of R600a/R23/R14", ***Advances in Mechanical Engineering,*** *9*(3): 168-781 (2017).

83. Uysal, E,. "Experimental Determination of the Optimal Superheat Value in Cold Storage Application", M.Sc., Karabuk University Institute of Science and Technology, Karabuk, (2018).

84. Ismaeel, H. "Thermodynamic Analysis of a Cascade Refrigeration System", ***Yüksek Lisans Tezi, Mechanical Engineering University of Gaziantep,*** Gaziantep, 49-74 (2012).

85. Chen, J., & Yu, J., "Performance of a new refrigeration cycle using refrigerant mixture R32/R134a for residential air-conditioner applications", ***Energy and Buildings,*** 40(11): 2022-2027 (2008).

86. Özkaya, M., and Gedik, B., "Experimental Investigation of the Performance of Different Refrigerants in Household Coolers", ***TUBAV Science Journal,*** 2(1): 1-9 (2009).

87. Çerkezoğlu, B., "CO2 kullanılan kaskad soğutma sisteminin analizi", ***Doctoral Dissertation, Fen Bilimleri Enstitüsü,*** Turkey, 32-54 (2010).

88. Mizutani, Y., Okido, T., Shono, Y., & Sakamoto, K., "Development of miscibility improved oil for R32", ***Transactions of the Japan Society of Refrigerating and Air Conditioning Engineers,*** *35*(4): 419-478 (2018).

89. Qi, Q., Deng, S., Xu, X., & Chan, M. Y., "Improving degree of superheat control in a direct expansion (DX) air conditioning (A/C) system", ***International Journal of Refrigeration,*** *33*(1): 125-134 (2010).

90. Karaöz, A. T., "CO_2-R404A Kaskad Sistem Tasarımı, İmalatı ve Testi", ***Doctoral Dissertation, Yüksek Lisans Tezi, TC Gebze Yüksek Teknoloji Enstitüsü, Mühendislik ve Fen Bilimleri Enstitüsü,*** Gebze, 12-19 (2010).

91. Xu, S., Fan, X., & Ma, G., "Experimental investigation on heating performance of gas-injected scroll compressor using R32, R1234yf and their 20wt%/80wt% mixture under low ambient temperature", ***International Journal of Refrigeration,*** 7(5): 286-292 (2017).

92. Usta, H., Menlik, T., & Kirmaci, V., "The Experimental Investigation of the Performance of R-404a/R-508b Refrigerants Couple in Cascade Cooling System", ***Journal of Polytechnic-Polytechnic Dergisi,*** 9(1): 13-19 (2006).

93. Arcaklıoğlu, E. "R12, R22, R502 Soğutucu Akışkanları Ve Alternatif Karışımlarının Soğutma Sistemlerindeki Termodinamik Analizi" ***Doktora Tezi, Kırıkkale Üniversitesi Fen Bilimleri Enstitüsü,*** Kırıkkale, 192-197 (2002).

94. Summary, E. "An Evaluation of R32 for the US HVAC & R Market", ***Prepared by Optimized Thermal Systems, Inc.*** Washington, 34-56 (2016).

95. Çengel, Y. A. and Boles, M. A., "Thermodynamics with an Engineering Approach", ***Güven Scientific İzmir Güven Bookstore,*** İzmir, 611-660 (2008).

96. Çakır, U., & Çomaklı, K., "Mevcut soğutucu akışkanlar ve alternatifleri. *X",* ***Ulusal Tesisat Mühendisliği Kongresi,*** Turkey, 1079-1087 (2011).

97. Fedele, L., Bobbo, S., Camporese, R., & Stryjek, R., "Vapour–liquid equilibrium measurements and correlation for the pentafluoroethane (R125) + n-butane (R600) system", ***Fluid Phase Equilibria,*** *227*(2): 275-281 (2005).

98. Özkol, N., "Applied Cooling Technique", ***TMMOB Chamber of Mechanical Engineers,*** 11(5): 112-145 (1999).

99. Bulgurcu, H., Kon, O., & İlten, N., "Soğutucu akişkanlarin çevresel etkileri ile ilgili yeni yasal düzenlemeler ve hedefler", ***Ulusal Tesisat Mühendisliği Kongresi,*** Turkey, 915- 927 (2007).

100. Ascoop, C. A., Simoons, M. L., Egmond, W. G., & Bruschke, A. V., "Exercise test, history, and serum lipid levels in patients with chest pain and normal electrocardiogram at rest: Comparison to findings at coronary arteriography", ***American Heart Journal,*** *82*(5): 609-617 (1971).

101. Internet: Bulgurcu, H., "Vapor Compression Cooling Cycles", **http://deneysan.com/Content/images/documents/sogutmacevrimleri_978667 87.pdf/** (2015).

102. Internet: Ekin Endüstriyel, "Lehimli Isı Eşanjörü Ürün Kataloğu", **https://www.ekinendustriyel.com/Kataloglar/LEHİMLİ_ISI_ESANJORU_URUN_KATALOG.pdf**/(2021).

103. Roberts, N. A., "Determination of the performance, leak scenario, flammability and oil return characteristics of a novel R22 replacement", ***Purdue University,*** United Kingdom, 20-29 (1998).

104. İsa, K. and Onat, A., "Energy efficiency in air conditioning and cooling systems", **Doğan Yayıncılık,** İstanbul, 40-76 (2012).

105. Internet: Onda SPA, "plate heat exchangers workıng prıncıple", **https://www.onda-it.com/media/2393/How-a-Plate-Heat-Exchanger-Works-Onda-SpA_2021.pdf/** (2021).

106. Reddy, D. R., Bhramara, P., & Govindarajulu, K., "Hydrocarbon Refrigerant mixtures as an alternative to R134a in Domestic Refrigeration system: The state-of-the-art review", ***International Journal of Scientific & Engineering Research,*** *7*(6): 87 (2016).

107. Internet: Karabulut, H., "Vapor Compression Cooling System Elements Lecture Notes" Harran University Faculty of Engineering, **http://eng.harran.edu.tr /~hbulut/Elemanlar.pdf**/(2010).

108. Internet: Emerson, "Display Case and Universal Controllers Series EC2", **https://kines.ru/photo/Alco_EC2U.pdf/** (2012).

109. Oruç, V., Devecioğlu, A. G., & Ender, S., "Improvement of energy parameters using R442A and R453A in a refrigeration system operating with R404A", ***Applied Thermal Engineering,*** 12(9): 243-249 (2018).

110. Çakır, U. and Çomaklı, K., "Current Refrigerants and Alternatives", ***X. National Plumbing Engineering Congress,*** USA, 1079-1087 (2011).

111. Mota-Babiloni, A., Navarro-Esbrí, J., Makhnatch, P., & Molés, F., "Refrigerant R32 as lower GWP working fluid in residential air conditioning systems in Europe and the USA", ***Renewable and Sustainable Energy Reviews,*** 8(0): 1031-1042 (2017).

112. Çomaklı, K. and Bakırcı, K., "Refrigerants Used in Cooling/Heating Systems and Alternatives", ***Mühendislik ve Makine Dergisi,*** 47 (562): 33-45 (2006).

113. Devecioğlu, A. G., & Oruç, V., "Energetic performance analysis of R466A as an alternative to R410A in VRF systems", ***Engineering Science and Technology, an International Journal,*** *23*(6): 1425-1433 (2020).

114. Bıtzer Kühlmaschinenbau GmbH, "Refrigerant Report 20", ***Refrigerant, Bitzer International,*** Sindelfingen, 3-9 (2019).

115. Heredia-Aricapa, Y., Belman-Flores, J. M., Mota-Babiloni, A., Serrano-Arellano, J. and García-Pabón, J. J. "Overview of low GWP mixtures for the replacement of HFC refrigerants: R134a, R404A and R410A," ***Int. J. Refrig.,*** 11(1):113–123 (2020).

116. Sheep. T. and Acar. M., "Refrigerants Used in Refrigeration Systems and Their Effects on Ozone Layer" ***Plumbing Engineering Journal,*** 8(8): 46-53 (2005).

117. Sanz-Kock, C., Llopis, R., Sánchez, D., Cabello, R., & Torrella, E., "Experimental evaluation of a R134a/CO2 cascade refrigeration plant", ***Applied Thermal Engineering,*** *73*(1): 41-50 (2014).

118. Internet: Ekin Industrial, “Bold Heat Exchanger Product Catalogue”, **https://ekinendustriyel.com/Admin/Kataloglar/Link?i=75&t=d&l=t/**(2019).

119. Internet: Ordel, “Udl 200 Data Collector”, **https://ordel.com.tr/tr/urunler/veritoplayicilar/udl200/**(2020).

120. Internet: Emerson Climate, "Ec2 Display Case Controllers", **http://frigopolska.pl /upload/dok/EN_EC2__Electronic_Case_Controller-35018.pdf/** (2005).

121. Internet: Refrigeration vapor compression cycle, “Refrigeration cycle animation video/vapor compression cycle explained”, **https://www.yesyen.com /refrigeration_cycle.php**/(2022).

122. Internet: Edward, W. “Green Energy Island Integration and Operation Optimization Research”,**https://www.researchgate.net/figure/a-b-cSchematic-and-T-s-diagram-for-the-ideal-vapor-compression-refrigeration-cycle_ fig2_326912104**/(2022).

123. Internet: Baskaran Ayyalusamy, “A performance study of Vapour compression refrigeration system using ZrO2 Nano particle with R134a and R152a”, **https://www.researchgate.net/figure/P-h-diagram-of-vapor-compression-refrigeration-cycle-Generally-the-vapor-compression_fig1_313722266/** (2022).

124. Internet: Diagram of vapour “diagram of the vapour-compression-refrigeration cycle”,**https://www.researchgate.net/figure/T-s-diagram-of-the-vapour-compression-refrigeration-cycle-considered-in-Fig-1_fig2_316144041** /(2022).

125. Internet: Hugo, R. “Mechanical Engineering Thermodynamics” **https:// www.youtube.com/watch?v=ZVsMi2IzKBs**/(2022).

126. Internet: Guilherme, M. “Can we use a Mollier diagram in a refrigeration cycle problem?”,**https://www.quora.com/Can-we-use-a-Mollier-diagram-in-a-refrigeration- cycle-problem/**(2022).

127. Internet: Word Press “What is thermstatic expansion valve? Working construction and applications”, **https://electricalworkbook.com/thermostatic-expansion-valve/**(2022).

128. Internet: Electrical workbook, “Automatic expansion valve”, **https:// electricalworkbook.com/automatic-expansion-valve/**(2022).

129. Internet: Shodiya, S. “A simple method on equipment selection methodology of vapor compression refrigerant electric vehicle air-conditioning system”, **https://www.researchgate.net/figure/Danfoss-EEV-type-ETS-6-a-Actual-view-b-cross-sectional-view-17_fig4_281307524**/(2022).

130. Internet: Outreach, “Middle shcool caroline”, **https://cloud1.arc.nasa.gov/solveII/outreach/middleschool-chlorine.htm/(2022).**

131. Internet: Ashrae “Classification of refrigerants according to ASHRAE standards“,**https://www.researchgate.net/figure/Classification-of-refrigerants -according-to-ASHRAE-standards_fig15_305737030/(2022).**

132. Internet: ECO-R600a, “Freeze products”, **https://eco-freeze.com/tr/products/ecor600a/(2022).**

133. Internet: AliBaba “refrigerant product”, **https://turkish.alibaba.com/ product-detail/SHINGCHEM-OEM-NEUTRAL-buy-refrigerant-gas-6256_5859937.html**/(2022)

134. Internet: Made in China, “High Purity R407c Refrigerant Gas for Refrigeration Industry China”, **https://fluorogas.en.made-in-china.com/product/JqbnovhykwRs/ChinaHigh-Purity-R407c-Refrigerant-Gas-for-Refrigeration-Industry-China. html**/(2022).

RESUME

Adel Mohmed A KRAIM completed his primary and secondary education at Houn School. He graduated from Houn High School in 1993. He started undergraduate studies at Houn's College of Engineering, From there, he moved to the Higher Institute of Refrigeration and Air Conditioning in Sukneh city in 1993 and successfully graduated in 1998. Immediately after the graduation, he started working as a teacher and lab supervisor at the Faculty of Engineering in Houn. He started the graduate studies at Middlesbrough University in the United Kingdom, Graduate Education Institute, Department of Advanced Manufacturing Systems Engineering. After obtaining his master's degree, he worked as a faculty member at the Higher Education Authority in Libya. He obtained a decision from the Ministry of Higher Education in Libya to complete a doctoral study in the field of energy at Karabuk University in Turkey in 2016.